CRITICAL SEISMIC PERFORMANCE ASSESSMENT OF CONCRETE BRIDGE PIERS DESIGNED FOLLOWING CANADIAN HIGHWAY BRIDGE DESIGN CODE

by

Md Rashedul Kabir

A THESIS SUBMITTED IN PARTIAL FULFILLMENT

OF THE REQUIREMENTS FOR THE DEGREE OF

MASTER OF APPLIED SCIENCE

in

THE COLLEGE OF GRADUATE STUDIES

(Civil Engineering)

THE UNIVERSITY OF BRITISH COLUMBIA

(Okanagan)

October 2017

The undersigned certify that they have read, and recommended to the College of Graduate Studies for acceptance, a thesis entitled:

CRITICAL SEISMIC PERFORMANCE ASSESSMENT OF CONCRETE BRIDGE PIERS DESIGNED FOLLOWING CANADIAN HIGHWAY BRIDGE DESIGN CODE

Submitted by Md Rashedul Kabir in partial fulfillment of the requirements of the degree of Master of Applied Science

Dr. M. Shahria Alam, Associate Professor, School of Engineering, UBC
Supervisor

Dr. Solomon Tesfamariam, Professor, School of Engineering, UBC
Supervisory Committee Member

Dr. Kasun Hewage, Professor, School of Engineering, UBC
Supervisory Committee Member

Dr. Homayoun Najjaran, Professor, School of Engineering, UBC
University Examiner

18 October 2017

(Date Submitted to Grad Studies)

ABSTRACT

Performance-based design (PBD) method is gradually taking over the traditional force-based design (FBD) for designing bridges in North America. Considering the importance of bridge structures in the transportation network, quantitative performance criteria were adopted in Canadian Highway Bridge Design Code (CHBDC) in 2014 and a supplement to CHBDC 2014 was published in 2016. In this study, a lifeline bridge pier is designed following the FBD method from CHBDC 2010 and PBD approach following CHBDC 2014 and the supplement to CHBDC 2014 to understand the impression of changes in bridge design codes. The dominating performance criteria in the new supplement to CHBDC 2014 for a lifeline bridge is the maintenance of repairable damage at a seismic event of 975 years return period. The performances of the designed bridge piers are assessed using 20 near-fault ground motions through incremental dynamic analysis. Fragility curves for the bridge piers are plotted to perform the seismic vulnerability analysis of the bridge piers designed following three different alternatives. A lifeline bridge pier is also designed following PBD from CHBDC 2014 using different ASTM grade steel of varying strength and fracture elongation in combination with different concrete strength. Performances of the designed bridge piers are evaluated for site-specific ground motion suits. Moreover, the impact of changing reinforcement strength on the designed bridge piers' seismic behavior is checked by fragility analysis. PBD from the supplement to CHBDC 2014 shows the highest damage probability. Whereas, the FBD from CHBDC 2010 and the PBD from CHBDC 2014 substantially reduce the risk of damage and improve the performance of the bridge pier. Practicing high strength steel reinforcement (HSR) in PBD of bridge piers can reduce the required percentage of reinforcement by 50% compared to conventionally used Grade 60 reinforcement. Construction difficulties can be avoided due to less congestion of rebars and cost of construction can be cut down without compromising the seismic performance. Damage vulnerability related to longitudinal steel strain reduces remarkably, and the collapse performance decreases when HSR are practiced in the design of bridge piers. Incorporation of high strength concrete can marginally improve the collapse performance.

PREFACE

Major portions of this study have been submitted to peer-reviewed technical journals for publications as listed below. All the analytical studies have been solely conducted, and the author prepared the initial drafts of all the papers listed below. His research supervisor provided continuous supervision and guided towards further development of the final versions of the manuscripts by giving valuable feedback and revisions.

List of Publications Related to this study:

Kabir, M.R., and Alam, M.S. 2017. Seismic performance evaluation of force-based and performance-based designed lifeline bridge pier following CHBDC. Submitted to Canadian Journal of Civil Engineering.

Kabir, M.R., and Alam, M.S. 2017. Effect of material strength on the performance-based design and dynamic performance of bridge piers as per CHBDC. Submitted to Bulletin of Earthquake Engineering.

TABLE OF CONTENTS

LIST OF TABLES

LIST OF FIGURES

LIST OF SYMBOLS

$\beta_{EDP\|IM}$	Dispersion Of The Demand
COV	Coefficient of Variation
DS	Damage State
EDA	Elastic Dynamic Analysis
EDP	Engineering Demand Parameter
ε_c	Concrete Strain
ε_{cc50}	50% of Confined Concrete Strain
ε_{cu}	Crushing Strain of Concrete
ε_{st}	Steel Strain
ε_{scr}	Buckling Strain of Longitudinal Rebar
ε_{sm}	Steel Strain at Maximum Tensile Stress
ε_{su}	Fracture Strain of Steel
ε_y	Yielding Strain of Steel
f'_c	Compressive Strength of Concrete
f_{cr}	Cracking Stress of Concrete
f_{sy}	Yield Stress of Steel
f_{yh}	Yield Strength of Transverse Steel
I	Importance Factor
IDA	Incremental Dynamic Analysis
IM	Intensity Measure
ISPA	Inelastic Static Pushover Analysis
K_{cr}	Cracked Stiffness
LS	Limit State
m	Effective Mass
NLTHA	Non-Linear Time History Analysis
PGA	Peak Ground Acceleration
PGV	Peak Ground Velocity
PSDM	Probabilistic Seismic Demand Model
PSV	Pseudo-Spectral Velocity

R	Response Modification Factor
SI	Spectral Intensity
$S(T)$	Spectral Acceleration for a Certain Period, T
T_a	Fundamental Period of Structure
UHS	Uniform Hazard Spectrum
σ_c	Compressive Stress in Concrete
σ_s	Longitudinal Steel Strain
ρ_s	Volumetric Ratio of Transverse Reinforcement

ACKNOWLEDGMENTS

On the eve of this great milestone of my life, I would like to take this opportunity to express my unfathomed gratitude to the Almighty Allah for all the blessings to reach the pinnacle of this achievement. However, this achievement would not be possible without the support of my supervisor Dr. M. Shahria Alam from day one of this exciting journey of M.A.Sc. at the University of British Columbia, Okanagan (UBCO). He has been an umbrella over my head through his mentorship, continuous support, guidance, knowledge and above all his friendship, which have shaped my research experience to an unforgettable one. He has always motivated me to dig deep to bring the best out of myself. I cannot express enough my appreciation for his inevitable contribution to pave me the right way during my research at UBCO.

I would like to express my appreciation for my master's dissertation committee members, Dr. Solomon Tesfamariam and Dr. Kasun Hewage for their guidance and support, which helped me to ameliorate my research quality. I would like to acknowledge the excellent facilities and support of UBCO to make my graduate experience a fruitful one. Additionally, grant like Queens Scholarship has played an instrumental role in effectively conducting my research.

I would like to thank all my research group members, especially Dr. A.H.M.M. Muntasir Billah, Dr. Farshad Hedayati Dezfuli and Mr. Qi Zhang for their guidance, which boosted up my confidence during the difficult phases of my research. I was fortunate to have some fruitful discussion and share the technical knowledge of research work with some excellent graduate students of the research group. Their friendship and critical feedback helped me to a great extent during this endeavor.

I would like to thank my parents for their unconditional support, which is the fundamental inspiration for this achievement. Finally, I would like to thank my wife, Ismat Zahan Zerin, whose spontaneous support, love and encouragement have ignited the spark in me in this journey and every avenue of my life.

DEDICATED TO MY PARENTS

Md. Shahjahan Bhuiyan

&

Nargis Jahan

Chapter 1 : INTRODUCTION

1.1 General

Earthquake is one of most devastating unforeseen natural catastrophe. The disastrous behavior of earthquake not only cost lives but also results in severe damage to structure and economic loss. Transportation network of any country comprises of a substantial portion of highway bridges. Any major damage to the bridges during seismic events causes breakdown of transportation links (Chang and Nojima, 2001; Choi et al., 2004; Padgett and DesRoches, 2007), leading to disruptive post-disaster service management. Extremely high cost and prolonged repair time of damaged bridges make the situation even more critical causing interruption to the total traffic system. Every year, billions of dollars are spent worldwide to repair damaged bridges and to construct new ones. History demonstrates the high susceptibility of highway bridges to earthquake damage. The 1971 San Fernando earthquake, the 1994 Northridge earthquake, the 1995 Great Hanshin earthquake in Japan, the 1999 Chi-Chi earthquake in Taiwan, the 2010 Chile earthquake, and the 2010 Haiti earthquake showed the devastating nature of earth movement and caused massive socioeconomic impact (Hwang et al., 2001). Twenty-five percent of bridges were damaged during the Northridge Earthquake in Los Angeles, and six of them collapsed (Basöz et al., 1999). Non-seismic design provision was the main cause of these collapses. Around $190 million was cost to repair the damaged bridges (Caltrans, 1994). The scenario in Canada is nothing exceptional. Mirza (2007) reported that the municipal infrastructure deficit had reached 123 billion dollars of which more than 30% is in transportation and transit sector in Canada. The sheer importance of bridges to the economy of Canada cannot be ignored. So, it is absolutely important that the bridges stay active even after massive earthquakes (Billah et al., 2013).

Keeping a bridge system functional during and after a seismic event is challenging. To minimize the adverse effect from an earthquake, maximum drift in the bridge pier needs to be limited (Billah and Alam, 2014a). Bridge piers experience huge lateral deformation in a traditional structural system and unrepairable damage at the plastic hinge regions due to excessive deformation during an earthquake. Predicting and controlling the deformation in bridge piers following the traditional force-based seismic design (FBD) process is merely possible due to some limitations (Priestley, 2000). To consider the inelastic response of the structure, *R* factor is used in

FBD approach, which is represented by the displacement ductility. This *R* factor reduces the elastic base shear demand to an acceptable design level. However, it does not assure any definite performance level (Sheikh and Légeron, 2014). The *R* value is chosen based on the assumed ductility of a bridge pier, but this *R* value can vary notably with the geometry of the structure and target performance level. Employing single *R* factor for multilevel performance and different structural elements may not be suitable. Next limitation of FBD is the constant stiffness presumption of the structure. The stiffness and force distribution varies with the changed deformation of the structure, and the yielding of structural elements occurs gradually; not at a time. Lastly, the key shortcoming is that the FBD cannot clearly describe the performance of the bridge structure to a certain level. To deal with these limitations of FBD approach, engineers have established alternative seismic design methodologies based on the performance of structural elements and materials than strength, which is termed as performance-based design (PBD). This design method reasonably eliminates the performance uncertainties in the traditional FBD method with specific and quantitative performance criteria. Since the force in not measurable during an actual seismic event, the PBD approach regards specified performance levels regarding drift ratios and material strains. Client based approach can also be considered in PBD as long as it explicitly demonstrates the performance levels to acceptable risks and associated costs (Priestley et al., 2007). Due to flexible design methodology meeting the performance requirement of structure regarding damage and serviceability, bridge designers are leaning towards the PBD.

The Canadian highway bridge design code (CHBDC) recently incorporated the PBD (CSA, 2014). Depending on the bridge type, the required serviceability and damage states are defined in terms of material strain in CBDC 2014. However, very limited information is available on the comparative performance of bridge piers designed following FBD and PBD. Zhang et al. (2016) investigated the comparative design and performance of FBD and PBD bridges and concluded that the PBD is too conservative leading to high reinforcement requirements and cost. However, a new and improved supplement to CHBDC 2014 (CHBDC, 2016) has recently been published with a substantial change in performance criteria for the PBD. To date, there is no study has been conducted on how the performance of bridge changes for the adoption of different design methods from CHBDC regarding probability-based seismic vulnerability. This study will play a significant role in giving an idea of the seismic performance of steel reinforced concrete bridge pier designed following different design guidelines; using a widely used tool, fragility curve, which gives a view

on the vulnerability of structural components. How the design changed during past seven years in CHBDC will also be investigated through the design of a lifeline bridge pier. With the evolution of PBD, fragility analysis getting the attention to assess the performance and seismic risk of the bridges to be constructed. An elaborate understanding will also be presented here to show the importance of high strength longitudinal steel on bridge design process and seismic performance for near-fault ground motions.

1.2 Research Significance

A Recent report from Natural Resources Canada (NRC) revealed that the western part of BC is the highly active seismic region with more than 200 seismic tremors a year (NRC, 2017). On an average 1500 earthquake occurs in Canada per year of which only 6.7% are more than three magnitudes in Richter scale and felt by humans. The Pacific-North American plate boundary along the west coast of the United States and Canada consists of the Juan de Fuca subduction fault off the Vancouver Island and the Cascadia subduction zone "megathrust fault' along the Northern Vancouver Island to Cape Mendocino California are pushing against each other creating a probability of 9 magnitudes of earthquake. Even the small magnitude earthquake can be devastating if it happens for a longer duration. Considering these facts, necessary precautions and understanding of current design practice of bridges are indispensable to oblige the saying "precaution is better than cure". Moreover, to study the suitability of higher grade reinforcing steel and high strength concrete in seismic application to avoid congestion during construction and reduce material demand while maintaining superior performance triggered the motivation behind this research.

1.3 Objectives of the Study

With the advancement in design methodology and material properties, PBD and choice of high strength steel as reinforcement in reinforced concrete structures are receiving special attention. The primary objective of this research is to investigate the design evolution in CHBDC from FBD method to PBD method in last decade for a lifeline bridge and performance assessment of a bridge pier designed using different steel alternatives. To thoroughly understand the effect of high strength steel reinforcements (HSR) on design and seismic performance of bridge pier, different

steel grades are combined with varying concrete strength. The specific tasks to achieve these objectives include:

- Comparing the seismic design methodology and the design outcomes of a lifeline bridge pier designed following CHBDC 2010, CHBDC 2014 and the supplement to CHBDC 2014.
- Assessing the performance of the designed bridge piers by conducting incremental dynamic analyses under near-fault ground motions.
- Evaluating the dynamic response of a lifeline bridge pier designed following PBD design method from CHBDC 2014 using reinforcing steels and concrete of varying strength.

1.4 Scope of the Research

This particular research focuses on the design evolution in CHBDC for a lifeline bridge pier and introduces the importance of steel strength in design. Unlike before, HSR are presently in mass production. However, application of HSR are very limited in Canada. Also, the design philosophy has changed after the adoption of PBD method in CHBDC 2014 (CSA, 2014). It is important to understand how these changes affect the dynamic response of a bridge pier and what reinforcing steel strength can offer in improving bridge performance. To accomplish the goals of this research, literature reviews on PBD of bridge piers and application of HSR are carried out first. A hypothetical bridge pier is selected to be designed following the FBD specified in CHBDC 2010 (CSA, 2010) and the PBD criteria stated in CHBDC 2014 and the new supplement to CHBDC 2014 (CHBDC, 2016). Design difference and dynamic response of these bridge piers are evaluated under near-fault ground motions. Finally, a lifeline bridge pier is designed using different steel reinforcement having code specified yield and elongation properties according to the most recent CHBDC guidelines. There have been many studies on bridge fragilities present in the literature on bridges in Canada that includes Tavares et al. (2012), Siqueiraa et al. (2014), Dezfuli and Alam (2017), and Parghi and Alam (2017). None of these studies have worked on fragility analysis and dynamic response assessment of the same bridge pier designed following different design alternatives and using varying strength steel reinforcements. This study will address the issues mentioned above, which will direct the design engineers towards the proper selection of design and reinforcing material.

1.5 Outline of the Thesis

This thesis contains six chapters including the present chapter 'Introduction'. This chapter outlines the main goals of this research along with the breakdown of steps to achieve the specified goals. Significance and scope of this study are also presented here. The dissertation contents are arranged in following chapters.

Chapter 2 portrays an overview of HSR application in bridge and building component design. History and development of high strength steel rebars, their manufacturing process, significant properties and application in structural engineering are discussed in light of existing studies. Philosophy and basics of PBD are also presented in this chapter focusing on bridges only. The necessity of PBD and importance of high strength steel in designing bridges are concluded in this chapter.

Chapter 3 explains the force-based and PBD methodology of a bridge pier according to CHBDC 2010, CHBDC 2014 and the supplement to CHBDC 2014 with design examples. Static pushover analyses and non-linear time history analyses are performed to assess the responses of the designed bridge piers. Incremental dynamic analyses (*IDA*) for twenty near-fault ground motion are carried out to plot the *IDA* responses for maximum hazard level, and the results are compared for the designed bridge piers.

Fragility analysis is a strong tool to evaluate the seismic performance of existing bridges and bridges to be built. In Chapter 4, analytical fragility analyses of the designed bridge piers are done by developing probabilistic seismic demand models. Fragilities are plotted in terms of maximum drift in bridge piers for four different damage states to predict the performance of the bridge piers under varying ground motion intensities.

Chapter 5 deals with the application of HSR and high strength concrete in PBD of bridge piers. Performance criteria for bridge piers stated in CHBDC 2014 are utilized in designing a lifeline bridge pier. Final design outcomes and their comparative performances are also discussed in this chapter in term of *IDA* plots and fragility curves.

Lastly, summary and conclusions from this study, discussion on limitations and future recommendations in this research area are proposed in Chapter 6.

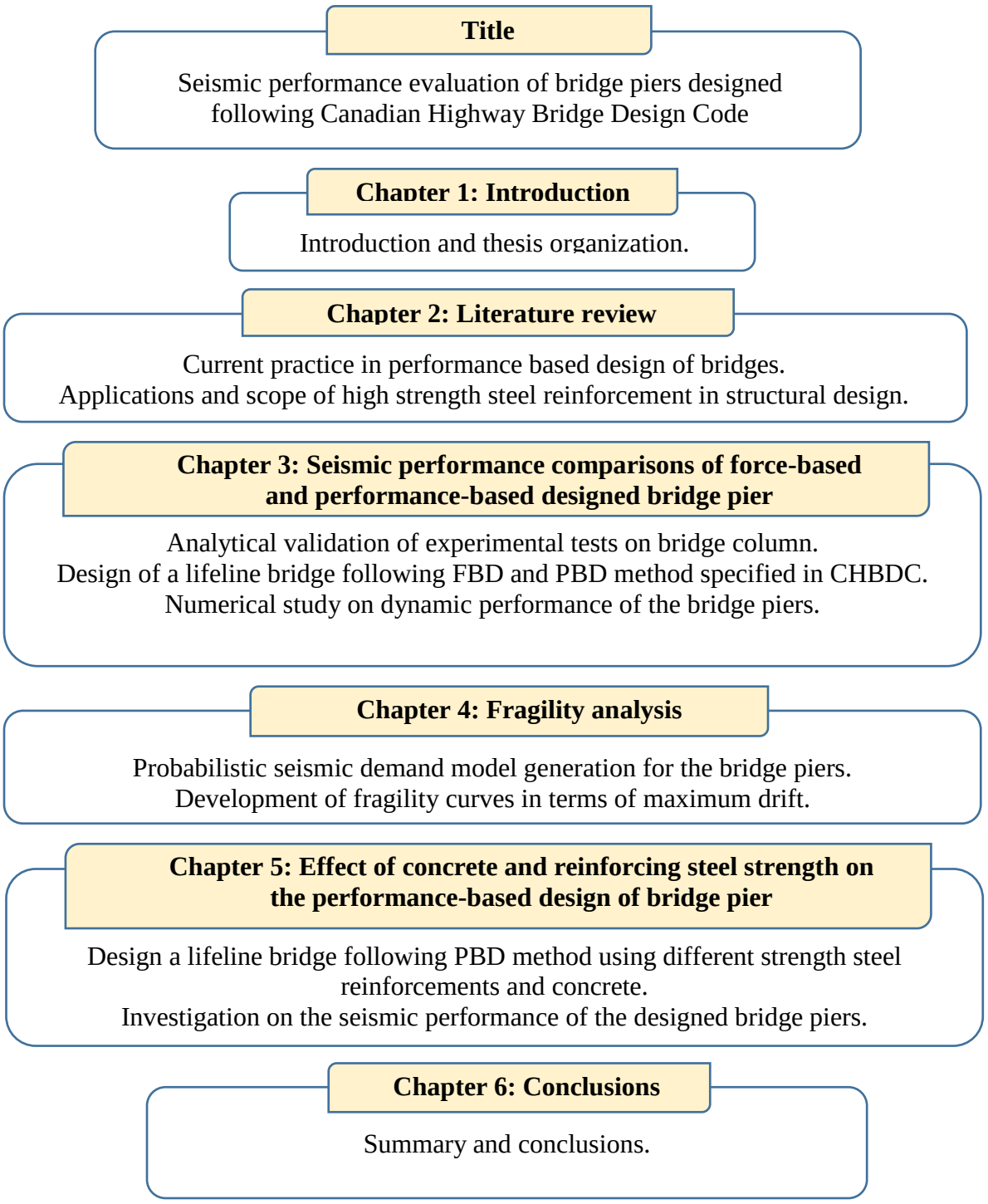

Figure 1.1 Thesis outline

Chapter 2 : LITERATURE REVIEW

2.1 Bridge Design

Bridges are an essential part of transportation network of a country and contribute actively in the sustainable development process. Disruption in this transportation network due to undesirable natural calamities can cause serious damages to life and economy. After the devastating 1971 San Fernando earthquake, researchers put extra effort in investigating the seismic effect on bridges, which acted as the turning point in the seismic design of structures. Many of the investigations on previous earthquakes show the deficiency in the design of bridges (Saiidi, 2011). However, recent post-earthquake field observations reveal that the bridges designed following modern design practices performed far better than the old bridges (Basöz et al., 1999; Hsu and Fu, 2004). Many of the existing highway bridges in North America were built when the seismic design was in the early stage of development (Roy et al., 2010). After the Loma Prieta earthquake in 1989, Northridge in 1994, and Kobe in 1995, engineers and stakeholders perceived the essence of designing and retrofitting structures to attain performance objectives, ensure life safety and lessen the damage cost associated with earthquakes. To improve the ductility of structure, the seismic design evolved from force-based to displacement-based design (Kowalsky et al., 1995; CALTRANS, 2004; ATC, 2003).

2.1.1 Force-based design (FBD) approach

FBD method was the most common design approach in designing buildings and bridges traditionally. To find out the demand on structure, load factors are associated with plastic range capacity of the structure (Allen, 1975). Figure 2.1 portrays a typical flow chart of designing a bridge pier following the FBD approach.

FBD approach possesses some inherited drawbacks such as the exclusion of varying stiffness with deformation in calculating time period of structure, uniform force reduction factor and concurrent yielding of elements (Priestley et al., 2007). Most importantly, FBD cannot establish a connection between structural performance and design. Ghobarah (2001) showed that the FBD method was not an effective design procedure to restrict damage in structures during large-scale earthquakes. Displacement was considered the main factor in designing bridges to

avoid the constraints related to FBD method by Priestly et al. (2007). The effective stiffness of the structure and displacement demand have to be calculated to find out the seismic base shear demand in displacement-based design. Many researchers found the direct displacement-based design very efficient and cost-effective in designing bridge structures (Kowalsky, 2002; Ortiz, 2006; Suarez and Kowalsky, 2006; Bardakis and Fardis, 2010). Reza (2012) studied the differences in FBD and displacement-based design regarding the design of a bridge with irregular column heights. However, a study from Reza et al. (2014) found that the FBD designed bridge performs better than direct-displacement based designed bridges in terms of displacement demand, residual deformation and cumulative energy dissipation capacity.

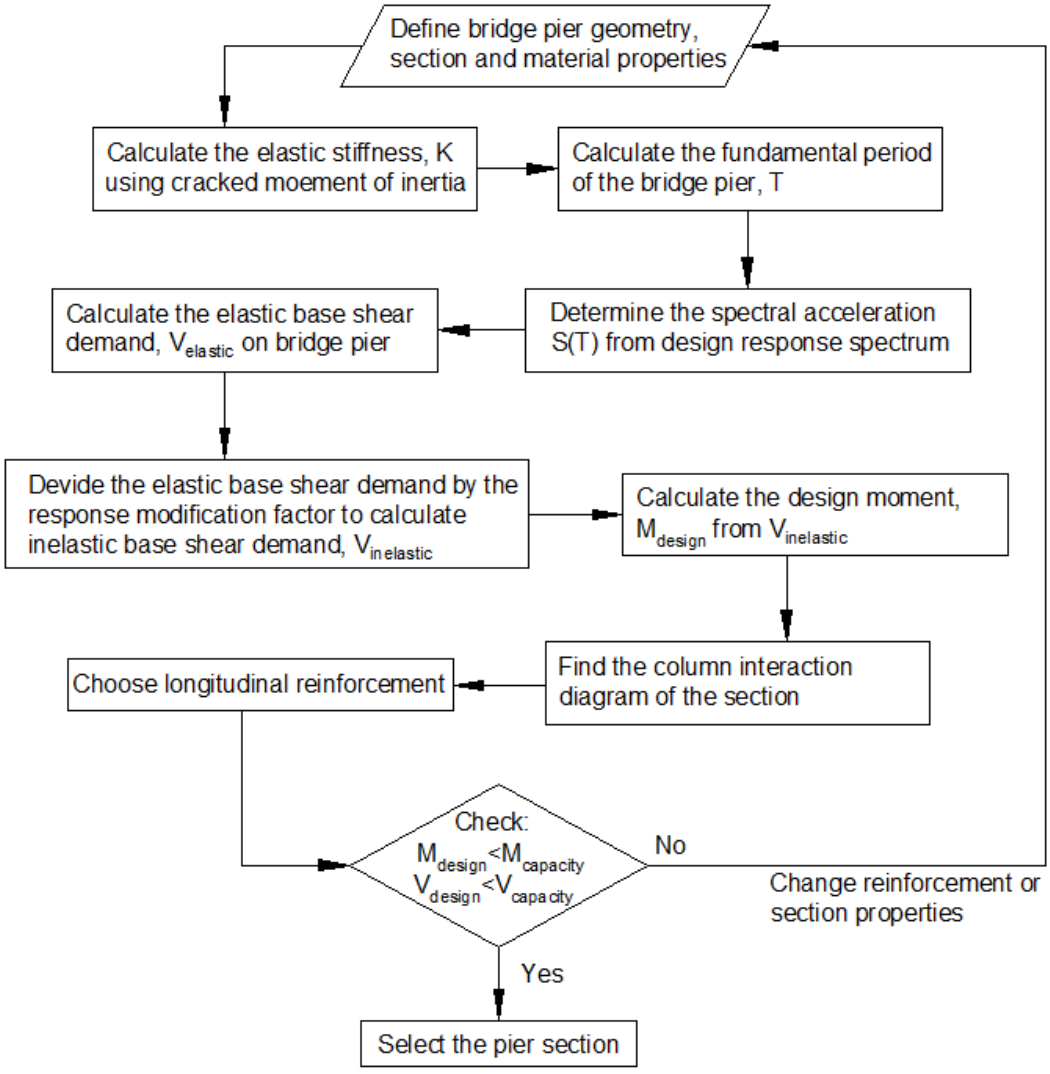

Figure 2.1 Flowchart showing the steps in FBD method of bridge pier

2.1.2 FBD in Canadian Highway Bridge Design Code

Canadian Highway Bridge Design Code till 2006 was mostly focused on the FBD of bridges. Elastic force demand from a particular site soil class and design response acceleration are calculated from the elastic stiffness of the structure. Ductility of the structure is assumed through incorporating a response modification factor, *R* based on the bridge configuration and expected performance level are treated with importance factor, *I*. Bridges are designed for the modified base shear demand but do not assure a target performance during a particular level of earthquake. The value of response modification factor (*R*) should vary with multiple performance levels, and the importance factor (*I*) should be related to the bridge properties and seismicity of the region (Sheikh and Légeron, 2014). National building code of Canada (NBCC) (NRCC, 2010) announced the increased seismic hazard levels for some regions in Canada. This initiated the obligation to evaluate the existing design of bridges and design of the to-be-built bridges. Bridge design codes such as AASHTO (2007), CHBDC 2010 (CSA, 2010) commonly use the FBD approach; however, there had been significant changes in terms of design and detailing to ensure ductility in the bridge structure (Mitchell et al., 2010).

2.1.3 Performance-based design approach

Modern bridges should be designed to satisfy the deformation requirement without any major damage to the structure. Higher energy dissipation capacity exhibits ductility in structure and allows them to deform in their inelastic region with a prior warning before failure. Plastic hinge location experiences the highest material strain under a seismic action and is critically designed to dissipate energy. Flexure failure is expected over brittle shear failure in structure. Global ductility of the structure depends on element level ductility and material ductility (Figure 2.2).

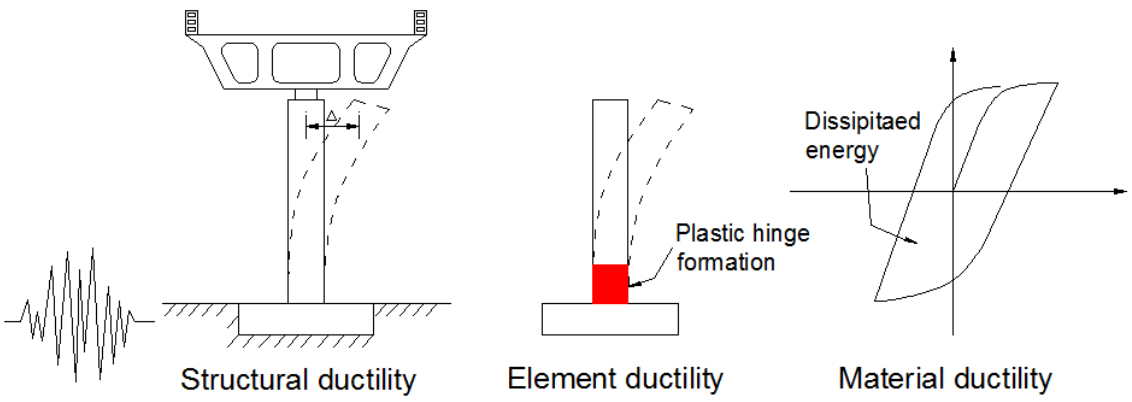

Figure 2.2 Ductility of structure

Performance-based seismic design of bridges can ensure the targeted performance while minimizing the economic losses and reducing the post-earthquake service demands (Floren and Mohammadi, 2001). A major benefit in PBD is that the PBD can minimize the uncertainties in traditional FBD method with specified performance criteria regarding displacement, drift or material strain limit. Life safety is the main concern in the FBD, whereas the PBD not only ensures that but also reduce post-disaster damage by ensuring the desirable performance of the structure. This widely reviewed design method for bridges is still in development process. Many design codes are yet to consider and implement the PBD method. The first initiation of PBD was in the 1980s in the United States and the reason behind was to get clear performance indication during and after a seismic event by the retrofitted buildings as demanded by the investors (Hamburger et al., 2004). The comparative performance assessment before and after retrofitting of a structure is critical for the safe investment by the project owners. Since then, PBD framework is being practiced and researched for several decades by engineers and researchers. Initial developments were focused on buildings as can be seen in many published documents like ATC 13 (ATC, 1985), ATC 14 (ATC, 1987) and FEMA-356 (FEMA, 2000c). The design of bridges is somewhat similar to the design of buildings. Reducing damage by protecting life safety and optimizing the cost are invariably the core of all structural design. Designers and engineers have taken many attempts to relate the structural performance to its serviceability. Performance-based assessment of bridge example was carried out by Forcellini et al. (2012) using the program BridgePBEE (Lu et al., 2011), which has the capability of running dynamic analysis of bridge structures and predicting

probable damage and loss along with the repairing time and cost. Most of the construction and rehabilitation projects of structures principally depend on the financial feasibility.

2.1.4 Performance-based design in bridges

Performance prediction of bridges has been extensively investigated by researchers in recent years. Priestley (2000), Floren and Mohammadi (2001), Mackie and Stojadinović, (2007), Saiidi (2011), Dawood and ElGawady (2013), Billah and Alam (2014b), Khan and Jiang (2015), Zhang et al. (2016) incorporated the PBD approach in investigating the bridge performance. First generation PBD of bridges based on drift, ductility and material strain response was summarized in National Cooperative Highway Research Program (Marsh and Stringer, 2013). There are few limitations of this first generation PBD specified by Hamburger et al. (2004). The weakest component dominates the global response leading to an overly conservative design. Damage in the non-structural members and their associated cost cannot be measured accurately. However, there may be possibility of higher damage cost in non-structural members than structural components. Also, it cannot correlate the performance with the coded design procedure, repair cost and time (Zhang, 2015). The next generation PBD methodology considered the uncertainties as started in 2001 the project ATC-58 (Hamburger et al. 2004) and completed in 2007 to bridge between engineers and clients. The phase two of the project commenced in 2012 and are expected to be finished in 2017. Repairing bridges is an important issue since almost fifty percent of the bridges in the USA were built before 1935 and reaching towards the end of their lifespan (Golabi and Shepard, 1997). To prioritize the retrofitting based on performance criteria, Gordin (2010) studied multi-criteria decision making (MCDM) in rehabilitating bridges and presented a decision matrix considering the damage severity, method of repairing, risk, construction supports and others.

2.1.5 PBD limit states

CHBDC adopted PBD method in 2014. Before that, the performance levels were merely descriptive in the CHBDC and the design engineers were not required to explicitly check the seismic performance of the bridge. A clear guideline based on quantitative performance limit was first introduced in CHBDC 2014 (CSA, 2014). Conflicting design outcomes following two different design approaches (Zhang et al., 2016) led to further modification in performance criteria specified in CHBDC 2014. Sheikh and Légeron (2014) showed that the bridge designed following

the CHBDC 2006 did not satisfy the performance objectives automatically. They correlated the engineering parameters with the bridge performances and outlined an implicit seismic design method to achieve target performance. Correlated engineering parameters with the performance levels and the limit states (*LSs*) from Sheikh and Légeron (2014) are shown in Table 2.1 and Figure 2.3 correspondingly.

Table 2.1 Descriptive and quantitative performance limits with engineering parameters

Limit state	Performance level	Serviceability	Performance description	Quantitative criteria
1A 1B	Fully functional	Serviceable	No or few easily repairable cracks. Yielding of main reinforcement	$\sigma_c = f_{cr}$ $= 0.4\sqrt{f_c'}$ $\sigma_s = f_{sy}$
2	Delayed operation	Limited service only	Concrete starts spalling and longitudinal cracks develop. Inelastic deformation initiates	$\varepsilon_c = -0.004$ $\varepsilon_s = 0.007$
3	Stable	Closure	Crushing of core concrete with strength degradation, buckling of longitudinal reinforcement, fracture of confinement.	$\varepsilon_c = \varepsilon_{cc50}$ $\varepsilon_s = \varepsilon_{scr}$ $\varepsilon_s = \varepsilon_{su}$ $= 0.07$

Note: f'_c= compressive strength of concrete; σ_c= stress in concrete; f_{cr}= cracking stress of concrete; σ_s= longitudinal steel strain; f_{sy}= yield stress of steel; ε_c= concrete strain; ε_s= steel strain; ε_{cc50}= 50% of confined concrete strain; ε_{scr}= buckling strain of main rebar; ε_{su}= fracture strain of steel.

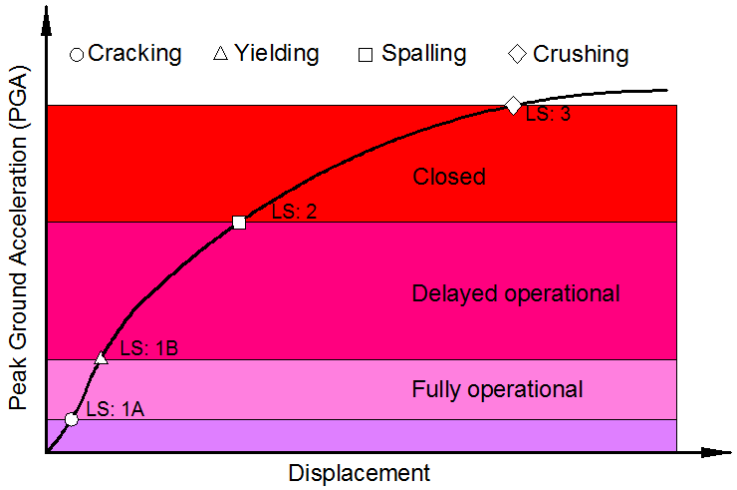

Figure 2.3 Graphical presentation of serviceability and limit states

2.1.6 Seismic hazard

The probabilistic approach that presents the maximum probability of exceedance is considered in various seismic design guidelines (Roy et al., 2010). The design earthquake hazard level in CHBDC 2000 (CSA, 2000) had the return period of 475 years, but the recurrence period for the extreme events varied from 1000 (CSA, 2000) to 2500 years (ATC, 2003). Later on, uniform hazard spectrum (*UHS*) at 2% in 50 years (2500 year return period) was developed by the Geological Survey of Canada (Adams and Halchuk, 2003). National Building Code of Canada, NBCC 2005 (NRCC, 2005) added the new *UHS* that significantly influenced the seismic design of structures. To design a bridge, CHBDC 2010 considers the earthquake of 10% probability in 50 years (return period 475 years). However, current CHBDC (CSA, 2014) employs three design level earthquakes in defining the performance objectives. The return period is commonly used to define the level of seismic events. A Poisson model described by Wang (2006) as shown in the Equation 2.1 presents the probability of n earthquakes happening within a time period of t years.

$$P(n,t,\tau) = \frac{e^{\frac{-t}{\tau}}(\frac{t}{\tau})^n}{n!} \qquad (2.1)$$

Here, τ is the recurrence interval of an earthquake equal or greater to a specific magnitude. Probability of design earthquake occurring at least once can be predicted by

$$P(n \geq 1,t,\tau) = 1 - e^{-\frac{t}{\tau}} \qquad (2.2)$$

In CHBDC 2014, the lower level earthquake has the return period of 475 years that means 10% probability in 50 years. Eurocode also exercises the similar level of earthquakes for the design level (Marsh and Stringer, 2013). Most of the bridges like Desmond Bridge, Tacoma Narrows Bridge were designed for the lower level event where the return period was not more than 100 years (Jones et al., 2013). Later on, the Port Mann Bridge and the Willamette River Transit Bridge were designed considering lower level design earthquake of return period 475 years. Target performance for the bridges mentioned above was to ensure elastic behavior with a little inelastic response. The performance-oriented design protocols as per CHBDC 2014, and the supplement to CHBDC 2014 for different types of bridges are shown in Figure 2.4.

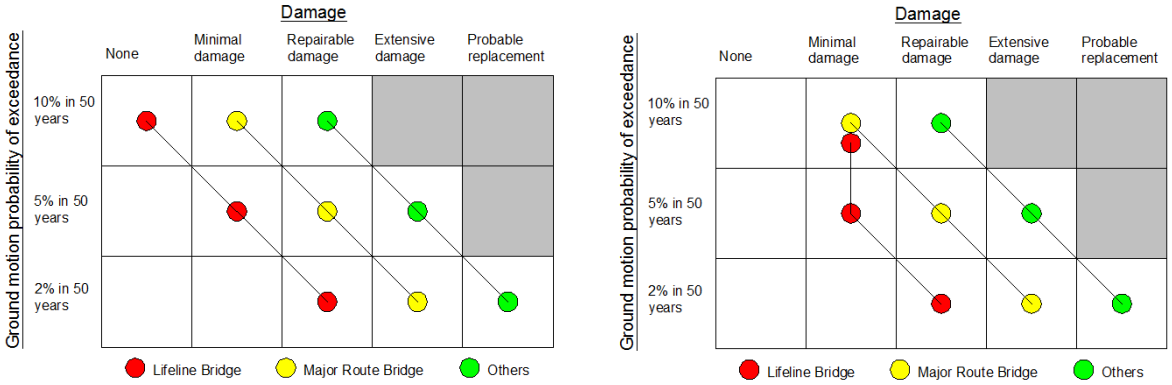

(a) (b)

Figure 2.4 PBD for different types of bridges according to (a) CHBDC 2014 (b) supplement to CHBDC 2014

2.1.7 Performance assessment guidelines in CHBDC

CHBDC (CSA, 2014) divides the bridge types into three categories: i) lifeline bridge, ii) major route bridge and iii) others. Lifeline bridge is the most critical, major and unique bridge, which possesses significant impact on the economy. Any service disruption in lifeline bridges during and post-disaster emergency hampers the economic recovery. Usually, this type of bridges are large in shape and requires a fortune in construction. Repairing a lifeline bridge costs a great deal of money and time. Port Mann Bridge, Second Narrows Bridges, and Oak Street Bridge are few examples of lifeline bridges in Canada. Major route bridges serve as post-disaster emergency response bridges. Emergency routes must be kept open after a seismic event and essential for

effective transportation and economy following an earthquake. It has the highest priority in retrofitting after lifeline bridge. Routes in Vancouver Island and the Lower Mainland can be considered as the major routes or disaster response routes. Major route bridges are also important for security and defense purposes. Bridges that are not included in the above two categories and less important in emergency response and post-disaster rehabilitation, are classified as other types of bridges.

Performance criteria in different codes are distinct for varying level of design. In most of the design guidelines, the performance criteria are mainly descriptive. No quantitative performance limits are set in terms of material strain or drift capacity of the structure. In New Zealand bridge manual (NZ-Transport, 2014), Chinese Specifications of Earthquake Resistant Design for Highway Engineering (China-MOC, 2008), LRFD (Load Resistance Factor Design) seismic analysis and design of bridges reference manual (FHWA-NHI, 2014), performance criteria are in more generalized form (Chen and Duan, 2013). Performance criteria were described previously in CHBDC 2010 (CSA, 2010) but quantitative limits were set in 2014 (CSA, 2014). These criteria vary with design levels and bridge types. CHBDC adopted material strain as the performance indicator of bridge structures. Usually, a structure is designed for the lower level of seismic event and checked for higher level events (Zhang, 2015). Life safety, serviceability, and economic criteria are the basis for the design of bridges for different level earthquakes. A bridge should remain serviceable when designed for a lower level earthquake, and the life safety should be ensured for a maximum level design (Bertero, 1996). Table 2.2 illustrates the comparative serviceability, design and performance criteria to design a reinforced concrete bridge using PBD approach according to CHBDC 2014 and the supplement to CHBDC 2014.

Table 2.2 Performance criteria according to CHBDC 2014 and the supplement to CHBDC 2014

Damage	Serviceability	Performance criteria (CHBDC 2014)	Performance criteria (CHBDC 2014 supplement)
Minimal 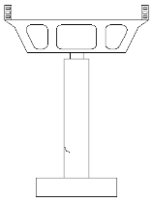	Fully serviceable to regular traffic. Any repair work does not hamper the service. Bridge remains elastic with minor damage.	Concrete compressive strain should be less than 0.004, and reinforcing bars should not yield.	Compressive strain limit in concrete is 0.006, and tensile strain in steel should not exceed 0.01
Repairable 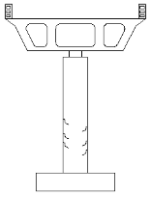	Usable to emergency traffic. Repairing can be done without bridge closure. Moderate damage due to some inelastic behavior. But repairing can be done in place without replacing any primary component.	Tensile strain in reinforcing steel cannot exceed 0.015	Maximum tensile strain in reinforcing bars must not cross 0.025
Extensive 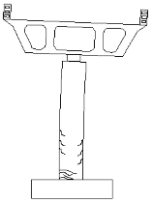	Bridge closure might require for repairing purpose and restricted emergency use. Visible damage due to concrete spalling and bar bucking. Bridge behavior is in inelastic range.	Confined concrete should not crush. Maximum allowable tensile strain in steel bar is 0.05	Core concrete strain should not exceed 80% of the maximum confined strain limit. Allowable tensile strain in steel is 0.05.
Probable replacement 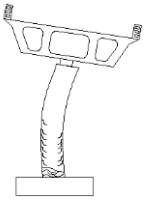	Bridge is in near collapse condition but evacuation should possible to maintain life safety. The bridge becomes unusable. Needs extensive repair work or replacement in some cases.	No criteria in terms of material strain are specified.	Confined concrete should not crush. Reinforcement strain should not exceed 0.075. For 35M or higher rebar size, the limit is 0.06.

FBD is not permitted for a lifeline bridge in the recent CHBDC 2014 (CSA, 2014) code. However, before that, a lifeline bridge was used to be designed using FBD method following the criteria that the bridge has to remain open to traffic for a lower level seismic event (475 years of return period) (Billah and Alam, 2016a). The minimum performance level specified for a lifeline bridge has been changed in the new supplement to CHBDC 2014. For ground motion with 10% probability of exceedance in 50 years, a lifeline bridge should not have any damage (CSA, 2014). In the supplement to CHBDC 2014, this damage criterion has been relaxed to minimal damage unless otherwise required by authority (CHBDC, 2016). Major modifications in the highway bridge design code happened to the performance criteria for different damage and serviceability conditions. For a ground motion with a return period of 975 years (probability of exceedance is 5% in 50 years), the damage in the lifeline bridge should be minimal, and it should be fully serviceable to the regular traffic, and no service disruption is expected from repair works (CSA, 2014). In the case of an extreme event with a return period of 2475 years, a lifeline bridge can offer limited service being accessible for emergency traffic only. Repairing should be done without any closure to the bridge, and at least one lane must be active during the repairing process. In designing a reinforced concrete bridge structure following PBD method, performance limits are set in term of concrete and reinforcing steel strain to satisfy the serviceability conditions. Table 2.3 displays the comparative performance criteria stated in CHBDC 2014 and the new supplement that has to be fulfilled in designing a regular lifeline bridge following the PBD approach.

Table 2.3 Performance criteria for a lifeline reinforced concrete highway bridge design

Ground motion probability of exceedance	CHBDC 2014			CHBDC 2014 supplement		
	Damage	Serviceability	Performance criteria	Damage	Serviceability	Performance criteria
10% in 50 years (T_r= 475 years)	None	Immediate	$\varepsilon_c \leq 0.004$ $\varepsilon_s \leq \varepsilon_y$	Minimal	Immediate	$\varepsilon_c \leq 0.006$ $\varepsilon_s \leq 0.01$
5% in 50 years (T_r= 975 years)	Minimal	Immediate	$\varepsilon_c \leq 0.004$ $\varepsilon_s \leq \varepsilon_y$	Minimal	Immediate	$\varepsilon_c \leq 0.006$ $\varepsilon_s \leq 0.01$
2% in 50 years (T_r= 2475 years)	Repairable	Limited	$\varepsilon_s \leq 0.015$	Repairable	Limited	$\varepsilon_s \leq 0.025$

Note: ε_c is the compressive concrete strain, ε_s is the strain in steel reinforcement, ε_y is the yielding strain of steel.

A seismic performance category is assigned to every bridge based on the fundamental period of the structure, bridge type and the site-specific spectral acceleration for the high-level seismic event with 2475 years return period. Lifeline bridges falls in the performance category two according to CHBDC 2014 (CSA, 2014) when $T< 0.5s$ and $S(0.2)< 0.20$ or $T\geq 0.5s$ and $S(1.0)< 0.10$ (here, T is the fundamental period of bridge structure, and $S(T_a)$ is the site-specific spectral acceleration for a particular period). In the recently published supplement to CHBDC 2014 (CHBDC, 2016), the performance category changed to one for the same criteria for a lifeline bridge where no analysis for seismic loads is required. For all other scenarios, the lifeline bridge includes in the performance category three. CHBDC 2014 recommends elastic dynamic analysis (EDA), inelastic static pushover analysis (*ISPA*) and non-linear time history analysis (*NLTHA*) for a regular lifeline bridge in the seismic events with 2% and 5% exceedance probability in 50 years. The new supplement to CHBDC 2014 (CHBDC, 2016) only requires the *EDA* and *ISPA* for regular lifeline bridges. The *ISPA* should account the non-linear response due to the formation of the plastic hinge in the ductile bridge elements and the soil-structure interaction (SSI), and P-delta effect need to be considered as applicable.

Roy et al. (2010) studied the retrofitting of a bridge bent using carbon fiber reinforced polymer (CFRP) following the performance-based approach. A one-third scale model of the bridge bent was experimentally tested to achieve certain limit states of the bridge with increasing intensity of loading. They concluded that the CHBDC 2010 performance criteria are very conservative and less economical. Zhang et al. (2016) investigated the effect on the design of bridge piers due to the changes in CHBDC code from force-based to PBD. A four span real-life reinforced concrete bridge with multiple column bridge bent was considered for the analysis. The major route bridge was designed following CHBDC 2006 (CSA, 2006) and CHBDC 2014 (CSA, 2014) specified FBD methods and the PBD method. The FBD method in CHBDC 2014 allows designing a major route bridge for 2475 years return period earthquake. However, before that, the design was restrained to earthquakes with 475 years return period. PBD permits design for all three levels of hazard. They found the longitudinal reinforcement requirement almost double in case PBD than that of FBD following CHBDC 2014 making the design overly conservative. Though the high reinforcement ratio limits the damage in the structure, it also causes problems in construction due to congestion. The performance limit states used in their study has now been changed in the new supplement to CHBDC 2014. Time history analyses were done to assess the performance of the bridge in terms

of strain limits. However, the study did not provide any specific solution to this issue related to high reinforcement ratio requirements. Also, how the dynamic response of bridges and their seismic vulnerability are affected by using different design alternative were not presented. Study on the design of lifeline bridges is limited in literature allowing space for possible research. The performance criteria requirements are also higher and more conservative in lifeline bridges than major route bridges considering their importance. It is important to understand the design evolution of lifeline bridge in CHBDC from FBD to PBD and their dynamic response to facilitate decision making analyzing all the design alternatives. The strength of steel can contribute greatly in design by reducing congestion. Moreover, employing different strength reinforcing bars in the design will satisfy the material strain criteria in different stages. Ductility of steel is also an important concern during the dynamic action to predict the probable performance of the structure. Copious amount of inspection is required to understand the effect and contribution of reinforcing steel strength in PBD. This particular study focuses on the design evolution in CHBDC for a lifeline bridge and impact of reinforcing steel properties on PBD following the supplement to CHBDC 2014 guidelines through extensive dynamic analysis.

2.1.8 Fragility

PBD technique ensures predefined performance during seismic motions, unlike the conventional design method. The uncertainties in the hazard and structural responses are counted in the probabilistic method in PBD. With the advancement in PBD, the seismic performance assessment of structure is gaining attention from both the academic and professionals. Fragility plots are a very popular seismic assessment tool that presents a conditional probability of demand exceeding the capacity of a structural component for a given intensity measure (Karamlou and Bocchini, 2015). The conditional probability is presented in Equation 2.3.

$$Fragility = P[LS|IM = y] \qquad (2.3)$$

Here, *LS* is the limit state of the structural component and *IM* is the intensity measure of ground motion. For a specific ground motion intensity, fragility plot presents the probability of particular damage that can happen to the structure. A typical fragility function is shown in Figure 2.5. There are a number of approaches available to define the fragility function of a structure. Earlier, most of the fragility analysis were based on site survey and opinions from experienced

panel members. The evolution of fragility analysis from expert-based to analytical are discussed elaborately in Billah and Alam (2015a). Among all, the non-linear time history analysis method in the analytical approach of generating fragility is the most popular one. Probabilistic resilience, life cycle cost and expected loss related to reconstruction and damage repairing cost can be predicted from fragility analysis of structural components and structures. To execute the loss assessment of a structure at a specific region, predicting the seismic vulnerability is the most important prerequisite (Zelaschi et al., 2015).

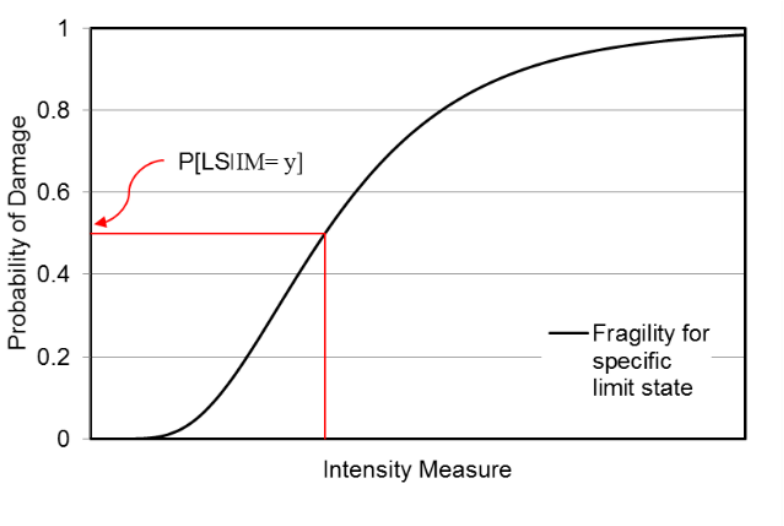

Figure 2.5 Typical fragility plot

2.1.9 Incremental Dynamic Analysis (IDA) approach of generating fragility

The incremental dynamic analysis method is a very attractive method of generating fragility curves when sufficient ground motion data are not available to execute the non-linear time history analysis (*NLTHA*) of the structure. The *NLTHA* requires a high number of numerical investigations but considered the most reliable method of developing fragilities by researchers (Shinozuka et al., 2000). In this *NLTHA* method, the site-specific ground motion suits are selected firstly. The analytical models of the study structures are prepared considering material and geometric uncertainties. The ground motions are applied to the structural models to run *NLTHA*. Maximum responses based on the engineering demand parameters (*EDPs*) are taken from the analyses results, and probabilistic seismic demand models (*PSDMs*) are generated through regression analysis. Limit states are defined from expert opinions, experimental investigations or

by analytically. Demand and capacity models are combined to plot the fragility considering lognormal distribution. The methodology is graphically presented in Figure 2.6 with corresponding equations. It is a very effective analytical method and extensively used by academics (Choi, 2002; Nielson, 2005; Padget, 2007; Tavares et al., 2012; Billah and Alam, 2014c). *IDA* is simply a combination of *NLTHA* where the ground motions are scaled to cover a range of ground motion intensity levels to apprehend the dynamic response of the structure with a limited number of seismic motions available. Due to the reliability of this method, many researchers have accepted *IDA* method in plotting fragilities of bridges (Zhang and Huo, 2009; Huo and Zhang, 2013; Billah and Alam, 2014c; Baker, 2015; Billah and Alam, 2016a).

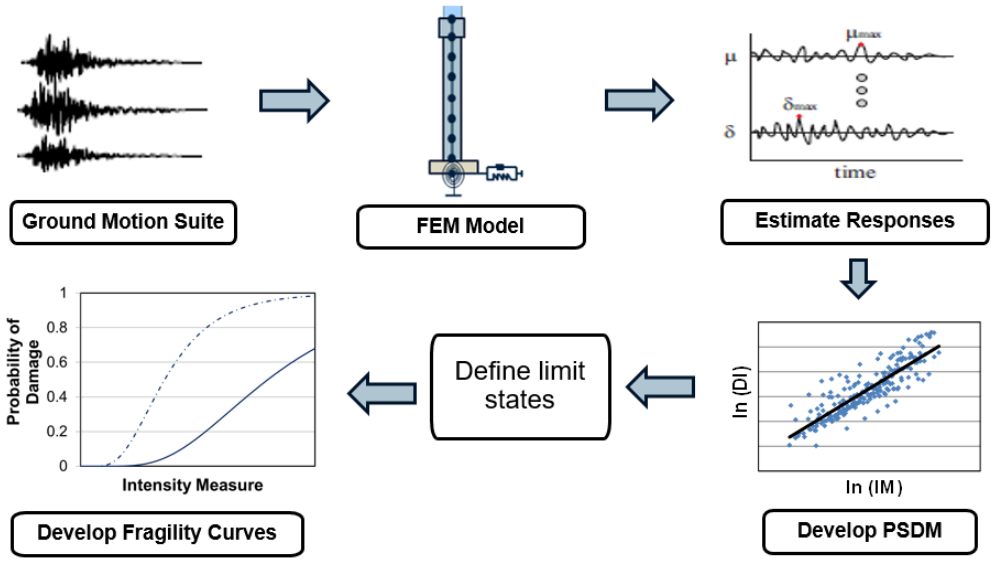

Figure 2.6 Generation of fragility plot following *NLTHA*

2.2 High Strength Steel

The very first reinforced concrete structure was built in 1884. From 1911 to 1966, Grade 33, Grade 40 and Grade 50 steels were in action to reinforce concrete structures. First high strength steel was experimentally tested for bridges in the USA in early 60's (Hognestad et al., 1960). Most common reinforcing steel used in USA and Canada is the Grade 60 steel conforming to American Society for Testing and Materials (ASTM), ASTM A615/A615 M. In the past 100 years, steel strength had enormous improvement that resulted in the present very high strength steel, ASTM A1035 with Grade 100 and Grade 120 (ASTM, 2007). ASTM included the Grade 80 in ASTM615 in 2009 (ASTM, 2009) and later in 2004, Grade 100, and in 2007 Grade 120 were added to ASTM A1035. Table 2.4 presents some common types of reinforcements used in construction industry. Advancement in high strength concrete and high-performance concrete demands an increased strength in steel reinforcement with the potential to reduce structural member size and cost of gigantic constructions notably without compromising the overall performance. Concrete strength as high as 100 MPa known as Ultra High-Performance Concrete requires a large quantity of Grade 40 or Grade 60 steel confinement resulting in congestion and troublesome construction. On the other hand, lower concrete strength needs a higher number of longitudinal reinforcements to satisfy the design when lower grade steels are used leading towards the same difficulty. Steel grade of 100 is newly acquainted into ASTM A615 standard. American Concrete Institute (ACI 318-14, 2014) and American Association of State Highway and Transportation Officials (AASHTO, 2014) now allow the use of 100 ksi steel in specified construction and 75 ksi and 80 ksi to other constructions. CHBDC permits using reinforcing bars of yield strength between 300 and 500 MPa (CSA, 2014), which is more conservative than the American Association of State Highway and Transportation Officials (AASHTO) and the American Concrete Institute (ACI) specifications. CHBDC 2014 recommends that all the reinforcing steel bar should conform requirements of Canadian Standard Association, CSA G30.18.

Table 2.4 Available reinforcing steel

Designation	Type of reinforcement	Scope
A 615	Carbon steel	Deformed and plain carbon steel for concrete reinforcements in cut length and coils
A 706	Weldable steel	Low alloy deformed and plain steel bars with restrictive mechanical properties and chemical composition to control the tensile strength and improved weldability.
A 767	Galvanized steel	Reinforcing steel coated with protective zinc
A 934	Epoxy coated steel	Epoxy coated prefabricated steel reinforcing bars
A 1055	Zinc and Polymer membrane steel	Dual coated reinforcing steel that provides galvanic cathodic protection and ensures anode to steel continuity during the construction process
A 955	Stainless steel	Corrosion resistant deformed and plain stainless steel with controlled magnetic permeability for concrete reinforcement
A 1035	Low carbon chromium steel	Low and high corrosion resistive low-carbon, chromium steel bars for concrete reinforcement

2.2.1 Limitation on HSR

The permissible concrete strain of 0.003 and to control crack width under service loads are the main reasons behind limiting the yield strength of steel in designing RC members. Steel strain coupled with steel stress controls the crack width (Nawy, 1968). It is important to limit yield strength of steel to some extent to prevent cracking and maintain aesthetics of structures. Also, the maximum stress of 87ksi is usable to produce 0.003 strain considering linear elastic behavior. Recent developments in concrete strength and properties allow higher limiting strain than 0.003, making the ACI 318 and AASHTO limit for steel strength (80ksi and 75ksi) needlessly conservative (Russell et al., 2011). A recent study from Salomon and Moen (2014) found that the deformability of A1035 steel is in agreement to AASHTO (AASHTO, 2015) requirement with 36% less steel.

2.2.2 Ductility of steel reinforcement

The total strain at the point of rupture defines the elongation at fracture. It is an important measure of ductility. Another parameter to express ductility is the strain hardening of steel. The ratio of the tensile stress and the yield stress describes the strain hardening, which allows RC member to deflect more. Elongation at the maximum stress level is also gaining popularity as a ductility measure recently (Firoze, 2010; ATC, 2014). Other criteria to measure ductility are the bend and re-bend test of reinforcement where the outer surface and inner surface experience tension and compression respectively. If the bend diameter is lower than specified, there is a possibility of rib split up even without fracture of steel. Even though a steel reinforcement satisfies the tensile and yield strength test, it might fail in the bend or re-bend tests to disclose any manufacturing defect or brittleness of the material. It is better not to bent HSR unless otherwise specified cause simple crack on steel surface may lead to corrosion. With the increase in yield strength in HSR, tensile to yield strength and uniform elongation reduces (ATC, 2014). Most of the cases with higher grades like 100ksi and 120ksi steel, the yield plateau completely vanishes. As defended by Federal Emergency Management Agency (FEMA), the ductility of a RC structure can be improved by providing low flexural reinforcement, adding confinement and compression reinforcement. Designing reinforcement for gravity loads only required adequate yield strength without much concern on the elongation of steel. Whereas, the seismic design requires special attention to the elongation percentage and tensile to yielding stress ratio of steel rebars (ATC, 2014).

Typical stress-strain curves for lower and higher grade steel grades are shown in Figure 2.7. Lower grade reinforcement shows an elastic region followed by a yield plateau and a strain hardening segment. Whereas, the HSR displays gradual loss in stiffness after an elastic part. 0.2% offset method is used to define the yield point, and a ‘roundhouse’ curve leads to the tensile strength (ATC, 2014).

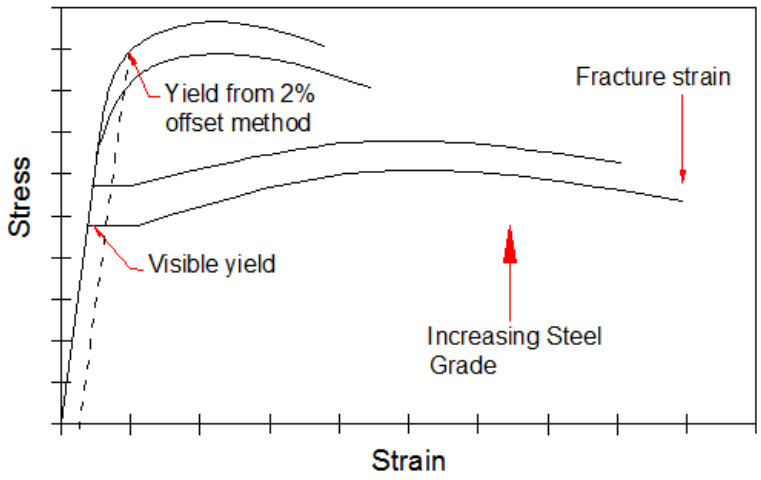

Figure 2.7 Typical stress-strain curve for different grade steel

2.2.3 Manufacturing process of HSR

The Quench and Temper technology is adopted to manufacture high-strength steel meeting highest quality standard in terms of strength, ductility, weldability, and durability. This process depends on temperature and time and causes a softer inner core compared to a hard outer shell at the end of the process. Water spray quenching of hot rolled steel bars is done under precise pressure and controlled design of nozzles. The outer surface layer becomes martensitic whereas the inner core remains austenitic causing a self-tempering process that helps in increasing yield strength of steel. At the end stage, soft austenitic core transforms to the ductile ferrite-pearlier core on the cooling bed. This process improves the ductility and fatigue property of steel and allows gradual yielding from core to surface with round shape in the stress-strain curve. Micro-alloying is also done to get desirable steel properties by certain alloy to the molten steel for grain refinement (ATC, 2014). The addition of vanadium and manganese helps in attaining higher yield strength. The final treatment process of steel manufacturing is summarized in Figure 2.8.

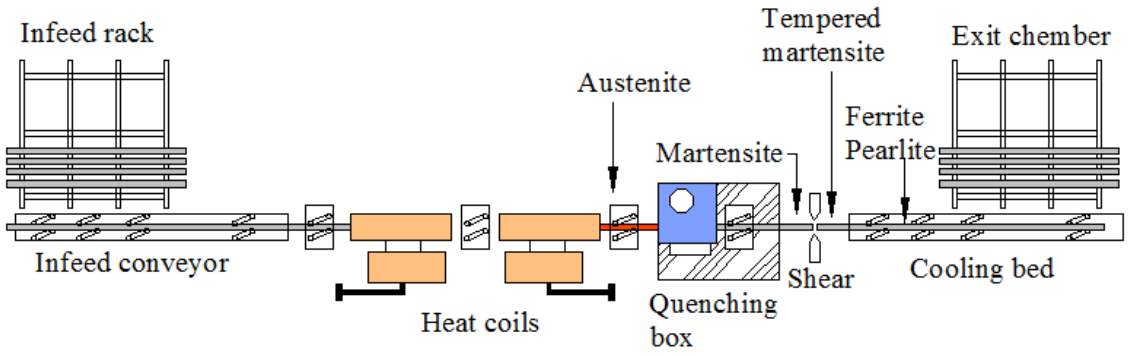

Figure 2.8 Final treatment process in manufacturing high strength steel

2.2.4 ASTM A1035

ASTM A1035 reinforcing bars have exceptional corrosion resistance capacity like stainless steel due to the high chromium content (up to 9%), which makes it a strong contender in RC structure construction as an alternative to stainless steel and epoxy coated bars (Russell et al., 2011). The stress-strain plot of A1035 does not show any yield plateau. 2% offset method is used to find out the yield strength, which is no less than 100ksi. Grade 100 (f_{ymin}= 100ksi) and Grade 120 (f_{ymin}= 120ksi) are currently producing in the market. However, some codes do not allow more than Grade 75 (AASHTO) and Grade 80 (ACI 318) in designing longitudinal rebars and Grade 100 in transverse reinforcement limiting the application of A1035 steel. The benefit of this high yield strength is left unutilized in those cases. El-Hacha and Rizkalla (2002) concluded that the A1035 has similar tensile and compressive yield with a Poisson ratio of 0.26. 0.2% offset method is most commonly used to determine the yield point by the researchers (DeJong, 2005; DeJong and MacDougal, 2006; Russell et al., 2011; Mast et al., 2008; Paulson et al., 2013). To specify the elongation in steel, NIST (2014) recommended using the uniform elongation at peak stress rather than total elongation. “Best-fit” model is proposed in some literature to model the behavior of HSR (Vijay et al., 2002; Rizkalla et al., 2005; Mast et al., 2008). Modulus of elasticity is reported 29,000ksi with a proportional limit of at least 70ksi (Mast et al., 2008). DeJong (2005) and DeJong and MacDougal (2006) conducted the fatigue test of high strength A1035 steel using #3, #4 and #5 bars for 1 million cycles and concluded the fatigue strength 45ksi, which was 87.5% higher than Grade 60 rebars. El-Hacha and Rizkalla (2002) published similar findings in their work. The yield and tensile strength of A1035 steel are nearly twice of typical Grade 60 rebars, but the ductility limit depends largely on material compositions. Important measures of ASTM A615 and

ASTM A1035 rebars are summarized in Table 2.5. Minimum elongation percentage at fracture are specified over an 8-inch gauge length. Promising HSR, ASTM A1035 steel, licensed under MMFX technologies has three major series: 2000, 4000 and 9000. The costliest and highest corrosion resistant is being the 9000 series has around 9% chromium content whereas the 2000 series has only 3% chromium content, which can be used where corrosion probability is low. However, all the series ensures minimum yield strength of 100 ksi.

Table 2.5 Measures of ASTM A615 and ASTM A1035 steel rebars

	ASTM A615			ASTM A1035	
	Grade 60	Grade 75	Grade 80	Grade 100	Grade 120
Minimum yield stress, ksi (MPa)	60 (420)	75 (520)	80 (555)	100 (690)	120 (830)
Minimum tensile stress, ksi (MPa)	90 (620)	100 (690)	105 (725)	150 (1035)	150 (1035)
Bar designation	Minimum percent elongation in 8” gauge length				
#3	9	-	-	7	7
#4 and #5	9	-	-	7	7
#6	9	7	7	7	7
#7 and #8	8	7	7	7	7
#9, #10 and #11	7	6	6	7	7
#14 and #18	7	6	6	6	6

Vijay et al. (2002) proposed the following equations (Equation 2.4 and 2.5) to calculate the strain-strain of ASTM A1035 steel #4 and #5 rebars (where σ is tensile stress, and ε is strain percentage). However, they demanded more research for the refined equations.

Bar #4: $\sigma = 1131.084\ [1- e^{-182.058\varepsilon}]$ (2.4)

Bar #5: $\sigma = 1192.662\ [1- e^{-168\varepsilon}]$ (2.5)

Yotakhong (2003) provided the formulation to determine #6 ASTM A1035 bar stress-strain behavior as follows.

Bar #6: $\sigma = 1220.238\ [1- e^{-185\varepsilon}]$ (2.6)

Later on, Moran and Lubell (2008) experimented application of HSR for deep beams and found polynomial equations for ASTM A1035 #4, #6 and #7 rebars.

El-Hacha and Rizkalla (2002) tested the #4, #6 and #8 rebars from ASTM A1035 and found the elastic modulus 200 GPa. The same experiment displayed the average shear strength of ASTM A1035 rebars 762 MPa. El-Hacha et al. (2006) further investigated on four beam specimens reinforced with ASTM A1035 rebars to find out the bond performance and splice length of HSR. They demonstrated the conservative estimation of boned length in ACI 318-02 and proposed the following Equation 2.7 to find the splice length required for ASTM A1035 steel rebars.

$$l_d = \frac{\frac{f_y}{\sqrt{f'_c}} - 51}{\frac{4}{9}\left(\frac{c'_{\min} + 0.5d_b + k_{tr}}{d_b}\right)}\, d_b \qquad (2.7)$$

Here,

$$k_{tr} = \frac{A_{tr} f_{yt}}{556sn} \qquad (2.8)$$

C_{si}= ½ clear spacing between splice rebars

C_b= bottom concrete clear cover

C_{so}= concrete side clear cover

D_b= nominal bar diameter

c'_{min}= minimum of C_{si} and C_b or C_{so}

2.2.4.1 Chemical composition

Excessive carbon content reduces the weldability capacity of reinforcement. During welding, the temperature rises to a level more than temper temperature. If the quenching and tempering process were not controlled properly, this high temperature during welding could lead

to lower yield strength of steel rebar. Chromium content plays an important role in resisting corrosion. ASTM A1035 reinforcing steel has a unique chemical composition that makes it suitable for the adverse environment and ensures sufficient strength (Faza et al., 2008). Chemical constituents of ASTM A1035 reinforcing steels of different series are presented in Table 2.6 as per ASTM (2007) and AASHTO (2015).

Table 2.6 Chemical composition of ASTM A1035 reinforcing bars

Element (%)	ASTM A1035		
	Series 9000	Series 4000	Series 2000
Carbon	0.15	0.20	0.30
Chromium	8-10.9	4-7.9	2-3.9
Manganese	1.5	1.5	1.5
Nitrogen	0.05	0.05	0.05
Phosphorus	0.035	0.035	0.035
Sulfur	0.045	0.045	0.045
Silicon	0.50	0.50	0.50

2.2.4.2 Previous studies on ASTM A1035

HSR can be used with regular strength concrete. For pure compression members like short columns, it is advantageous to use HSR along with high strength concrete. HSR have huge potential to be used in industrial, commercial, residential and transportation projects. Construction productivity can be increased by using HSR in several parts of construction phases. Research on HSR like ASTM A1035 is facing advancement due to its prospect in the construction industry.

2.2.4.3 Flexure reinforcement

A RC member should display large deformation and adequate cracking at ultimate load to provide ample warning before complete failure. At service loading condition, the deformation should be small with minimal cracking. Steel strain and stress are the deciding factors in calculating the deflection and cracking. For lower strength steel, only yielding in tension steel ensures the high strain whereas, for HSR, yielding is not mandatory (Mast et al., 2008). Through

extensive studies on the beams subjected to axial and flexural loading, Mast et al. (2008) proposed the suitability of ASTM A1035 reinforcement in tension and compression controlled RC members. They used the concrete compressive strength 6.5ksi and ultimate strain at compression 0.003. The steel was Grade 100 (f_y = 100 ksi) with a modulus of elasticity 29,000ksi. The elastic-plastic stress-strain model was considered. They concluded that for a section with balance reinforcement less than 1.75%, an elastic-plastic model of 100ksi steel underestimated the nominal moment capacity and between 1.75% and 2.7% it overestimated marginally (only 2.5%). Tension controlled strain limit of 0.0066 for 100ksi HSR showed similar ductility as Grade 60 reinforcement for a simple beam. Also, the crack widths under service load were very close to the acceptable limit. Recent research from NIST (2014) suggested that reduced amount of HSR member in place of Grade 60 steel reinforced member subjected to cyclic loading demonstrates equivalent deformation capacity and flexural strength. Mast et al. (2008) suggested limiting reinforcement yield strength to 80ksi to match concrete strain 0.003 in the compression face to avoid compression failure. Experimental studies from Seliem et al. (2006), McNally (2003), Malhas (2002), Vijay et al. (2002) and Florida DOT (2002) supported the conclusions from Mast et al. (2008) to apply A1035 steel as flexural reinforcement. McNally (2003) found reduced ductility of structure for A1035 steel whereas Seliem et al. (2006) and Florida DOT (2002) concluded increased ductility resulting from lower reinforcement ratio due to the high yield strength of A1035 steel. Russell et al. (2011) demonstrated that the present limit for fatigue in AASHTO LRFD applies to A1035 steel. Full-scale experiment on deep beam was carried out by Moran and Lubell (2008) using high strength steel as reinforcement. Strut and Tie model was employed to find out the capacity of deep beams, which were in good agreement with the CSA A23.3-04, ACI 318-05 and Eurocode 2 provided equations. Salomon and Moen (2014) tested one to one replacement of Grade 60 rebars with ASTM A1035 steel and found 70% higher flexure capacity. Reducing the rebar size resulted in 15% higher capacity. Crack width reduced almost 50% after reducing the clear cover when A1035 was used. It also helped in ductility improvement and gaining flexural rigidity in the section.

2.2.4.4 Shear reinforcement

High stress in steel may result in cracks in concrete and reduce the concrete contribution in carrying the shear (Brown et al., 2006; Lubell et al., 2004; Tureyen and Frosch, 2003). Reduced longitudinal reinforcement reduces the compression zone depth, which is the primary shear

carrying region (ATC, 2014). Some studies have been performed on the viability of the use of high strength steel as shear reinforcement (Budek et al., 2002; Munikrishna, 2008; Ou et al., 2012). National Cooperative Highway Research Program (NCHRP) research project indicated the feasibility of the use of higher grade steel as shear reinforcement and found a minor difference in concrete crack width with Grade 60 and Grade 100 rebars (Shahrooz et al., 2011). Sumpter (2007) examined the feasibility of HSR application as shear reinforcement in concrete members. The beam tested by Sumpter (2007) had shear span to depth ratio of 3 and both ASTM A615, and A1035 steel were employed as longitudinal and transverse reinforcement. He tried to maintain very high stress in steel through overloading and found an ignorable difference in the specimens at service loading. Specimens reinforced with A1035 shear steel showed marginally higher capacity than that of A615 steel. Concrete dominated the shear behavior, and the stress in shear reinforcements never exceeded 80ksi. Thus the high strength of A1035 steel was not fully utilized. Florida DOT (2002) concluded similar findings on the generated stress in shear reinforcements. Test result from five RC beam and four prestressed girders by Russell et al. (2011) found the current AASHTO LRFD specification allowable for A1035 steel of Grade 100. NIST (2014) concluded that the spacing for high strength transverse reinforcement should be reduced to $5d_b$ and $4d_b$ for Grade 80, and Grade 100 and Grade 120 longitudinal reinforcements respectively.

2.2.4.5 Compression member

Increasing the strength of transverse reinforcement provides better control on longitudinal bar buckling than regular strength steel confinement (Muguruma et al., 1991). Cusson and Paultre (1994) concluded improved ductility and strength under high strength confinement. Nagashima et al. (1992), Razvi and Saatcioglu (1994), and Nishiyama et al. (1993) had identical conclusions. Study on HSR also provided improved behavior in axial column reinforced with A1035 transverse steels (El-Hacha and Rizkalla, 2002; Stephan et al., 2003; Restrepo et al., 2006). Analytical results from Russell et al. (2011) indicate that for a compression member, AASHTO LRFD design specifications are applicable for A1035 steel for both longitudinal and transverse reinforcement design.

2.2.4.6 Development length

There have been extensive studies done in last 25 years on the development length of reinforcement in normal and high strength concrete. Azizinamini et al. (1993), Azizinamini et al. (1995), Hamad and Itani (1998), Harajli (2004) and Holschemacher et al. (2005) studied the bond behavior of steel in concrete whereas Esfahani and Kianoush (2005) and Firas et al. (2011) experimented the bond development of fiber reinforced polymer (FRP) in concrete. High strength concrete displays very strong bond strength due to its high compressive strength and elastic modulus (Holschemacher et al., 2005; Azizinamini et al., 1993). The inclusion of steel fibers in high-performance concrete reduces the crack width and increases the bond resistance leading to more ductile failure. (Harajli et al., 2002; Chao et al., 2009). To develop high bar stress in HSR, longer development length is expected. Saleem et al. (2013) investigated the development length of ASTM A1035 HSR from MMFX Technologies of Irvine, California embedded in ultra-high performance concrete from pullout and beam tests. Two sizes of high strength rebars, #10 and #22 of 690 MPa yield strength were used in predicting their bond strength. Saleem et al. (2013) found the development length $12d_b$ and $18d_b$ for #10 and #22 rebars correspondingly from beam test. They also concluded that the equation provided by ACI 408R-03 can reasonably predict the development length for HSR. However, it was observed that pullout test was effective only in case of small diameter HSR. Some studies revealed that the load-slip relationship of A1035 steel with concrete is pretty similar to A615 steel (Ahlborn and DenHartigh, 2002; El-Hacha et al., 2006) and some suggested improved performance due to the rib configuration in A1035 steel (Sumpter, 2007; Zeno, 2009). Peterfreund (2003) studied A1035 steel in bridge deck and found the ACI 318 requirement adequate without the presence of confining reinforcement. However, Seliem et al. (2009) found that ACI 318 underestimates the development requirement with no confinement and ACI 408 described the requirement adequately and suggested to use confinement in developing HSR. #5 and #7 steel rebars without any confining reinforcement were tested by Ciancone et al. (2008) to determine the hook behavior of A1035 steel. Lower bar size developed the yield capacity whereas the higher one could not. It is suggested to use confinement and adequate cover for A1035 steel development (Ciancone et al., 2008; Russell et al., 2011). A more detailed investigation was carried out by Sperry et al. (2015) to determine the important factors affecting the anchorage length of hooked bars in concrete for high strength steel application. 337 beam-column joint specimens were tested on varying hook number, concrete compressive strength and cover, hook angle and

spacing, embedded length, hook position and bar diameter. Maximum stress of the hooked bar and concrete were 141 ksi and 16.5 ksi respectively. They found that the ACI 318-14 overestimates the strength of larger hook bar, the contribution from concrete and transverse confinement. Hooked bar angle and concrete cover did not affect anchorage length. Increasing bar diameter and far casting from column core increase the anchorage capacity. Hassan et al. (2012) investigated the splice length of large diameter high strength steel (yield strength ranged from 730-750 MPa) rebars from 20 full-scale RC beam test. Their study revealed ACI 318 provision for bond and development could extend to #20 bars with 25% increase to account for safety. Also, transverse reinforcement ratio is a crucial parameter for splice strength of large diameter HSR.

2.2.4.7 Ductility

Bridge decks reinforced with HSR can produce AASHTO, and ACI provided ductility at ultimate loading with an added benefit against corrosion (Salomon and Moen, 2014). Most of the ASTM A615 Grade 60 rebars have tensile to yield strength ratio of 1.5 (Bournonville et al., 2004). Though ASTM does not provide any minimum requirement for this, it is expected that the HSR will have similar ratio to ensure ductile failure of RC members with prior warning. CHBDC 2014 specifies the minimum elongation at rupture in a 200 mm gauge length should be 12% for 25M bars and smaller and 10% for 30M bars and larger (CSA, 2014). However, these limitations are for maximum steel strength of 500 MPa.

2.2.4.8 Corrosion performance

High corrosion resistance capacity of A1035 steel has make it an appealing choice in present construction industry along with other ASTM rebars like A955 (Ji et al., 2005). Though the chromium content in A1035 steel (up to 9%) is less than stainless steel (greater than 10.5%), it is sufficient to impart a reasonable degree of protection against corrosion than A615 or A706 steels. The microcomposite Fe-C-Cr- Mn alloy are 2-10 times more effective in resisting corrosion than black steel (A615 or A706). Relative performances of different grade steels in terms of corrosion resistance are shown in Table 2.7 from Russell et al. (2011).

Table 2.7 Corrosion performance of different steel grades (Russell et al., 2011)

Steel Grade	Material	Relative performance to A615 steel
A615	Black steel	1
A706	Black steel	0.5-0.8
A955 2101	Duplex stainless steel	2-10
A955 304	Austenitic stainless steel	>10
A955 316	Austenitic stainless steel	>20
A1035	Microcomposite alloy	2-10

2.2.4.9 Application in bridge

Most of the applications of ASTM A1035 steel are limited to bridge deck as "one-to-one" replacement of regular steel to fight corrosion (Russell et al., 2011; Salomon and Moen, 2014). Bridge decks are designed on serviceability criteria, and it is expected that the Grade 60 and the HSR like A1035 will behave similarly (Rizkalla et al., 2005; Hill et al., 2003). Currently, MMFX Inc. is the lone supplier of A1035 steel. Russel at al. (2011) listed seventeen projects where more than 60ksi steel were employed. Most of them were 75ksi (maximum limit in AASHTO) steel that indicates the gaining popularity of HSR in bridge design and construction in recent years. Salomon and Moen (2014) investigated the flexural performance of corrosion resistive A1035 steel in reduced bar size and clear cover replacing Grade 60 rebars in one and two layers in one way slab over a bridge girder and found higher capacity even with 36% less steel. Fatigue resistance is an important concern especially in bridge construction rather than buildings. For HSR like Grade 100 and Grade 120, it is recommended to test for fatigue (ATC, 2014). Also, lower reinforcement ratio for HSR will reduce the flexural stiffness that will affect the drift demand in bridge pier. Ziehl et al. (1998; 2004) suggested to maintain minimum longitudinal reinforcement requirement even for HSR to avoid problems related to passive yielding and the cost cutback is not very significant when less than 1% longitudinal rebars are provided.

2.2.5 Prospect of HSR

HSR show gradual yielding without sudden loss of stiffness, unlike mild steel. Elastic-plastic assumption yields to a conservative prediction of flexural strength capacity for HSR.

Growing interest in high strength A1035 reinforcements started in 2002 with the commercial production to fight corrosion (Malhas, 2002). Previous studies showed the feasibility of A1035 steel application both in buildings and bridge decks (Yotakhong, 2003; Seliem et al., 2008). Previously Malhas (2002) showed the possibility of compression zone failure in beams with one to one replacement of A1035 steel that triggered the motivation to work on strain limit to ensure the ductile failure of HSR (Mast et al., 2008; Shahrooz et al., 2010).

The report prepared by Russell et al. (2011) evaluated the bridge design specifications provided by AASHTO LRFD to use high strength reinforcing steel with no well-defined yield plateau for concrete strength up to 10ksi and 15ksi in some cases. According to them, no major change is required in AASHTO LRFD bridge design code considering maximum steel yield strength of 100ksi. To ensure ductility, they recommended strain limit in steel in A1035 Grade 100 rebars minimum 0.008 and maximum 0.004 for tension and compression controlled sections respectively.

Paultre et al. (2001) studied the potential and effect of high strength steel as transverse reinforcement in combination with high strength concrete. The column concrete strength varied between 80 and 120 MPa and the tie strengths were 400MPa and 800MPa with varying spacing. They found a negative impact of high strength concrete on the displacement ductility and energy dissipation capacity of the column. On the contrary, HSR as transverse ties in the column provided similar ductility with reduced confining steel. However, they also concluded that the HSR may not always be effective for every column configuration.

The project of Applied Technology Council (ATC, 2014) worked on the Building Code Requirements for Structural Concrete and Commentary (ACI, 2014) to find out whether any update requires in ACI 318-14 to use Grade 80, Grade 100 and Grade 120 reinforcements to design for seismic, wind and gravity loads. The nuclear industry has a special interest in using high strength reinforcement for speedy construction, and reduced congestion as the lower elongation associated with HSR are not a concern due to very small non-linear deformation demand of the components. Bridge industry is also showing interest in HSR to pursue the goal (ATC, 2014).

2.2.6 Cost and current applications

The cost of ASTM A1035 series 4100 is almost equal to that of ASTM A615 epoxy coated steel (Tadros, 2017). For a constant member section, replacement of Grade 60 reinforcement with HSR can be done by using same size bars with higher spacing or by providing smaller size bar at the same spacing. Larger spacing reduces the congestion and allows easier consolidation of concrete, but it is difficult to bend higher size HSR. On the other hand, smaller diameter HSR reduces the cost by decreasing overall reinforcement volume and cost, easy to bend and easy to construct (ATC, 2014). Replacing Grade 60 reinforcement with Grade 80 rebars reduces 4% overall cost of concrete structure (NIST, 2014). Price et al. (2014) concluded that if the ACI 318 limit on steel yield stress was avoided, HSR could substantially reduce the reinforcement requirement with a speedy construction. At present, the Abu Dhabi International Airport Departure Bridge and the Lesner Bridge in Virginia Beach, Virginia are utilizing ASTM A1035- CS alloy reinforcement.

2.2.7 Benefits of HSR

- HSR has the potential to reduce steel reinforcement requirement up to 50% compared to regular Grade 60 steel. Fewer bars needed and the spacing increases allowing more space for concrete placement and easy compaction. Bar diameter can also be reduced.
- Concrete volume can be saved by reducing structural member size with appropriate selection of steel grade resulting in reduced dead load. Usable floor space increases due to reduced column sizes.
- Formwork required for the structural members will be less with light cage weights. Site storage space requirement will reduce as well.
- Steel fabrication will require less labor work. Less material handling will improve the site safety.
- The cost in logistic supports will be less. Carrier costing will reduce to carry less number of reinforcements through trucks. Jobsite storage, logistics, and transit will improve.
- With reduced reinforcements, fewer workers are required to install steel rebars onsite. Also, it will free up the crane time leading to a speedy construction.
- The size of the foundation can be optimized with reduced member sections and loads.

- Most importantly, overall construction cost can be minimized with reduction of construction time.

2.2.8 High strength steel design consideration and limitations

- HSR does not show well-defined yield plateau (Seliem et al., 2009) and plastic elongation like Grade 60. This affects the flexural behavior of structural elements such as beam and columns significantly due to low ductility.
- As the flexural reinforcement reduces due to HSR, concrete compressive strength should be high enough to maintain the neutral axis position in compression zone of the section to have the complete benefit of HSR with tension controlled behavior.
- If the concrete member section size is reduced to utilize the benefit of high strength of steel, congestion in the member will be similar to that of Grade 60 steel. Moreover, additional transverse rebars have to be provided to control longitudinal bar buckling (ATC, 2014).
- Minimum reinforcement requirement should be checked with design codes to avoid abrupt tension induced failure.
- HSR are not effective in reducing the concrete crack width and member deflection capacity for improved serviceability when provided in lower numbers (Shiro and Hitoshi, 1996).
- Due to the higher yield strength of HSR, larger development requires, which is not practical for larger diameter bars.
- A limited number of experimental investigations on the performance of HSR concrete members to establish proper design method.
- At a very high temperature (5370 Celsius), the relative reduction in yield and tensile strength of HSR are similar to conventional rebars (Aoyama, 2001).
- Designers should be extra cautious to avoid mix up in steel grades to avoid unnecessary hindrance in construction.

2.3 Summary

Numerous studies from previous research show the growing interest of PBD in structural engineering. Considering the importance of bridges, enormity and investment in bridge project, PBD approach is desirable to ensure life safety and reduce loss due to damage after a seismic event. The performance criteria in CHBDC transformed to more precise quantitative form in 2014

from descriptive statements. However, noticeable changes in the performance limits occurred in the supplement to CHBDC 2014. It is essential for the engineers to understand how the changes in code affect the dynamic performance of the bridge piers to decide on the proper design method.

For improved constructability and to lessen reinforcement congestion for better concrete consolidation, high strength steel has no alternative. Moreover, superior corrosion resistance capacity has made ASTM A1035 steel a very attractive choice for bridge deck applications. The scope should not be limited and must be extended to the application in bridge pier, which is considered the most critical element of a bridge structure. Prior dynamic analysis of RC bridge pier reinforced with high yield strength steels with reasonable ductility needs to be investigated before field applications.

With the advancement in PBD, strength criteria of material properties are getting attention to satisfy the required performance limit for design. Criteria set by CHBDC 2014 is highly conservative. Minimal damage is allowed for a lifeline bridge even at an event of 975 years return period. To reduce reinforcement percentage without compromising the performance can be achieved by using high strength steel.

Chapter 3 : SEISMIC PERFORMANCE COMPARISONS OF FORCE-BASED AND PERFORMANCE-BASED DESIGNED BRIDGE PIER

3.1 Background

PBD has been developed by the researchers to overcome the deficiency associated with FBD, especially for reinforced concrete structures rather than steel structures since steel behavior is more predictable than reinforced concrete. PBD is a powerful approach that allows the engineers to design the bridges to have a predictable and dependable behavior during seismic events. After the first introduction of PBD concept back in the 1980s (Hamburger et al., 2004), most of the applications were confined to design of buildings (SEAOC, 1995; ATC, 1996; FEMA, 1996). However, bridges have got the attention due to their importance in the transportation network and seismic vulnerability during earthquakes. Plentiful studies have been done since the commencement of 21st century on the improvement of PBD of bridges using deferent materials (Priestley, 2000; Mackie and Stojadinović, 2007; Marsh and Stringer, 2013; Billah and Alam, 2016a). CHBDC first adopted the PBD in 2014 (CSA, 2014). Though some performance goals were specified in CHBDC 2006 (CSA, 2006), the traditional design method could not satisfy the criteria automatically (Sheikh and Légeron, 2014). CHBDC 2014 allows designing a bridge using both force-based and PBD depending on the type of bridge (CSA, 2014). For a lifeline bridge, PBD is compulsory in CHBDC 2014.

Designing bridges based on performance goal are not a novel technique, rather it includes the conventional method of seismic design with necessary advancement (Ghobarah, 2001). A few bridge projects are already in action in Canada like the Port Mann Bridge, Vancouver (Jones et al., 2013) and the Vancouver Evergreen Line Rapid Transit Project (Khan and Jiang, 2015). Bridges designed with conventional force-based approach prevents loss of life, but the loss associated with the damage and repairing cost can be substantial. Improper design choice and lack of performance awareness may lead to an inaccurate decision and cost a great deal of money. It is necessary to design bridges against different hazard level considering the performance objectives to limit the economic losses. This study will present comparative performance of bridge piers designed following force-based and performance-based methods that will aid the engineers in decision making with a clear vision of improvement in current CHBDC design practice.

3.2 Validation of model

A finite element program SeismoStruct (SeismoStruct, 2015) is employed in modeling the bridge piers. The program had been used by researchers to model bridges and bridge components very efficiently (Alam et al., 2008; Billah and Alam, 2015b; Kabir et al., 2015; Fakharifar et al., 2015a). However, to verify the efficacy of the program, a steel reinforced square column from Correia et al. (2008) and a high strength steel reinforced circular bridge column from Restrepo et al. (2006) are selected. Comparison between two frame element formulation, displacement-based, and forced-based was done by Correia et al. (2008). For this purpose, a reinforced concrete bridge column using low-performance material was experimentally tested by Correia et al. (2008). The control column had 400 mm x 400 mm cross-section with 1850 mm height and 60 mm clear cover. Main longitudinal reinforcements consisted of 12-D13 bars, and the transverse reinforcements were D6 bars with 50 mm center to center spacing. An axial load of 160 kN was applied during application of the loading history. The displacement control cyclic load history as shown in Figure 3.1a was applied at 1450 mm from column base. The details can be found in Correia et al. (2008). Seismic testing of full-scale bridge column using high strength concrete and high strength steel was carried out by Restrepo et al. (2006). The 914mm diameter bridge pier was reinforced with 42- #5 (15.8 mm diameter) longitudinal bars and #3 (9.7 mm diameter) hoops spaced at 40 mm. The clear height of the column was 2444 mm, and the clear cover was 38 mm. Force-controlled load history was applied until flexural yielding occurred and after that, the displacement controlled cyclic load was in action (Restrepo et al., 2006). The loading protocol used in the experiment is shown in Figure 3.2a. Constant axial load of 2669 kN was applied on top of the bridge column. Fixed base is considered during analysis of the bridge pier since the footing was prestressed to the strong floor. Material properties measured in both the experiments are listed in Table 3.1. The program SeismoStruct is capable of predicting collapse load and large deformation in structure considering both material and geometric non-linearity (Pinho et al., 2007). 3-D inelastic force-based beam-column elements are considered in modeling the bridge piers. Material models are calibrated using the values provided in Table 3.1 to catch the strength, deformation and stiffness transition under reverse cyclic loading.

Table 3.1 Material properties used in model validation

	f'_c (MPa)	f_y (MPa)	f_{su} (MPa)	ε_{su} (MPa)	f_{yh} (MPa)
Correia et al. (2008)	20.6	367	-	-	367
Restrepo et al. (2006)	56.5	648.1	1067.3	5.2	827.4

Here, f'_c = Uniaxial compressive strength of concrete, f_y = Yielding stress of longitudinal bars, f_{su} = Ultimate stress of longitudinal bars, ε_{su} = Strain at ultimate stress of longitudinal bars, f_{yh} = Yielding stress of transverse bars

Figure 3.1b displays the comparative hysteretic performance of experimental and analytical results of the steel reinforced square concrete column. Results obtained from the analytical modeling of Correia et al. (2008) shows that SeismoStruct can predict the test results reasonably where the variation in maximum shear capacity is only 8.3% (Figure 3.1b). The energy dissipation capacity from the numerical analysis is found 152 kN-mm, which is 5.72% higher than the experimental result. This is due to higher loop area inside the hysteretic curve and indicates that the program predicts the residual deformation little more than the experimental outcome (14% more maximum residual deformation). The parameter post-elastic and elastic stiffness ratio and the shape defining parameters are adjusted to conform the stress-strain behavior accurately in Manegotto-Pinto model. Material modeling and fiber-based element modeling approach are discussed in details in Chapter 5. Values for the calibrated parameters are b = 0.015, R_0 = 20, a1 = 18.5, a2 = 0.15, a3 = -0.025 and a4 = 15. Figure 3.2b portrays the shear force, and drift capacity of the high-performance material made bridge pier from the numerical model of Restrepo et al. (2006), which is in good agreement to the experimental results. The maximum shear force is calculated 1311 kN, which only 0.77% higher than the experimental results respectively. Moreover, the cumulative energy dissipation capacity from the hysteretic curve is determined 523.9 kN-mm that is only 1.06% more than that of the lab test. The calibrated hardening and cyclic response parameters used in modeling to better represent the experimental data are b = 0.015, R_0 = 19.5, a1 = 18.8, a2 = 0.05, a3 = 0.25 and a4= 0. Validating the experimental results with the simulation clearly express the effectiveness of the program in predicting the simulated seismic behavior of steel reinforced column and bridge pier for a wide range of material properties.

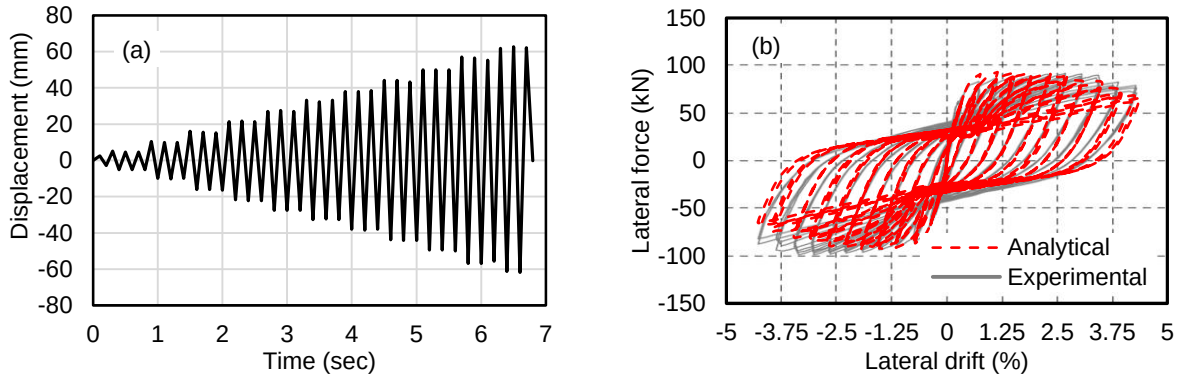

Figure 3.1 Comparison of analytical results with experimental results from Correia et al. (2008); (a) loading protocol (b) analytical validation

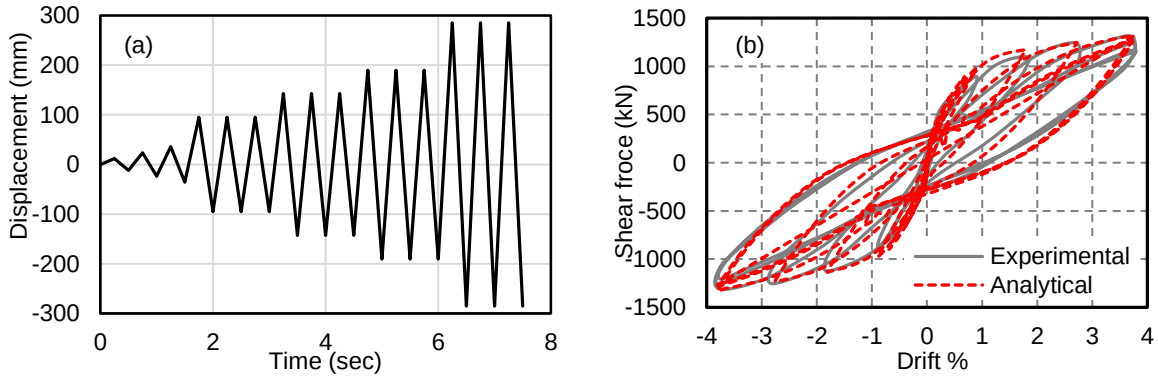

Figure 3.2 Comparison of analytical results with experimental results from Restrepo et al. (2006); (a) loading protocol (b) analytical validation

3.3 Geometry and Design of Bridge Piers Following CHBDC

Design and geometric configuration of steel reinforced concrete bridge piers following different design guidelines are described in this section. Concrete of 35 MPa compressive strength and ASTM A615 Grade 60 steel (415 MPa yield strength) are considered to design the bridge piers seismically following two design methods, forced-based design approach, and PBD approach. Most of the bridges are designed following the traditional force-based method where for simple bridges seismic demands are calculated by single-mode spectral method (Zhang et al., 2016). Whereas, PBD is relatively new design method, which has recently been adopted in CHBDC (CSA 2014). Performance of the bridge is controlled by designing it to meet certain target performance levels for various hazard probability is the main concept of PBD. A lifeline bridge assumed to be

located in Vancouver, Canada is designed as per CHBDC. At a seismic ground motion probability of 2% in 50 years, a lifeline bridge should remain open for immediate use. Though CHBDC 2014 allows designing a lifeline bridge using PBD method only; to understand the variation in design outcomes and seismic performance of same bridge pier designed with different design code alternatives, FBD approach is also embraced from CHBDC 2010. The diameter of the bridge pier is 915 mm, and the height is 5250 mm as shown in Figure 3.3. Aspect ratio is maintained 5 to ensure flexure dominated behavior of the bridge pier (Billah and Alam, 2016a). Considering a simple regular bridge supported on a single pier bridge bent, the 10% axial load ratio is considered in designing the bridge column. Soil-structure interaction is disregarded in this particular study for simplicity. Cracked stiffness from Priestley et al. (1996) is used to calculate the fundamental time period of the bridge pier following the equation $T=2\pi\sqrt{(m/k_{cr})}$ where m is the effective mass and k_{cr} is the cracked stiffness of the bridge pier.

Korinda (1972) and Hage (1974) demonstrated the importance of accurate flexural stiffness calculation of structure considering both lateral and gravity loads. With the increase in steel strength, the cracking probability of concrete will increase. Changes will occur in the flexural stiffness of the cracked section. This reduced stiffness will necessitate the recalculation of the moment of inertia of the section. This modification will vary with the reinforcement grade and reinforcement ratio. The importance factor and the response modification factor are taken 3 and 3 respectively, and the site coefficient of 1.5 for soil profile type III from CHBDC (CSA, 2010) are considered in calculating the base shear demand. It is recommended that, in an earthquake event of 475 years return period, a lifeline bridge should remain open to traffic for immediate use. A constant lumped mass of 2300 kN is applied at the top of bridge column to represent weight coming from the superstructure. The design moment, axial force and base shear demand are 5020 kN-m, 2300 kN, and 950 kN respectively. Reinforced concrete sectional analysis software Response 2000 (Bentz, 2000) is employed in generating the moment-curvature capacity of the column section. It has the capacity to perform flexural strain compatibility calculation with the moment-curvature relationship. A user-friendly graphical interface to define material properties and section geometry and dimensions allow the user to interpret the results easily. The material properties can easily be modified to plot stress-strain curves. Previous studies effectively used Response 2000 in sectional analysis (Karim and Yamazaki, 2001; Setzler and Sezen, 2008; Xu and Zhang, 2011; Salomon and Moen, 2014; Özer and Soyöz, 2015; Colley et al., 2015). Design spectral acceleration is taken

from Vancouver design response spectrum for soil type C. To check the performance of FBD bridge pier, displacement demands are calculated for return periods of 475, 975 and 2475 years. FBD of the bridge pier requires 16-55M longitudinal bars, which yields 4.87% longitudinal reinforcement ratio. The transverse spiral reinforcements are 20M bars spaced 50 mm at the center in the plastic hinge region as shown in Figure 3.3 and 65 mm to the rest. For the PBD, spirals configuration and sizes are the same. The only variation is in longitudinal reinforcement based on design methodology.

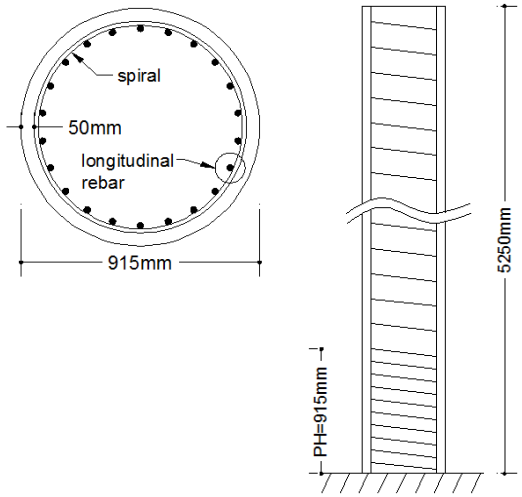

Figure 3.3 Cross-section and elevation of steel reinforced concrete bridge pier

It is not very likely that the FBD and the PBD will yield same design results. FBD is entirely based on the elastic force demand on structure reduced by the structure ductility. It is not targeted to satisfy any performance level of a structure such as drift, displacement or material strain. On the contrary, PBD can be done following any method (i.e., static pushover analysis, non-linear time history analysis) but has to be checked following the specified method (Zhang et al., 2016). Performance criteria are defined in terms of material strain limit for different hazard level earthquakes and seismic performance or damage category in CHBDC 2014. Deformation and strain give a clear indication of damage in structure than forces and stresses (Moehle, 1996). The strain limit and displacement in structural components can be interrelated as well as the level of specified damages. To meet certain performance criteria is not an easy task for engineers considering the construction and economic feasibility.

Performance criteria for bridges first included in CHBDC in 2014. After that, the supplement on the code in 2016 had noticeable changes in terms of performance criteria. Drift in bridge pier cannot always define the damage properly; rather the material strain level is the key parameter that dictates the damage in structure more distinctly. However, drift is more easily visible and predictable in case of a seismic event and most commonly used framework to present seismic performance and vulnerability. The study is intended to design the bridge piers regarding material strain level specified in CHBDC (CSA, 2014; CHBDC, 2016) to find out the design variations and show their behavior during actual ground motions in terms of drift capacity. For a lifeline bridge, CHBDC 2014 (CSA 2014) specified the damage must be repairable for higher level design (seismic ground motion probability 2% in 50 years). For seismic ground motion with a probability of 5% in 50 years, the bridge should have minimal damage with immediate service to the traffic. These damage and service criteria are presented in terms of material strain (concrete compressive strain and steel strain for reinforced concrete bridge pier) as shown in Table 3.2. For lower level design, CHBDC 2014 (CSA 2014) specified that there should be no damage whereas the supplement proposed that the strain in steel cannot exceed 0.01 (CHBDC, 2016). Updated and previous performance criteria to design a reinforced concrete lifeline bridge pier are concisely presented in Table 3.2. The level of analysis is also specified in CHBDC 2014. For the highest level of design, inelastic static pushover analysis accounting non-linearity in structural elements and elastic dynamic analysis are required. However, in this particular study, pushover analysis is performed to select the longitudinal reinforcement targeting the performance criteria and displacement demand estimated from response spectrum analysis. Non-linear time history analyses are also carried out to check the performance of the PBD bridge piers under seismic motions. The program SeismoStruct (SeismoStruct, 2015) can show the material strain levels for stated performance criteria with reasonable accuracy (Billah and Alam, 2016b). Concrete and reinforcing steel are modeled following the models proposed by Mander et al. (1988) and Menegotto and Pinto (1973) respectively.

Figure 3.4a shows the static pushover performance of the FBD bridge pier with 4.87 percentage of longitudinal rebars. Strain criteria of the materials are marked on the pushover curve. The dashed vertical lines represent the displacement demand for three events probabilities. Supplement to CHBDC 2014 specifies the concrete strain should not exceed 0.006 and the strain in steel should be less than 0.01 under the displacement demand of 1 in 475 years (10% probability

in 50 years) and 1 in 975 years (5% probability in 50 years) events for a lifeline bridge pier. The FBD pier satisfies the displacement demand with minimal damage for the both seismic events. As stated in CHBDC 2014, for a lifeline bridge, steel cannot yield during a seismic event with a probability of 5% and 10% in 50 years, and the tensile strain in steel should be limited to 0.015 during a seismic event with a probability of 2% in 50 years. Compared to the criteria defined in CHBDC 2014, the FBD bridge pier satisfies the criterion for the seismic event with a return period of 2475 years (Figure 3.4a) but fails to meet the steel yielding criterion during a seismic event with a probability of 5% in 50 years.

An iterative approach is used in designing the longitudinal reinforcements of the bridge piers following the performance-based criteria in CHBDC 2014 and the supplement to CHBDC 2014. Percentage of reinforcement is fixed to a stage where it just meets the performance criteria. Longitudinal reinforcement percentage in bridge pier is decreased to 1.22 from 4.87 targeting the performance criteria that the steel strain should be less or equal to 0.025 for an extreme seismic event (CHBDC, 2016). The pushover curve (Figure 3.4b) indicates the adequacy of main rebars to satisfy all performance criteria. This also satisfies the criteria that the concrete and steel strain needs to be limited within 0.006 and 0.01 respectively for an event with return period 975 years. Looking into the performance limits stated in CHBDC 2014 that the concrete strain has to be below 0.004 and the longitudinal steel must not yield for a 1 in 975 years event, the FBD bridge pier fails to maintain steel yielding the criteria. Steel strain reaches to yield strain earlier than the displacement demand imposed by the mid-level seismic event. The most conservative criterion is the steel yielding criteria for the mid-level event as can be seen from Figure 3.4a. Meeting this criterion results in very high longitudinal reinforcement ratio (6.1%). The previous study from Zhang et al. (2016) found similar results for major route bridges. CHBDC 2014 (CSA, 2014) does not allow reinforcement ratio more than 6% to avoid congestion, which turns out to be very difficult to maintain the performance criteria within this range. However, increasing the percentage of longitudinal rebar increases the stiffness of the structure and results in lower displacement demand. Limit strains in the materials also occur at higher load and displacement. 20-55M longitudinal reinforcements fulfill the performance criteria according to CHBDC 2014, which is almost 25.3% higher reinforcement than FBD pier. On the other hand, bridge pier designed following the updated version of performance on CHBDC 2014 (CHBDC, 2016) yields about 75% less longitudinal reinforcement than that of FBD. Since the steel performance strain limit for an

event of 5% probability in 50 years increased almost five folds in the recent supplement to CHBDC 2014 (CHBDC, 2016), longitudinal steel ratio demand drops drastically. The design results with reinforcement details are displayed in Table 3.3 and Figure 3.5.

Table 3.2 Performance criteria for reinforced concrete lifeline bridges (CSA, 2014)

Seismic ground motion probability	Service	Damage (CHBDC 2014)	Damage (CHBDC 2014 supplement)	Performance criteria (CHBDC 2014)	Performance criteria (CHBDC 2014 supplement)
10% in 50 years	Immediate	None	Minimal	-	$\varepsilon_c \leq 0.006$ and $\varepsilon_{st} \leq 0.01$
5% in 50 years	Immediate	Minimal	Minimal	$\varepsilon_c \leq 0.004$ and $\varepsilon_{st} \leq \varepsilon_y$	$\varepsilon_c \leq 0.006$ and $\varepsilon_{st} \leq 0.01$
2% in 50 years	Service limited	Repairable	Repairable	$\varepsilon_{st} \leq 0.015$	$\varepsilon_{st} \leq 0.025$

Here, ε_c = Concrete compressive strain, ε_{st} = steel strain

Table 3.3 Design cases and details

ID	Design basis	f'_c (MPa)	Steel grade	f_y (MPa)	Reinforcement percentage	Longitudinal rebar detail
F_35/415	CHBDC 2010	35	60	415	4.87%	16-55M
P_35/415_s	CHBDC 2014 supplement	35	60	415	1.22%	16-25M
P_35/415	CHBDC 2014	35	60	415	6.1%	20-55M

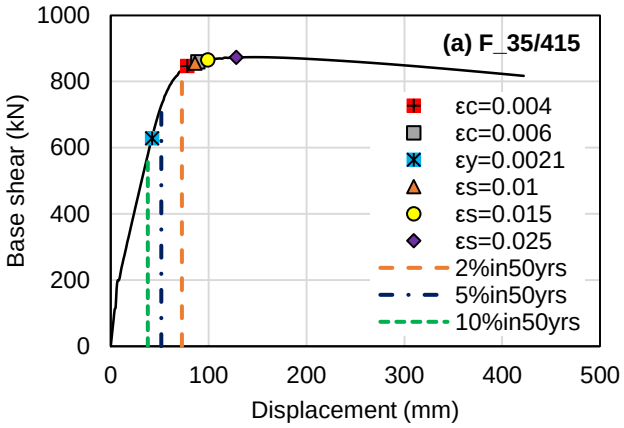

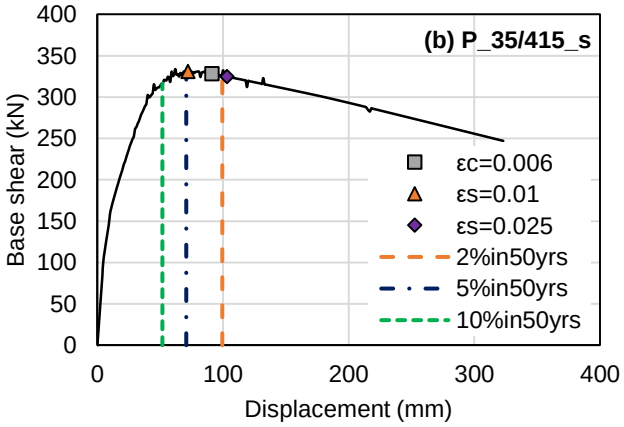

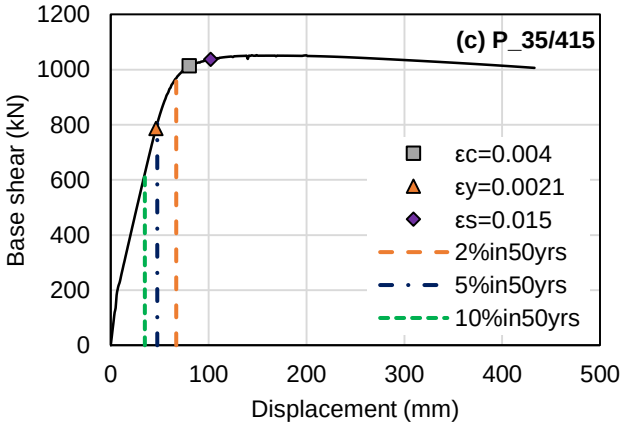

Figure 3.4 Static pushover analysis

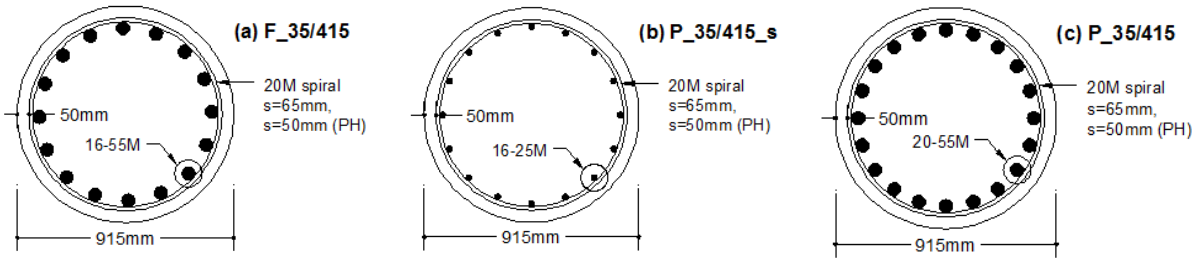

Figure 3.5 Cross sections of designed bridge piers

3.4 Seismic Ground Motions

Twenty near-fault earthquake ground motions of varying magnitude and peak ground acceleration (*PGA*) are selected to symbolize medium to strong ground motions. The near-fault ground motions range from *PGA* value of 0.37g to 1.07g. If the subject structure is within 15 km of a fault, then it can be categorized as NF (Caltrans, 2004). However, 10 km fault distance is defined as near fault in CHBDC 2014 (CSA, 2014). In this study, ground motions with epicentral distance less than 10 km are considered as near fault motions (Table 3.4). The south coast of British Columbia is susceptible to megathrust due to the movement of the Juan de Fuca oceanic plate under North American plate (Wagstaffe, 2016). Hundreds of small faults spread like matrix under the British Columbia providence. There are possibilities of shallow earthquakes below some major cities including Vancouver as well with faults under 10 km. According to Somerville (2002), NF ground motions incorporates high ground displacement, peak velocities, and long period velocity pulse. NF ground motions create pulse-like loading and apply high input energy on structures. Billah and Alam (2014a) studied the vulnerability of a bridge bent retrofitted with four alternatives for near-fault and far field ground motions. They concluded that the retrofitted bridge bents are more susceptible to near-fault ground motions and induce higher ductility demand. The ground motions shown in Table 3.4 are acquired from Pacific Earthquake Engineering Research (PEER) Center earthquake database (PEER, 2011) in such a way that they represent the characteristics of the site of the bridge pier. Naumoski et al. (1988) stated that the ratio of peak ground acceleration (*PGA*) and peak ground velocity (*PGV*) of a ground motion indicate the frequency content and for western Canada, this ratio is close to 1.0. However, Parghi and Alam (2017) studied the fragility of a retrofitted bridge pier located in Vancouver for 20 ground motion suites whose *PGA/PGV* ratio varied between 0.46 and 1.56 due to non-availability of adequate ground motion data in that

particular region. *PGA/PGV* ratios for the chosen ground motions in this study are between 0.37 and 1.14 and assumed to represent seismic motions in Vancouver. More than fifty percent ground motions selected have the *PGA/PGV* ratio range of 0.6-1.14. To generate sufficient data to plot the fragility curves, all the ground motions are taken into consideration. The near-fault ground motion records are scaled to the design spectrum of Vancouver for 5% damping ratio of C soil type SeismoMatch (SeismoMatch, 2014). Figure 3.6 demonstrates the response spectra for the different suits of ground motions for both the original and matched motions with quartiles.

Table 3.4 Characteristics of the earthquake ground motion histories

Sl. No.	Earthquake	Year	Richter magnitude	Epicentral distance (km)	PGA (g)	PGA/PGV
1	Tabas	1978	7.4	1.2	0.90	0.81
2	Tabas	1978	7.4	1.2	0.96	0.92
3	Loma Prieta	1989	7	3.5	0.70	0.42
4	Loma Prieta	1989	7	3.5	0.46	0.50
5	Loma Prieta	1989	7	6.3	0.67	0.40
6	Loma Prieta	1989	7	6.3	0.37	0.54
7	C. Mendocino	1992	7.1	8.5	0.63	0.51
8	C. Mendocino	1992	7.1	8.5	0.65	0.71
9	Erzincan	1992	6.7	2	0.42	0.37
10	Erzincan	1992	6.7	2	0.45	0.79
11	Landers	1992	7.3	1.1	0.69	0.53
12	Landers	1992	7.3	1.1	0.79	1.14
13	Nothridge	1994	6.7	7.5	0.87	0.51
14	Nothridge	1994	6.7	7.5	0.38	0.75
15	Nothridge	1994	6.7	6.4	0.72	0.60
16	Nothridge	1994	6.7	6.4	0.58	1.11
17	Kobe	1995	6.9	3.4	1.07	0.78
18	Kobe	1995	6.9	3.4	0.56	0.80
19	Kobe	1995	6.9	4.3	0.77	0.45
20	Kobe	1995	6.9	4.3	0.42	0.67

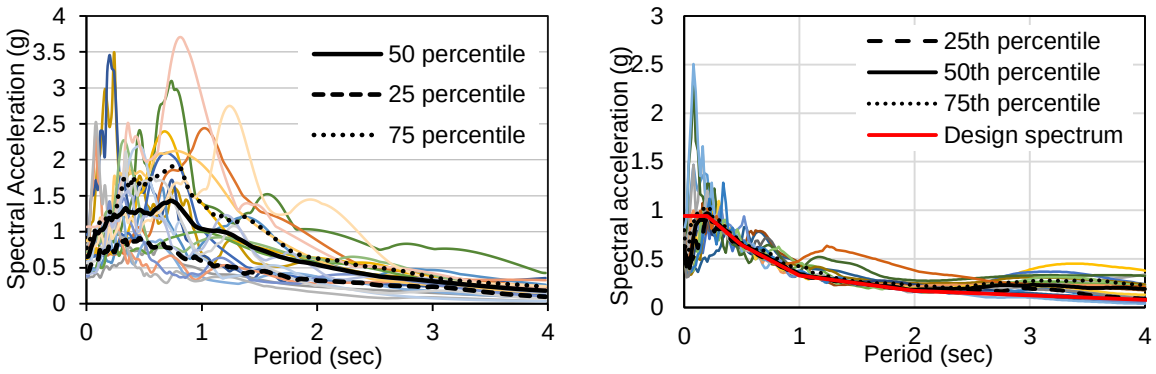

Figure 3.6 Spectral motion records (a) original near-fault motions spectra (b) matched ground motion spectra

3.5 Performance Assessment

To assess the performance of the bridge piers designed following the PBD method, dynamic time history analyses are carried out. The above-mentioned ground motions are scaled to match Vancouver response spectrum for an event with a probability of 2% in 50 years. The performance limit set for this particular hazard level is the strain in reinforcing steel cannot exceed 0.015 and 0.025 in CHBDC 2014 (CSA, 2014) and the supplement to CHBDC 2014 (CHBDC, 2016) respectively. Maximum strain induced in the longitudinal reinforcements from the time history analyses are presented in Figure 3.7. From the results, it can be seen that the performance criteria are met for most of the ground motions. For the bridge column P_35/415_s, only four out of twenty ground motions induced higher strain than specified (Figure 3.7a). Likewise, for the bridge pier P_35/415, four ground motion noticeably exceeded the strain limit in steel reinforcement (Figure 3.7b). However, the median strain value remains 0.015 and 0.023 for P_35/415 and P_35/415_s bridge piers correspondingly, which is within the specified limit.

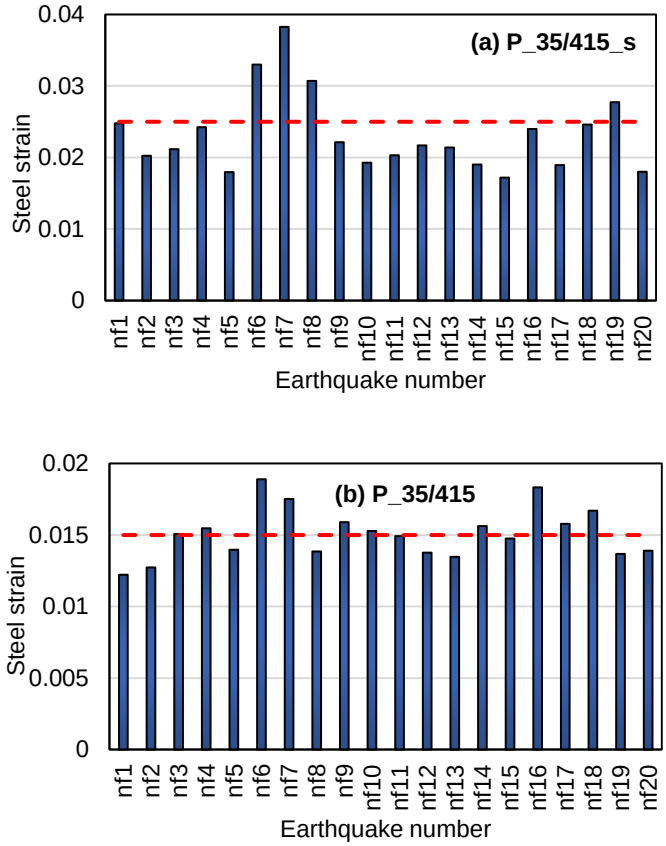

Figure 3.7 Maximum steel strain from time history analysis

3.6 IDA Performance

The incremental dynamic analysis method is widely used in estimating the bridge performance thoroughly under seismic actions (Billah and Alam, 2014a; Pang et al., 2014; Baker, 2015; Billah and Alam, 2015b; Fakharifar et al., 2015b; Chandramohan et al., 2016). *IDA* was first introduced by Luco and Cornell (1998) and further described elaborately in FEMA (2000b; 2000c), Vamvatsikos and Cornell (2002), and Yun et al. (2002). Series of non-linear time history analyses are carried out for a ground motion record increased in intensity until the structure becomes unstable or the range of response of the structure is captured. This *IDA* is performed for multiple earthquake records to attain the data on the variation of demand and capacity of the structure. Ground motion intensity levels should be selected to cover the whole limits of structural response from yielding to failure (Billah and Alam, 2014a).

3.6.1 PGA vs. Maximum drift

A suit of 20 near-fault ground motion records as shown in Table 4 are used in executing the *IDA* to determine the maximum drift capacity and yield behavior of the bridge piers under dynamic loading. These seismic motions are matched to highest level design spectrum (2% probability in 50 years) for Vancouver before implementing *IDA*.

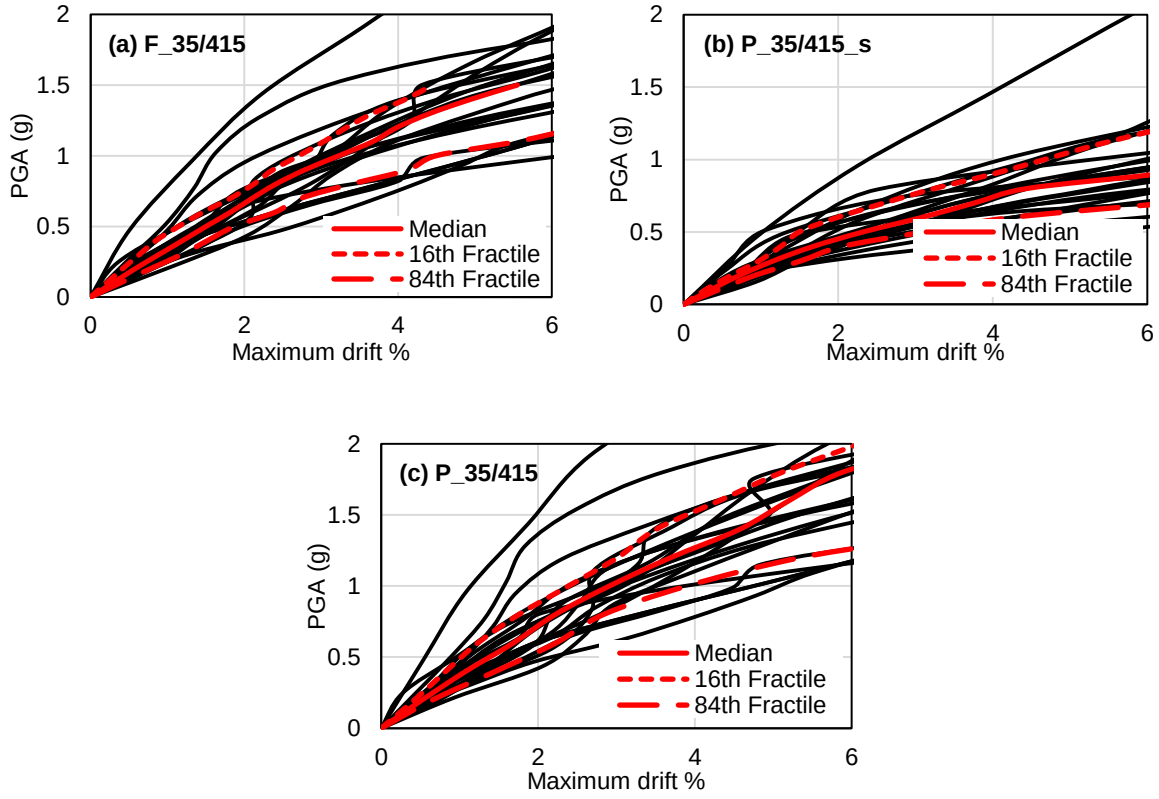

Figure 3.8 *IDA* curve for maximum drift

The *IDA* plots are produced from the non-linear time history analysis of the bridge pier for force-based and performance-based designs. Figure 3.8 shows the *PGA* versus maximum drift percentage of the bridge pier for individual ground motion records. All the plots show somewhat elastic behavior before starting non-linearity, and scattered curves indicate how the response varies even for same intensity earthquakes. The diversified frequency content of ground motions can be attributed to such behavior. PBD pier (P_35/415) designed following CHBDC 2014 show higher stiffness than the FBD pier (F_35/415) and the PBD pier (P_35/415_s) designed following the supplement to CHBDC 2014 in the elastic zone. Higher reinforcement ratio results in higher

stiffness of the structure. However, the inelastic behaviors of the bridge piers are quite diversified with gradual softening towards failure for PBD bridge columns (Figure 3.8b and 3.8c) and undulating behavior for FBD bridge column (Figure 3.8a). The PBD pier (P_35/415_s) fails to take more than 3g *PGA* earthquake whereas the FBD (F_35/415) and PBD (P_35/415) columns can take more than 3g *PGA* for some ground motions. The *IDA* curves are random lines or function of intensity measures (IM) (Vamvatsikos and Cornell, 2002). To understand their comparative performance with more reliable data, the curves are also summarized in terms of 16^{th}, 50^{th} and 84^{th} fractile values. Mean, median and 84^{th} fractile values are mostly used in engineering design (Billah and Alam, 2014). Figure 3.8 displays the developed 16%, 50%, and 84% fractile curves in terms of maximum drift for distinct ground motion intensities at 2% in 50 years probability level. For *PGA* 1g, 16% near-fault ground motion records cause maximum drift of 2.71%, 4.67% and 2.39% for FBD pier (F_35/415), PBD pier following the supplement to CHBDC 2014 (P_35/415_s) and PBD pier following CHBDC 2014 (P_35/415) respectively. At the same ground motion intensity level, 3.23%, 6.12% and 2.91% maximum drifts are induced for F_35/415, P_35/415_s and P_35/415 bridge piers correspondingly by 50% of the seismic motions. The FBD pier (F_35/415) displays 4.49% maximum drift by 84% ground motions at *PGA* 1g. On the other hand, P_35/415_s and P_35/415 piers show 186% higher and 13.2% less maximum drift compared to F_35/415 pier. The FBD method from CHBDC 2010 and the PBD method from CHBDC 2014 both are effective in lowering the maximum drift of bridge pier. Serviceability and damage of bridge piers are presented in terms of maximum drift by several researchers. Repairable damage is specified by 0.5% (Liu et al., 2012; Ghobarah, 2001) and 1.5% maximum drift (Kim and Shinozuka, 2004; Fakharifar et al., 2015b) and the near collapse are by 2% (Liu et al., 2012), 2.5% (Ghobarah, 2001; Kim and Shinozuka, 2004; Fakharifar et al., 2015b) and 5% (Banerjee and Shinozuka, 2008). In this present study, the repairable damage is calculated from the pushover analysis using the material strain criteria. For F_35/415 pier, the maximum drift of 2% (using criteria $\varepsilon_{st} \leq 0.025$) and for P_35/415_s and P_35/415 piers, the maximum drift of about 2% is considered as repairable damage state from the criteria $\varepsilon_{st} \leq 0.025$ and $\varepsilon_{st} \leq 0.015$ respectively and 4% drift as collapse limit. When the near-fault ground motions are matched to 2% in 50 years probability level, 50% motions of 1g *PGA* cause unrepairable damage in bridge piers irrespective of design methods. Collapse limit reaches to FBD column by 50% motions of 1.2g *PGA*. The P_35/415_s pier designed following the supplement to CHBDC 2014 demands 33% less PGA to reach the collapse drift limit

by 50% ground motions considered. Lower stiffness due to less reinforcement ratio can be attributed to such behavior of P_35/415_s pier (75% less longitudinal reinforcement than F_35/415). The PBD bridge column P_35/415 designed according to CHBDC 2014 is within collapse prevention range when 50% motions are considered with *PGA* 1.4g.

3.6.2 Yield displacement

Strain in steel is considered as an important factor since the design of both the PBD bridge columns are governed by steel strain level. Yielding in steel does not occur at the same displacement level under different dynamic loading. The Higher frequency with a high number of cycles with lower intensity earthquake can cause the bridge pier yield faster than a higher intensity earthquake with lower cycles and frequency. Displacements at yielding of the F_35/415, P_35/415_s and P_35/415 bridge piers under scaled ground motions are shown in Figure 3.9. Median yield displacement for FBD column is 44.5 mm (Figure 3.9a) with a standard deviation of 3.07 mm. The PBD bridge pier P_35/415 shows higher median yield displacement, and P_35/415_s shows lower median yield displacement compared to F_35/415 pier under dynamic motions. P_35/415_s pier is exhibiting 26.9% lower median yield displacement (Figure 3.9b) whereas P_35/415 pier is showing 8% higher than F_35/415 pier (Figure 3.9c) at a 2% in 50 years probability level seismic motions.

Uncertainties in load, material properties, design, and construction process can cause unexpectedly higher load and lower resistance causing damage to structures. To fight the issue, most of the design code uses load factor higher than 1 and material resistance factor lower than 1. North American design codes for buildings and bridges specify the material properties of steel as minimum requirements. Mirza and MacGregor (1979) found that the beta function can be a potential repetitive of the yield strength of steel rebars. Bournonville et al. (2004) studied the variability in properties of ASTM A615, A616 and A706. Statistical analysis was conducted to find the probability distribution function of yield strength, tensile strength and weight of reinforcement. They found similar distribution like Mirza and MacGregor (1979) for both yield and tensile strength of steel reinforcement except higher size A615 steels. In this particular study, yield displacements follow the Weibull distribution, which is valid for extreme conditions since uncertainties in material properties are not considered in this study. The median yield displacement can be used to determine the displacement ductility of the bridge piers for seismic vulnerability

analysis. Though CHBDC adopted material strain as performance limit, maximum drift and displacement ductility are often used by researchers as a deciding performance parameter in the seismic evaluation of bridge structures. Fragility plots are developed on the demand parameter, maximum drift later in this particular study.

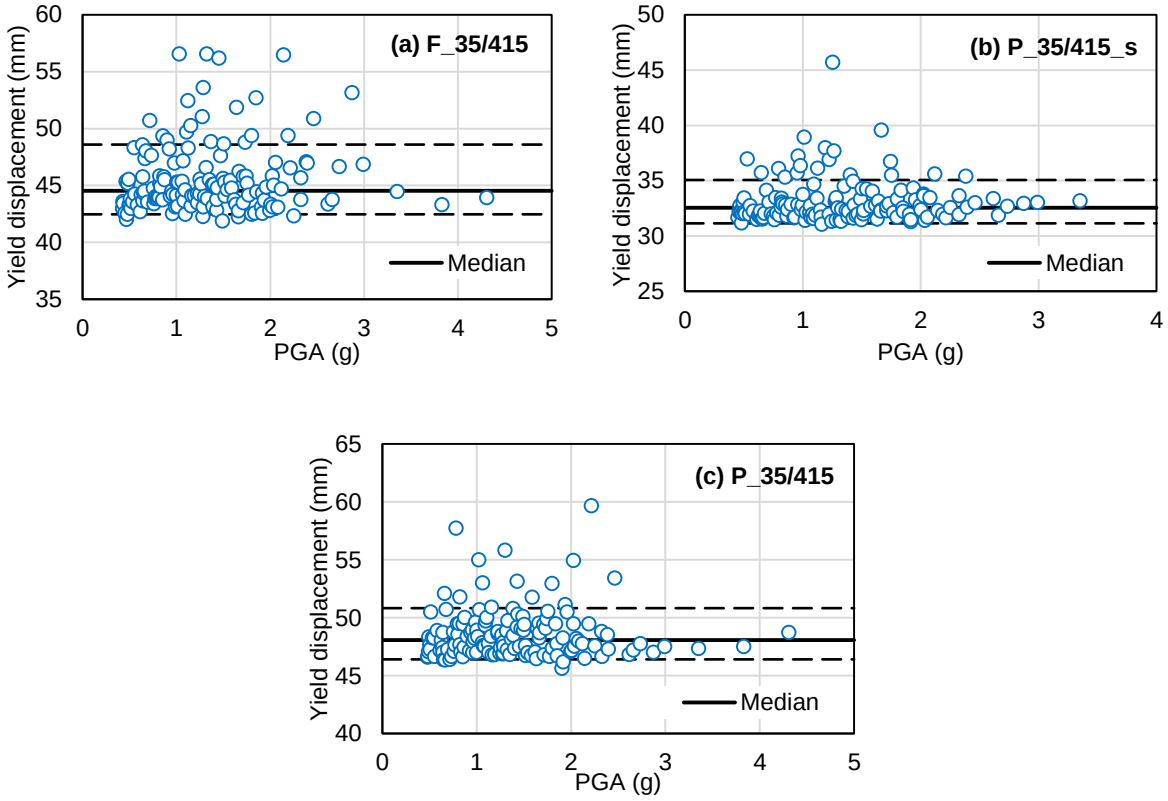

Figure 3.9 *IDA* curve for yield displacement

3.6.3 Crushing displacement

The crushing displacement changes with the increased longitudinal reinforcement ratio. Additional main rebar increases the stiffness of the member and partly contributes to the confinement of the core concrete. The median crushing displacement in the P_35/415_s bridge pier is found 214.3 mm (Figure 3.10b) with a standard deviation of 18.65 mm from the incremental dynamic analyses. Similar to the yield displacement, the PBD bridge pier P_35/415 and FBD pier F_35/415 show higher crushing displacement under seismic ground motions. Bridge pier designed following CHBDC 2014 displays 257 mm crushing displacement, which is 20% higher than P_35/415_s (Figure 3.10c). As can be seen from Figure 3.10a, the F_35/415 pier exhibits the

median crushing displacement of 250.9 mm at seismic motions with 2475years of return period. Although the longitudinal reinforcement ratio is almost five folds in P_35/415 pier compared to P_35/415_s, the crushing displacement increases only 20%. With increased longitudinal reinforcement percentages, the variation in crushing displacement also increases with increased standard deviation. Crushing starts earlier in the PBD bridge column P_35/415_s at a *PGA* as low as 0.8g. Whereas, crushing in the P_35/415 pier initiates at a *PGA* of 1.5g. The FBD from CHBDC 2010 and PBD from CHBDC 2014 yield to stronger bridge piers requiring higher intensity earthquake for the same level of damage.

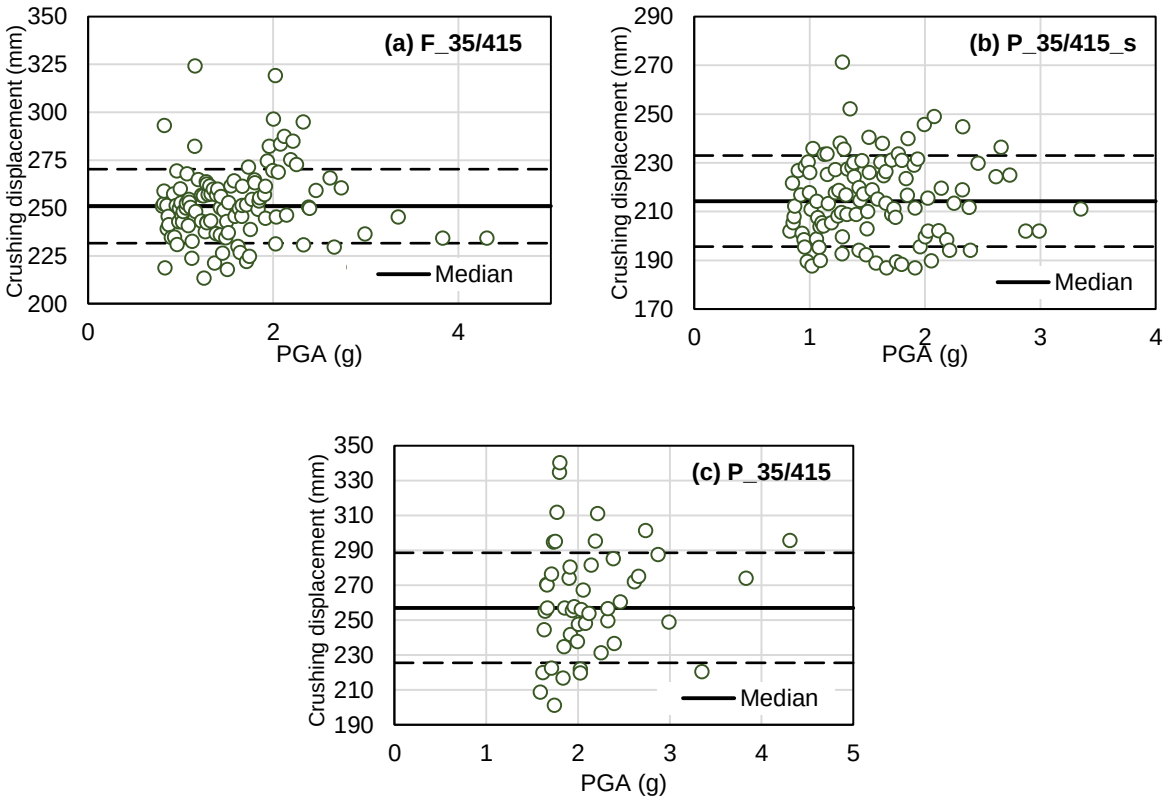

Figure 3.10 *IDA* curve for crushing displacement

3.7 EDP and IM Relationship

For a given intensity measure (*IM*) of seismic motions, the engineering demand parameters (*EDP*) are determined from the inelastic simulation of structures. The response of the structure can be portrayed in terms of pertinent engineering parameters like displacement, strain, residual deformation, force-induced and acceleration in structure. Interstorey drift, drift ratio, floor

acceleration are some commonly used *EDP* in building analysis. For bridge structures, pier deformation, drift, residual drift, abutment displacement, isolation bearing displacement and strain are the characterizing engineering parameters used to identify the response depending on the structural components involved in the analysis. Maximum drift is the most widely used response parameter in fragility analysis of bridge piers. Whereas, peak ground acceleration (*PGA*) and the spectral acceleration are the most commonly used intensity measure seismic fragility analysis (Mackie and Stojadinovic, 2004; Nielson and DesRoches, 2007a; Shinozuka et al., 2003). In this study, *PGA* is considered the *IM* of the ground motions to measure the response of the bridge piers in terms of maximum drift percentage. A comparatively new intensity measure acceleration spectral intensity (*SI*) are examined to understand the variation of *EDP* with the *IM*.

3.7.1 Maximum drift % vs. PGA

The relationship between the bridge piers maximum response and the ground motion parameter *PGA* are displayed in Figure 3.11. As the ground motion intensity increases, the maximum drift in bridge piers increases. These increments do not follow a linear path. Rather, the maximum response becomes scattered, and dispersion in demand increases with the increasing ground motion intensity. R-squared values shown in the figures do not support the linear fit of *PGA* with maximum drift of bridge piers. The range of r-squared values from the regression model is 0.45-0.72. However, at *PGA* less than 1g, the lower dispersion may allow predicting the response of structure considering linear variation of *EDP* and *IM*. Most suitable correlation between *PGA* and maximum drift is the logarithmic correlation in developing the probabilistic seismic demand model, which is discussed in Chapter 4.

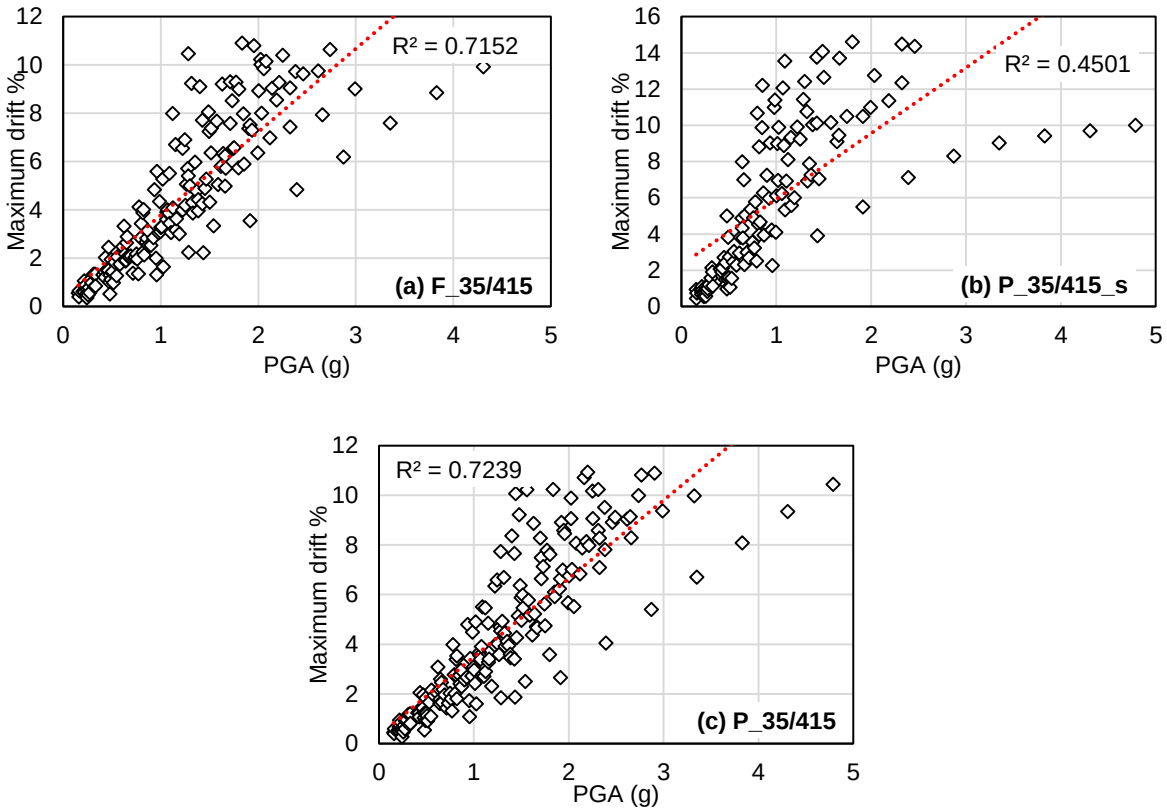

Figure 3.11 *IDA* performance: Maximum drift % vs. *PGA*

3.7.2 Maximum drift % vs. Spectrum Intensity

Spectrum Intensity (*SI*) is showing potential as a ground motion intensity measure in predicting seismic response of soil deposits (Bradley et al., 2009). *SI* of a ground motion was first defined by Housner (1963) as the integral of pseudo-spectral velocity (*PSV*) from 0.1 to 2.5 sec of the ground motion. 5% damping ratio is commonly used in calculating the *PSV*. The correlation between the maximum drift response of the designed bridge piers and the spectral intensity as a ground motion measure is shown in Figure 3.12. Compared to *PGA*, *SI* shows smaller dispersion in demand parameter. Maximum drift follows an increasing trend with increased *SI*. This trend is somewhat linear for the FBD bridge pier F_35/415. With decreasing longitudinal reinforcement in the PBD, the dispersion in demand parameter increases. The linearly fitted r-squared value from the regression model varies from 0.61 to 0.78. A simplified predicting equation to determine the *EDP* based on *SI* as an *IM* can also be proposed. Further investigation on the correlation between *SI* and *EDP* are expected to consider the potency of spectral intensity as a ground motion intensity measure.

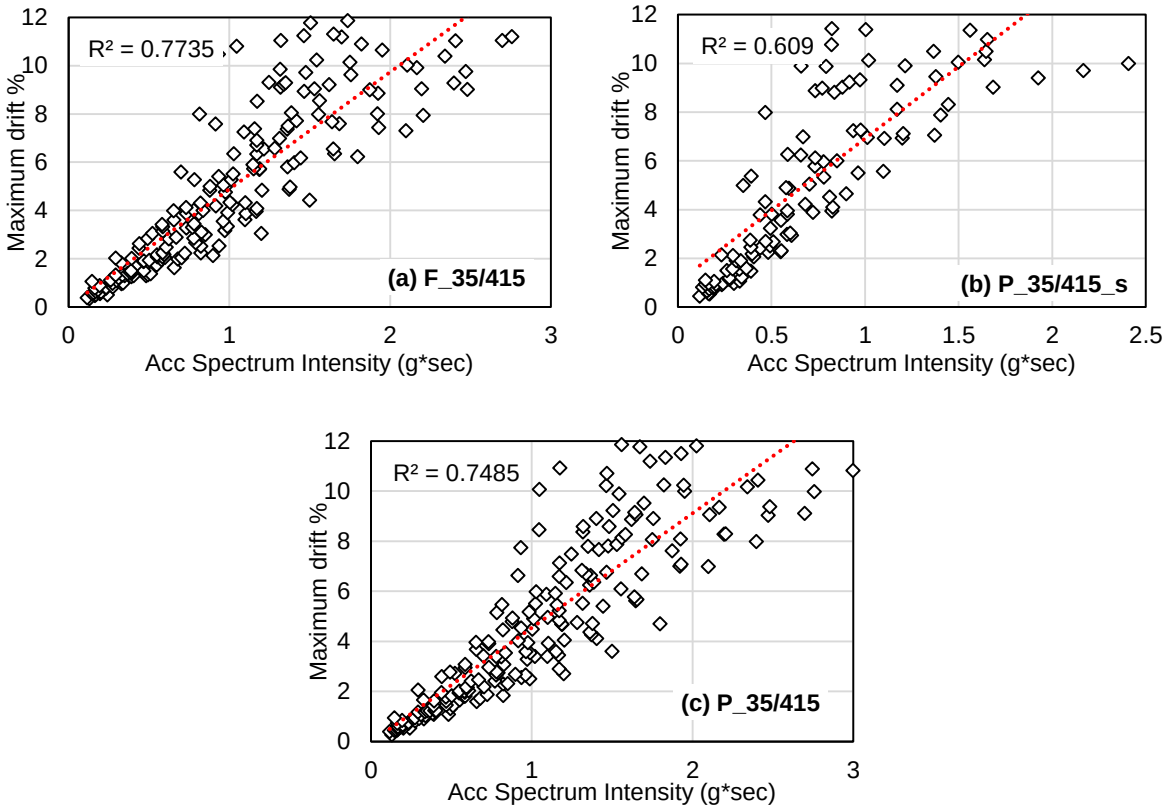

Figure 3.12 *IDA* performance: Maximum drift % vs. Acceleration Spectrum Intensity

3.8 Summary

This chapter introduces the primary objectives of this study and follows the roadmap to attain the goals. Seismic analyses of a lifeline bridge pier designed following three different design alternatives from CHBDC are conducted in this section. Numerical models of the bridge piers are developed and analyzed for 20 site-specific near-fault ground motions. Incremental dynamic analyses are carried out to assess the performances of the designed bridge piers. In total, 600 models are analyzed to develop the *IDA* plots and evaluate the behaviors of the bridge piers under dynamic motions. The results from this chapter are wrapped in brief as followings.

- In determining the response of bridge columns under simulated earthquake, the program SeismoStruct can be used with acceptable accuracy. The validation of experimental load-drift results with the analytical outcomes expresses the competency of the program for a wide range of material properties.

- The FBD of the lifeline bridge pier resulted in 4.87% longitudinal reinforcement. The response modification factor for a single pier bridge bent is only 3 in CHBDC 2010, which yields very high demand in shear. CHBDC does not specify any restriction on single pier bridge bent for a lifeline bridge, which results in very high reinforcement ratio. The pier designed following CHBDC 2014 performance criteria requires 6.1% main reinforcement ratio to satisfy the performance criteria that the steel should not yield at a ground motion with a probability of 5% in 50 years. Such highly conservative design results in reinforcement ratio even more than the maximum allowable limit in CHBDC.
- Following the supplement to CHBDC 2014, the governing design criteria for the lifeline bridge are found to be the repairable damage in a seismic event with a return period of 2475 years. However, this criterion is less conservative compared to the criteria defined in CHBDC 2014 and resulted in only 1.22% longitudinal reinforcement ratio. Maximum steel tensile strain of 0.01 (almost five folds to the Grade 60 steel reinforcement steel strain) describes the minimal damage criteria in the supplement to CHBDC 2014, which previously was the tensile yielding of steel in CHBDC 2014.
- Lower reinforcement requirement in the bridge pier designed according to the supplement to CHBDC 2014 will minimize construction cost and construction hindrance by reducing reinforcement congestion. However, the reduction in performance must be checked to decide on the most suitable design method.
- The *IDA* plots reveal that the conservative PBD of bridge pier undoubtedly experiences lower drift at a certain intensity ground motion. Nonetheless, the drift also shows improved performance when FBD method is used from CHBDC 2010 in designing a lifeline bridge pier.
- Increased longitudinal reinforcement percentage increases the median yield displacement and median crushing displacement of bridge piers making it stronger against earthquakes.

Chapter 4 : FRAGILITY ANALYSIS

4.1 Background

Fragility analysis is a probabilistic method of measuring the potential damage to the structural components and the structure and widely used as a seismic risk assessment tool. The failure and damage to the bridges after a seismic event can severely hamper the transportation facilities. To mitigate the damage cost, economic and life loss, it is utmost important to understand the vulnerability of the bridge structure. The money invested by the stakeholders in constructing and repairing bridge projects requires assurance over the performance of the newly constructed or retrofitted bridge. Establishing fragility curves can provide insight into the probabilistic performance of the bridges, which possess critical importance in prior earthquake planning and post-disaster response management.

Many of the bridges in North America are designed and constructed before the availability of any seismic design provision. The catastrophe happened in the Northridge earthquake acted as an alarm to the structural engineers. After that, every bridge design code went through critical investigation and earthquake resistant design came into action. Eventually, PBD is taking the place of traditional FBD due to its capability of depicting structural performance explicitly. For better perception on the bridge performance designed following different design method and risk assessment of the bridges, fragility analysis is a viable option. This chapter of the study will play a significant role in giving an idea of the probability-based seismic vulnerability of bridge pier designed following different design guidelines. This chapter of the study is designed to discuss the methodology of fragility analysis using probabilistic seismic demand model (*PSDM*). The process of defining the damage states are also described here with corresponding damage fragility.

4.2 Seismic Fragility

Fragility function is a probabilistic tool that describes the probability of a structure being damaged beyond a certain damage level for a given ground motion intensity level (Billah and Alam, 2013; Billah and Alam, 2014c). The conditional probability of damage can be expressed as

$$Fragility = P[LS|IM = y] \qquad (4.1)$$

where limit state (*LS*) is the specified damage level of the structure at the given ground motion intensity measure (*IM*) and *y* is the realized condition of the ground motion intensity measure. Current seismic performance assessment of structures are leaning towards the fragility analysis since it describes the likelihood of damage to the structure exceeding a certain level.

The demand placed on the structure to satisfy a specific performance level by a ground motion intensity measure is displayed by fragility plots. Probabilistic seismic demand model (*PSDM*) is used to correlate the *EDP* and the *IM*. Two common approaches to develop *PSDM* are the scaling approach (Alam et al. 2012; Zhang and Huo, 2009) and the cloud approach (Choi et al., 2004; Mackie and Stojadinović, 2004; Nielson and DesRoches, 2007a, 2007b). In the current study, the cloud method is employed in evaluating the seismic fragility functions of the bridge piers. Maximum drift in the bridge pier is considered as the *EDP*, and the *PGA* of each ground motion is taken as *IM*. Various choices of *IM* such as *PGA*, peak ground velocity (*PGV*), Arias intensity (*AI*), spectral acceleration (S_a), spectral displacement (S_d) at first mode period are proposed by several researchers; but PGA is acknowledged as the most effective and optimum *IM* (Padgett and DesRoches, 2008). The logarithmic correlation between median *EDP* and *IM* can be expressed as below assuming the power law function in the cloud approach from Cornell et al. (2002).

$$EDP = a\,(IM)^b \; or, ln\,(EDP) = ln\,(a) + b\,ln\,(IM) \qquad (4.2)$$

where a and b are coefficients, which can be estimated from a regression analysis from *IDA*. Gardoni et al. (2003) recommended that the *EDPs* follow the log-normal distribution. The dispersion of the demand, $\beta_{EDP|IM}$ can be estimated from Equation 3 (Baker and Cornell, 2006).

$$\beta_{EDP|\,IM} = \sqrt{\frac{\sum_{i=1}^{N}(\ln(EDP)-\ln(aIM^b))^2}{N-2}} \qquad (4.3)$$

where N= number of total simulation cases.

Fragility curves are generated using the following equation from Padgett (2007).

$$P[LS|IM] = \Phi[\frac{\ln(IM)-\ln(IM_n)}{\beta_{comp}}] \qquad (4.4)$$

where $\Phi[\,]$ is the standard normal cumulative distribution function and

$$ln(IM_n) = \frac{\ln(S_c) - \ln(a)}{b} \quad (4.5)$$

IM_n is defined as the median value of the intensity measure for the selected damage states, which are discussed in the next section. The dispersion component is presented in Equation 4.6 (Padgett, 2007).

$$\beta_{comp} = \frac{\sqrt{\beta_{EDP|IM} + \beta_c^2}}{b} \quad (4.6)$$

$$\beta_c = \sqrt{\ln(1 + COV^2)} \quad (4.7)$$

where S_c is the median and β_c is the dispersion value for a particular damage state of bridge component. The dispersion is calculated using the Equation 4.7 (Nielson, 2005). The coefficient of variation (*COV*) is assigned to each damage state for associated uncertainty. Smaller values of *COV* are assumed for slight and moderate damage states ($COV_{slight} = COV_{moderate} = 0.25$) and larger values for the higher damage states ($COV_{extensive} = COV_{collapse} = 0.5$) (Billah and Alam, 2014a).

4.3 Limit States (LSs)

Damages in the bridges can be experienced by service disruption like cracking and spalling of concrete or in the form of collapse like crushing of concrete. Any damage can cause service interruption and economic loss. Cracking in concrete and spalling of concrete cover occur during small to moderate earthquakes. No life safety concern is associated with this serviceability limit states. At an extreme event with less probability, significant damage can happen to the confined core concrete through crushing and fracture of the previously buckled rebars (Goodnight et al., 2015). Life safety and collapse limit state are portrayed by the later damage conditions. In an experimental investigation of the load history protocol and design parameters on the performance limit of circular bridge piers, Goodnight et al. (2015) found the damage sequence in RC columns as cracking in concrete, yielding of longitudinal rebars, crushing of concrete cover, yielding of confining steel, buckling of longitudinal rebars and fracture of the previously buckled reinforcements.

4.3.1 FEMA LSs

Limit states (*LSs*) are defined on different types of *EDPs* such as bridge pier ductility, pier displacement, isolation bearing displacement, bearing shear strain percentage, pile displacement, and abutment displacement. HAZUS-MH (FEMA, 2003) defined four limit states (slight, moderate, extensive and collapse), which are most commonly used in seismic fragility analysis. In this study, *LSs* are measured from static pushover analysis on bridge pier drift capacity. Drift percentage at the initiation of cracking, yielding of longitudinal steel, spalling of concrete cover and crushing of core concrete are considered as slight, moderate, extensive and collapse limit states for the bridge piers respectively. Material strain levels are defined to predict the damages in the bridge piers. The cracking strain of concrete is considered 0.0014 and the concrete spalling are assumed to occur at a compressive strain of 0.004 as recommended by Priestley et al. (1996). Longitudinal rebar yields at 0.0021 strain calculated from the yield strength and elastic modulus of steel. Paulay and Priestley (1992) suggested equation, $\varepsilon_{cu} = 0.004 + 1.4\rho_s f_{yh}\varepsilon_{sm}/f'_c$ is used in defining the crushing strain of concrete. Here, ε_{sm} = steel strain at maximum tensile stress (0.14); f'_c= concrete compressive strength (35 MPa); f_{yh} = yield strength of transverse steel (400 MPa); and ρ_s = volumetric ratio of spiral (2.2%). The crushing strain of concrete is found to be 0.057, which exceeds the limit 0.05 founded by Paulay and Priestley (1992). Very high importance factor (I=3) due to the significance of lifeline bridge and lower force reduction factor (R=3) due to single column design led to very high shear force demand and high transverse reinforcement ratio. However, the maximum limit proposed by Paulay and Priestley (1992) for the crushing of concrete is considered in this study. Different limit states are shown on the static pushover analysis curve for bridge piers F_35/415, P_35/415_s, and P_35/415 (Figure 4.1a). Yielding in bridge columns happens at a displacement 42 mm, 31 mm and 46 mm respectively for F_35/415, P_35/415_s, and P_35/415. From the incremental dynamic analysis of the bridge columns, the median values for yield displacement are found 44.5 mm, 32.6 mm and 48.1 mm (Table 4.1). The variations in yield deformation results from static analysis and *IDA* are only 5.95%, 5.16%, and 4.57% respectively for F_35/415, P_35/415_s, and P_35/415 piers. In case of crushing displacement, the variation becomes 2.41%, 1.56% and 1.98% for F_35/415, P_35/415_s and P_35/415 piers correspondingly (Table 4.1). These small variations testify the reasonable accuracy of damage state definition form static pushover analysis. Summary of different *LSs* physical appearance and criteria are presented in Table 4.2.

Table 4.1 Comparison of *IDA* and *ISPA* performance

Pier ID	Yielding		Crushing	
	Median yield displacement (mm)	Yield displacement from *ISPA*	Median crushing displacement (mm)	Crushing displacement from *ISPA*
F_35/415	44.5	42	250.9	245
P_35/415_s	32.6	31	214.3	211
P_35/415	48.1	46	257.0	252

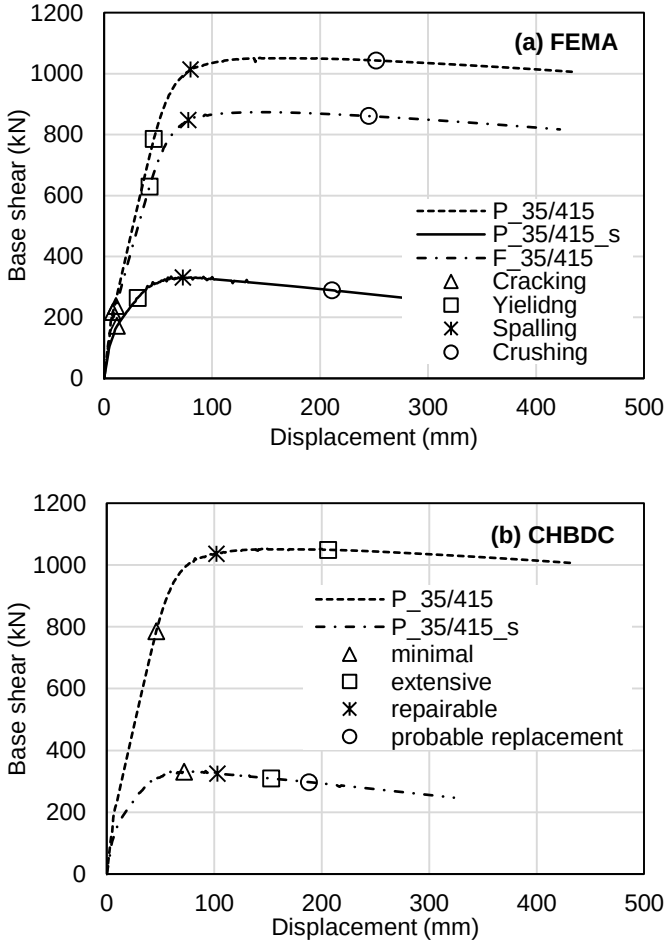

Figure 4.1 Limit states from pushover analysis

Table 4.2 Damage states of bridge piers following FEMA

Limit State	Physical Phenomenon (FEMA, 2003)	F_35/415		P_35/415_s		P_35/415	
		Displacement (mm)	Drift %	Displacement (mm)	Drift %	Displacement (mm)	Drift %
Slight	Cracking and minor spalling	11	0.21	12	0.23	8	0.15
Moderate	Moderate cracking and spalling	42	0.80	31	0.59	46	0.88
Extensive	Degradation without collapse	78	1.49	73	1.39	80	1.52
Collapse	Failure leading to collapse	245	4.67	211	4.02	252	4.80

4.3.2 CHBDC LSs

The damage states in CHBDC 2014 and the supplement to CHBDC 2014 are defined as minimal, extensive, repairable and probable replacement. The damage criteria and corresponding drift limits are shown in Table 4.3. Fig. 4.1b portrays the damage states over the pushover curves for the PBD bridge piers. For the P_35/415 bridge pier, no quantitative limit is specified in CHBDC 2014 for probable replacement of the bridge pier. Bridge pier designed following the Supplement to CHBDC 2014 criteria is likely to experience extensive damage at a drift of 2.91% and may need to be replaced when the drift reaches to 3.58%. On the other hand, the P_35/415 pier designed according to CHBDC 2014 performance criteria encounters only extensive damage at 3.92% drift.

CHBDC 2014 defines material strain limit for different serviceability conditions. However, no damage limit is defined to represent the cracking or slight damage in CHBDC 2014 (Zhang,

2015). Spalling of concrete is mostly related to the minimal damage specified in CHBDC 2014. Yielding is also defined as a criterion for minimal damage though spalling in concrete does not start onset of steel yielding (Zhang, 2015). To avoid such incertitude, limit states are defined following both the CHBDC specified criteria and following existing methods in the literature (Billah and Alam, 2016a) to develop the fragility of the designed bridge piers.

Table 4.3 Damage states of bridge piers following CHBDC

Limit State	Quantitative performance criteria		P_35/415_s (CHBDC 2014 supplement)		P_35/415 (CHBDC 2014)	
	CHBDC 2014 supplement	CHBDC 2014	Displacement (mm)	Drift %	Displacement (mm)	Drift %
Minimal	$\varepsilon_c \leq 0.006$ $\varepsilon_y \leq 0.01$	$\varepsilon_c \leq 0.004$ $\varepsilon_y \leq \varepsilon_y$	72	1.37	46	0.88
Repairable	$\varepsilon_y \leq 0.025$	$\varepsilon_y \leq 0.015$	103	1.96	102	1.94
Extensive	$\varepsilon_{cc} \leq 0.8\varepsilon_{cu}$ $\varepsilon_y \leq 0.05$	$\varepsilon_{cc} \leq \varepsilon_{cu}$ $\varepsilon_y \leq 0.05$	153	2.91	206	3.92
Probable replacement	$\varepsilon_{cc} \leq \varepsilon_{cu}$ $\varepsilon_y \leq 0.06$ (d_b≤35M) $\varepsilon_y \leq 0.075$ (d_b>35M)	Not specified	188	3.58	-	-

Note: d_b = longitudinal bar diameter

4.4 Probabilistic Seismic Demand Models

Incremental dynamic analyses of the three bridge piers designed following three different design approaches have been carried out to determine the probability of reaching a certain damage state under near-fault ground motions. *PSDMs* are developed through regression analysis using the peak responses of the bridge piers at each *IMs* for all types of ground motions. Parameters *a*, *b* and

$\beta_{EDP|IM}$ are calculated from the regression analysis. Fragility curves for the bridge piers are established using these parameters and Equation 4.3 to 4.7.

Figures 4.2a shows the *PSDMs* for maximum drift demand of F_35/415 pier and Figures 4.2b, 4.2c displays for P_35/4151_s and P_35/415 piers respectively under near-fault motions. R-squared values are in proximity for all the *PSDMs*. Also, the r-squared values vary between 0.78 and 0.86, which indicates reasonably well correlation between the *EDP* and *IM*. The fragilities are estimated from the limiting capacity of each damage state and *PSDMs* parameters.

Table 4.4 compares the effect of different design methods on the demand models. The regression parameters from Equation 2 are presented here along with dispersion. From the table, it is clear that PBD following the new supplement to CHBDC 2014 yields higher values than FBD from CHBDC 2010 and PBD from CHBDC 2014 in case of maximum drift of the bridge pier. These explain the higher susceptibility of bridges to near-fault ground motions when designed following the PBD method from the new supplement. In comparison to F_35/415 and P_35/415, P_35/415_s shows higher intercept (ln(a)) and slope (b) of the regression model, which increases the demand placed on the bridge piers. Higher dispersion indicates the increased variation of demand values predicted by the regression models.

Table 4.4 *PSDMs* for different design methods

	F_35/415	P_35/415_s	P_35/415
EDP→	Maximum Drift %		
a	3.44	5.49	3.13
b	1.11	1.13	1.10
$\beta_{EDP\mid IM}$	0.330	0.453	0.333

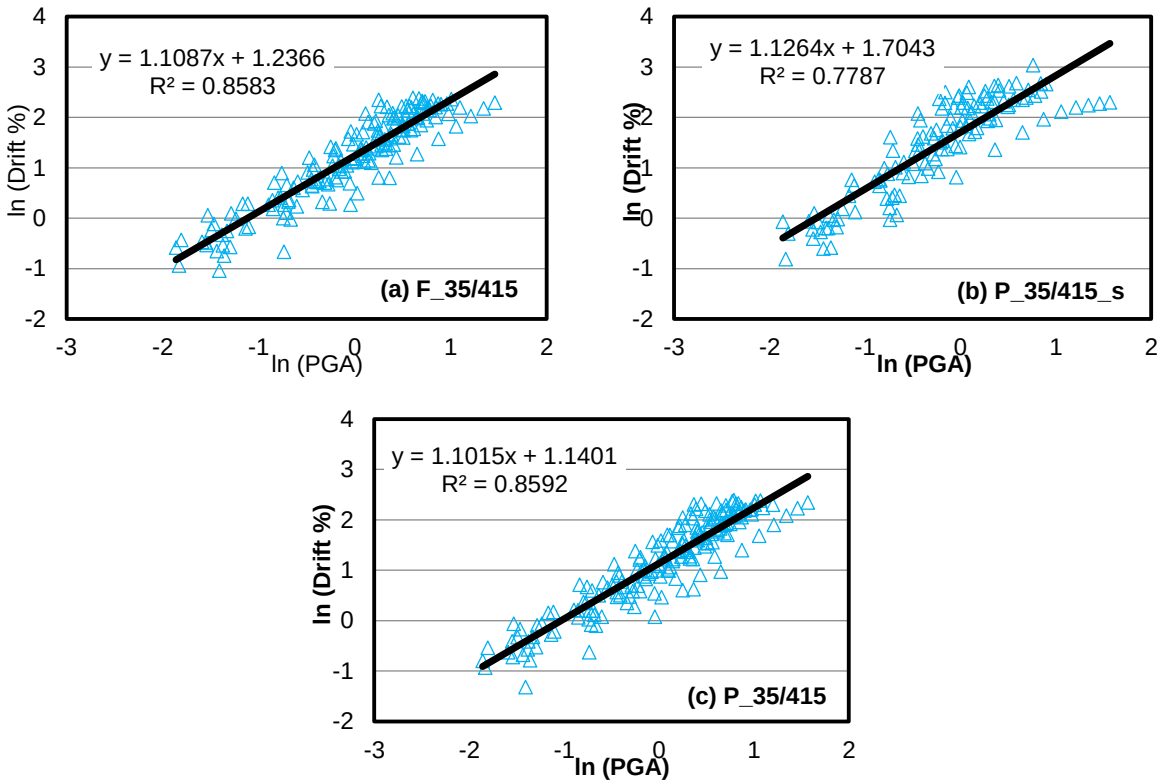

Figure 4.2 Probabilistic seismic demand models (*PSDMs*)

4.5 Fragility Analysis

Fragility functions are presented in the form of fragility curves of the designed bridge piers. *PSDMs* developed for the bridge piers are used to calculate the parameter *a* and *b*. Following the Equation from 4.3 to 4.7 and employing the limit states obtained from static pushover analysis, fragility curves for the bridge piers are generated for FEMA and CHBDC specified damage states.

4.5.1 Fragilities for FEMA specified DSs

Figure 4.3 demonstrates the fragility curves of the three reinforced concrete bridge piers designed according to force-based and PBD method specified in CHBDC for near-fault ground motions up to *PGA* 2g. Among the three piers, the PBD pier P_35/415_s designed following the supplement to CHBDC 2014 is the most vulnerable one. It is clear from Figure 4.3 that for these particular loadings, site scenario and pier configuration, the damage probability of a bridge pier lessens if PBD from CHBDC 2014 or FBD from CHBDC 2010 is employed.

At *PGA* value 1g for near-fault earthquakes, the probability of slight, moderate, extensive and collapse damage to all the bridge pier is essentially 100%. Damage in P_35/415_s starts earlier than F_35/415 and P_35/415 pier. 50% slight damage happens in F_35/415 and P_35/415_s pier at a *PGA* value as low as 0.08g and 0.07g respectively. The same damage probability is found at *PGA* 0.08g in P_35/415 pier. Extensive damage probability becomes 0.5 for the bridge column designed following CHBDC 2014 performance code at *PGA* 0.34g while for the pier designed with the FBD method from CHBDC 2010, the similar damage starts at 14.7% lower *PGA* earthquake. The PBD pier P_35/415_s is the most sensitive to damage where the 50% extensive damage possibility is found at 0.12g *PGA* (58.6% and 64.7% lower than F_35/415 and P_35/415 respectively). The behavior of bridge piers regarding collapse fragility varies substantially. Collapse probability in F_35/415 and P_35/415 piers starts just after 0.6g and 0.75g *PGA* correspondingly. However, P_35/415_s pier exhibits initiation of collapse damage at a lower *PGA* (0.25g *PGA*). At design *PGA* 0.463g, there is 12% probability that the PBD pier designed following the supplement to CHBDC 2014 will collapse. However, the FBD of the pier from CHBDC 2010 and PBD from CHBDC 2014 lower the probability to almost 0% at design *PGA* of 0.463g. The collapse in the P_35/415 pier designed following CHBDC 2014 performance codes shows strong behavior maintaining the collapse possibility to 50% at 1.89g *PGA* earthquake. Extremely high percentage of longitudinal reinforcement ratio not only increases the stiffness and yield performance, but maximum response capacity during dynamic loading also increases remarkably leading to higher ductility in structure. At *PGA* 1g, expected collapse damage risks are 13.6%, 66.4% and 6.3% for F_35/415, P_35/415_s and P_35/415 piers correspondingly.

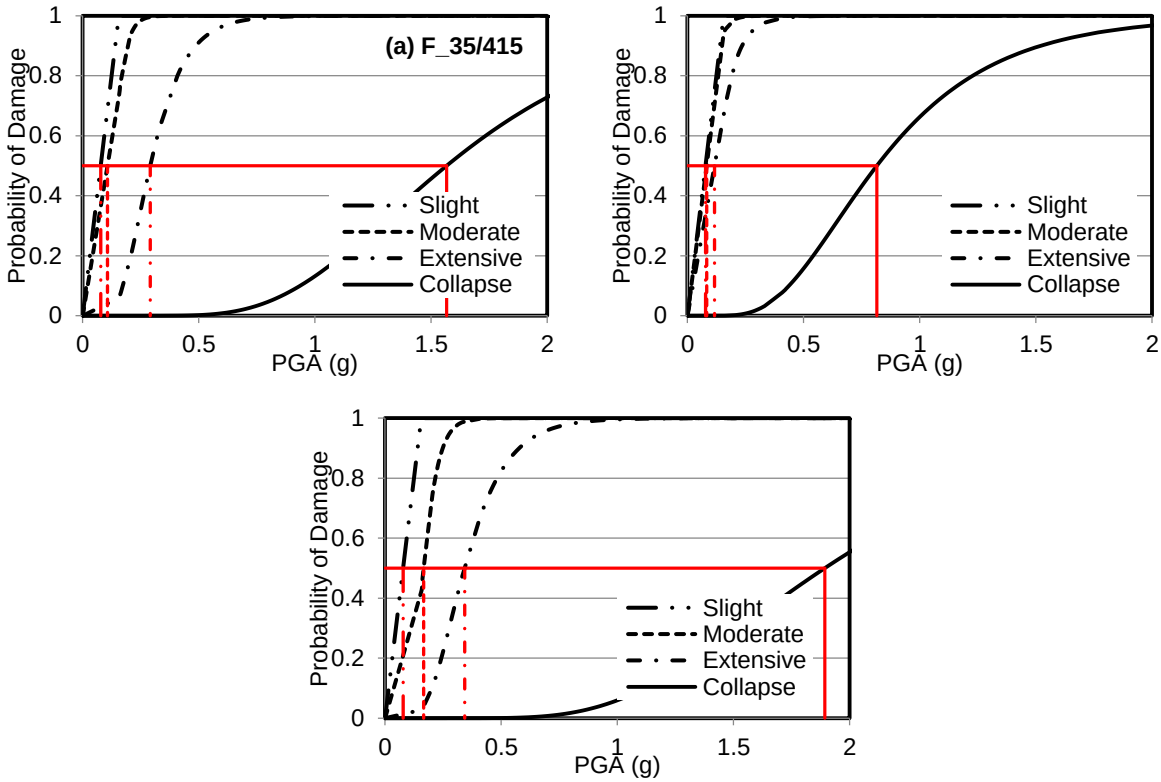

Figure 4.3 Fragility curves for FEMA specified limit states (a) FBD pier, (b) PBD pier following the supplement to CHBDC 2014 (c) PBD pier following CHBDC 2014

Table 4.5 Summary table I from fragility analysis

Pier	Design code	Damage probability	Slight damage		Moderate damage		Extensive damage		Collapse	
			PGA	% change in PGA compared to FBD	PGA	% change in PGA compared to FBD	PGA	% change in PGA compared to FBD	PGA	% change in PGA compared to FBD
F_35/415	CHBDC 2010	0.25	0.04g	-	0.06g	-	0.22g	-	1.20g	-
		0.50	0.08g	-	0.11g	-	0.29g	-	1.57g	-
		0.75	0.12g	-	0.17g	-	0.39g	-	2.06g	-
P_35/415_s	CHBDC 2014 supplement	0.25	0.04g	0	0.05g	16.7↓	0.06g	72.7↓	0.60g	50.0↓
		0.50	0.07g	12.5↓	0.08g	27.3↓	0.12g	58.6↓	0.82g	47.8↓
		0.75	0.11g	8.3↓	0.12g	29.4↓	0.18g	53.8↓	1.13g	45.1↓
P_35/415	CHBDC 2014	0.25	0.04g	0	0.09g	50.0↑	0.26g	18.2↑	1.43g	19.2↑
		0.50	0.08g	0	0.17g	54.5↑	0.34g	17.2↑	1.89g	20.4↑
		0.75	0.12g	0	0.21g	23.5↑	0.45g	15.4↑	2.50g	21.4↑

Table 4.6 Summary table II from fragility analysis

Pier	PGA	Slight damage		Moderate damage		Extensive damage		Collapse	
		Damage probability	% change in damage compared to FBD	Damage probability	% change in damage compared to FBD	Damage probability	% change in damage compared to FBD	Damage probability	% change in damage compared to FBD
F_35/415	0.25g	1.00	-	0.98	-	0.38	-	0	-
	0.5g	1.00	-	0.99	-	0.91	-	0.01	-
	1.0g	1.00	-	1.00	-	0.99	-	0.13	-
	1.5g	1.00	-	1.00	-	1.00	-	0.46	-
P_35/415_s	0.25g	1.00	0	0.99	1.0↑	0.92	142.1↑	0.01	100↑
	0.5g	1.00	0	0.99	0	0.99	8.8↑	0.16	150↑
	1.0g	1.00	0	1.00	0	1.00	1.0↑	0.66	407.7↑
	1.5g	1.00	0	1.00	0	1.00	0	0.89	93.5↑
P_35/415	0.25g	1.00	0	0.90	8.2↓	0.22	42.1↓	0	0
	0.5g	1.00	0	0.99	0	0.83	8.8↓	0	100↓
	1.0g	1.00	0	1.00	0	0.99	0	0.06	53.8↓
	1.5g	1.00	0	1.00	0	1.00	0	0.29	36.9↓

Fragility performances of the bridge piers are summarized in tabulated form as displayed in Table 4.5 and Table 4.6. *PGAs* that cause 25%, 50% and 75% probability of different damage levels for force-based and PBD column are outlined in Table 4.5. Percentage variation in *PGA* for PBD pier compared to FBD pier are also presented. Likewise, damage probability and their variation at 0.25g, 0.5g, 1g and 1.5g *PGA* seismic motions are compiled in Table 4.6. It is apparent that from the tables that the damage probability decreases when PBD method from CHBDC 2014 and FBD method from CHBDC 2010 are adopted; especially the collapse performance improves significantly. Current PBD practice following CHBDC 2104 supplement decreases ground motion intensity requirement 12.5% for 50% slight damage, 52.9% for 50% moderate damage, 64.7% for 50% extensive damage and 56.6% for 50% collapse probability of bridge pier compared to PBD method from CHBDC 2014. The P_35/415 pier designed following CHBDC 2014 performance criteria takes roughly 54.5%, 17.2%, and 20.4% higher intensity earthquake for similar moderate, extensive and collapse damage probability than F_35/415 pier. Though the supplement to CHBDC 2014 provides performance criteria in such a way to ensure economic feasibility and reduced construction hindrance due to reinforcement congestion, very low longitudinal reinforcement resulted from relaxed criteria and comparatively poor seismic performance, make the supplement to CHBDC 2014 less attractive for a lifeline bridge pier. Table 4.6 demonstrates that at high-intensity earthquakes, FBD from CHBDC 2010 can also noticeably decrease the slight, moderate and extensive damage probabilities. Besides, at low-intensity motion (0.5g *PGA*), collapse probability reduces significantly in F_35/415 and P_35/415 pier compared to P_35/415_s pier.

4.5.2 Fragilities for CHBDC specified DSs

Fragilities of the PBD bridge piers following the CHBDC damage states are presented in Fig. 4.4. Minimal, repairable and extensive damage limits are indicated quantitatively in CHBDC 2014 (CSA, 2014), and the damage probabilities of P_35/415 pier are displayed in Fig. 4.4b. There is 50% probability of minimal, repairable and extensive damage at 0.17g *PGA*, 0.51g *PGA* and 1.4g *PGA* earthquake respectively when the bridge pier is designed following CHBDC 2014. The bridge pier P_35/415_s shows the same minimal damage at *PGA* 0.12g. Since the minimal damage criteria changed from steel yielding to 0.01 strain limit in steel in the newly published supplement, it increased the minimal damage drift to 1.37% from 0.88% (Table 4.3). However, the minimal damage fragility increases due to lower reinforcement demand in the bridge pier P_35/415_s.

Likewise, the other damage case scenarios are also similar. 50% repairable and 50% extensive damage probability happens at 56.8% and 45.7% lower *PGA* earthquakes in P_35/415_s pier than that of P_35/415 pier. The relaxed performance criteria in the supplement to CHBDC 2014 leads to lower longitudinal reinforcement ratio. This reduced main reinforcement increases the seismic damage vulnerability in the bridge pier. 0.76g *PGA* ground motion shows 50% damage probability that may cause failure to the pier P_35/415_s and necessitate the replacement. At *PGA* 1g, the repairable and extensive damage probability in pier P_35/415_s are 100% and 96% respectively. Whereas, for P_35/415 pier these probabilities are 98% (2% lower) and 21% (78% lower) correspondingly.

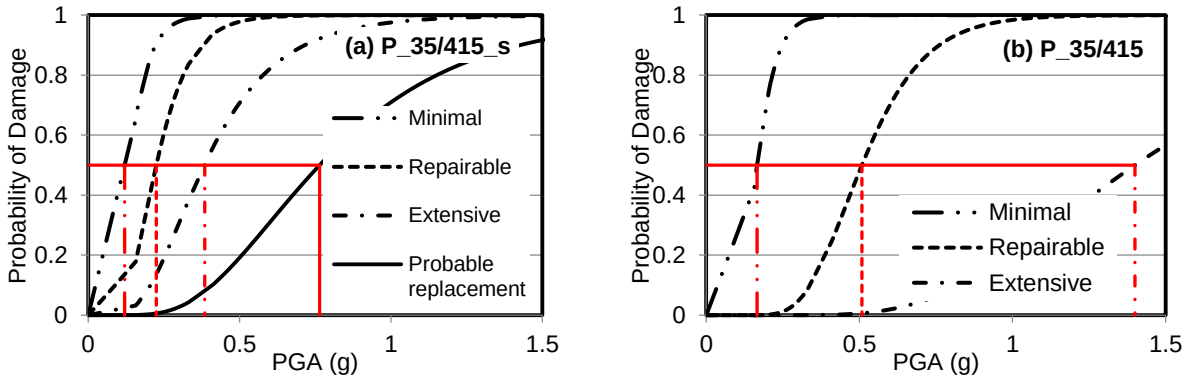

Figure 4.4 Fragility curves for CHBDC limit states (a) PBD pier following the supplement to CHBDC 2014 (b) PBD pier following CHBDC 2014

4.6 Summary

Fragility analyses of the lifeline bridge piers designed following the FBD and PBD approaches are carried out and presented in this section. Designing the bridge pier according to the supplement to CHBDC 2014 yielded only 1.22% longitudinal reinforcement ratio whereas the highly conservative CHBDC 2014 performance criteria and the FBD from CHBDC 2010 guidelines resulted in 6.1% and 4.87% longitudinal reinforcement correspondingly. It is evident that the seismic vulnerability of these bridge piers will be different due to their main reinforcement ratio. Damage states are defined individually for each bridge pier from static pushover analysis. *PSDMs* are developed from the *IDA* results, and fragility curves are plotted using equations described in this chapter. The following outcomes are summarized from this section.

- Limit states of the bridge pier can be defined from static pushover analysis with reasonable accuracy. The median yield displacement and median crushing displacement of the designed bridge piers obtained from *IDA* are in proximity to the corresponding values derived from inelastic static pushover analyses plots.
- CHBDC specified damage states for bridge piers are minimal, repairable, extensive and probable replacement. Definite performance criteria for concrete cracking and slight damage are absent in CHBDC performance guidelines. Minimal damage is associated with steel yielding and concrete strain of 0.004 as stated in CHBDC 2014, which is dubious. No specific criteria present in the CHBDC 2014 for collapse or probable replacement of bridge pier. The supplement to CHBDC 2014 has quantified all the damage criteria with noticeable modifications.
- For the bridge pier P_35/415 designed following CHBDC 2014, the damage states in term of maximum drift are found 0.88%, 1.94%, and 3.92% respectively for minimal, repairable and extensive damage. For the pier P_35/415_s, the similar *LSs* are calculated at 1.37%, 1.96%, 2.91% and 3.58% for the probable replacement.
- Limit states are developed using FEMA mentioned physical phenomenon. All the slight, moderate, extensive and collapse damage limits are tabulated in Table 4.2. Collapse criteria of FBD and PBD bridge piers vary significantly.
- Bridge pier designed following CHBDC 2014 code shows lowest seismic vulnerability considering the *LSs* from both FEMA and CHBDC. The pier P_35/415_s designed according to criteria from the supplement to CHBDC 2014 shows higher damage probability than P_35/415 due to lower reinforcement ratio. The performance in term of fragility is much better in the FBD bridge pier F_35/415 than the P_35/415_s pier. *PGA* at 50% collapse probability decreased about 47.8% when the new performance criteria used than that of traditional FBD method. Moreover, at *PGA* 0.5g, the collapse possibility increases about 150%. The newly published performance criteria in the supplement to CHBDC 2014 can be used in designing lifeline bridge piers for economic benefit, but the seismic performance is not even with the FBD pier from CHBDC 2010 and the PBD pier from CHBDC 2014.

Chapter 5 : EFFECT OF REINFORCING STEEL STRENGTH ON THE PERFORMANCE-BASED DESIGN OF BRIDGE PIER

5.1 Background

Reinforcement in RC structure is a critical ingredient that can control the behavior of the structure during a seismic event. Very limited number of research are available in the literature on the dynamic behavior of RC structural elements reinforced with high strength steel under simulated earthquake loading. To date, there is no research has been published on the effect of reinforcing steel strength on the PBD of bridge column. A number of ASTM steel grades are available to design bridge piers. However, it would be time-consuming and pricey to test the dynamic performance of bridge components to investigate the effect of steel strength and ductile properties. Simulating with proper validation can give an insight on the seismic performance of the RC bridge piers before in-field applications.

This chapter focuses on the performance of a lifeline bridge pier designed following the CHBDC 2014 and reinforced with various ASTM grade longitudinal steel rebars and varying concrete strength. The geometric and design details of the studied bridge pier are elaborately discussed with appropriate simulation technique. Twenty ground motions are selected from PEER ground motion database (PEER, 2011) to assess the performance of the designed bridge pier through dynamic analysis. Responses of the bridge piers are plotted in terms of *IDA* curves and fragility curves to apprehend the effect of reinforcing steel and concrete strength on the PBD of the bridge pier.

5.2 Bridge Pier Geometry

The bridge pier considered in this study is a circular reinforced concrete bridge pier located in Vancouver, BC and is seismically designed first following CHBDC 2010 (CSA, 2010). The considered bridge is a lifeline bridge. In the event of the design earthquake (return period of 475 years), a lifeline bridge needs to remain open for immediate use to all traffic as per CHBDC 2010. Therefore, the piers need to be designed to achieve this targeted performance. According to CHBDC 2010, the importance factor of I=3 and the response modification factor of R=3 are considered for this lifeline bridge. The diameter of the column designed is fixed to be 1.83 m.

Plastic hinge length is calculated 1.83m, equal to the diameter of the bridge pier, which is greater than 450mm and one-sixth of the clear height of the pier. Figure 5.1 shows the elevation and cross-section of the bridge pier. The FBD of the column yielded reinforcement of 48-25M longitudinal rebars and 16 mm diameter spirals at 76 mm pitch in the plastic hinge length and 100 mm outside the plastic hinge length with a 50 mm clear cover. The height of the pier is 9.14m with an aspect ratio of 5, which ensured the flexure dominated behavior. A constant mass of 850 ton is applied at the top to represents the weight of the superstructure. The yield strength of the spirals is considered 400MPa and the modulus of elasticity for all reinforcements are fixed at 200GPa. For the PBD, all the transverse reinforcement details are regarded invariable except the concrete and longitudinal reinforcement properties and details.

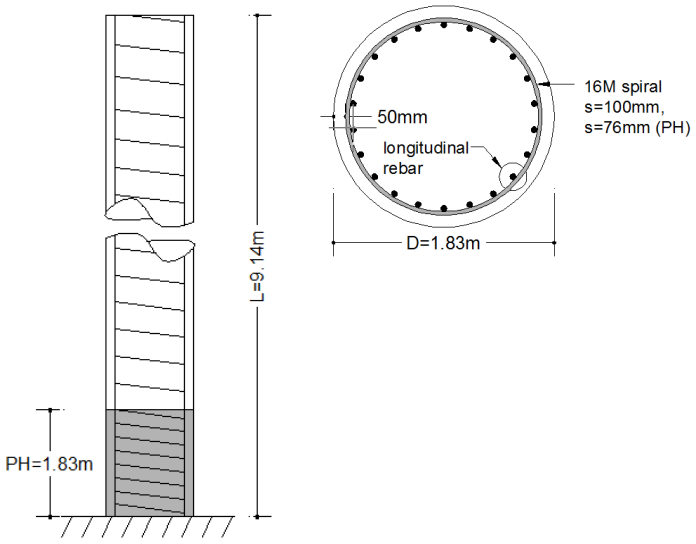

Figure 5.1 Elevation and cross-section of the reinforced concrete bridge pier

5.3 Material Properties

High strength concrete in construction is very common due to improved performance of structural members benefited from higher compressive strength and greater elastic modulus. Reduced member sections appeal the designers in using high strength concrete. Incorporation of high strength steel in design has the potential to reduce RC section leading to economic design. Combination of three ASTM steel grades and concrete of different compressive strength are selected in this study to design the bridge piers before assessing their seismic performance.

5.3.1 Steel

High strength steel rebars are characterized by lower carbon than that of low strength steel rebars. Chromium content is higher in HSR like ASTM A1035 to provide higher tensile properties compared to ASTM A615 steel. The actual stress-strain plots for various grade steel tested in WJE laboratories are shown in Figure 5.2 (Graham and Paulson, 2008). Monotonic axial compression testing was carried out in accordance to ASTM E9. The total elongation was measured over a gauge length of 8 inches. It displays the fracture elongation or increase in length over 8 inches gauge length.

As displayed in Figure 5.2, ASTM A1035 (Grade 100 and Grade 120) steel bar exhibits a linear trend in stress-strain plots up to 600MPa. A well-defined yield plateau is absent in the stress-strain curve of ASTM A1035 steel bars. The 2% offset method is usually used to find out the yield strength of steel grade equal and higher to 100. The maximum tensile strength reached beyond 1000MPa at strain range of 0.04 mm/mm to 0.06 mm/mm. Fracture elongations of the ASTM A1035 rebars were found 7.35% and 7.09% for Grade100 and Grade120 rebars respectively. The total elongation of steel rebar can vary from 0.08 to 0.10 for ASTM A1035 steel (Graham and Paulson, 2008).

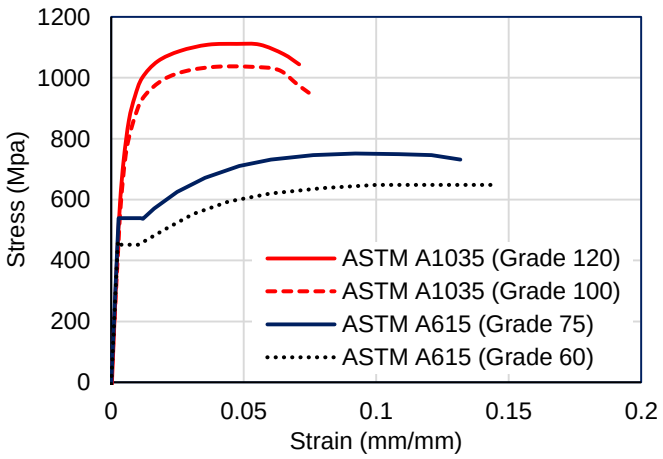

Figure 5.2 Stress-strain curves for various grades of steel rebar (from Graham and Paulson, 2008)

In this current study, the three types of steel grade are considered and combined with three different strength concrete in designing the bridge piers and analyzing them under earthquake

loadings. Minimum yield strength specified by ASTM are used in the analyses. However, total elongation of the steel rebars are taken from Graham and Paulson (2008) described stress-strain curves (Figure 5.2) to account for the ductility of the actual case scenario. Though the fracture elongation depends on the bar diameter, for simplicity uniform fracture percentage are considered irrespective of assigned diameter. The total elongation for ASTM A615 Grade 80 rebars is assumed 12.25% from the mean of the total elongation test data presented in Overby et al. (2015).

Table 5.1 Material properties of the steel grades used in analysis

ASTM Grade	Designation	Yield strength (ksi)	Yield strength (MPa)	Total elongation
60	A 615	60	415	14.3%
80	A 615	80	550	12.25%
120	A1035	120	830	7.09%

5.3.2 Concrete

Three different concrete strengths of 35MPa, 50MPa, and 70MPa are used in designing the lifeline bridge pier. Table 5.2 shows the typical properties of the concrete. To find out the concrete strain at peak stress, several researchers proposed linear relationship as a function of the compressive strength of concrete. For normal strength concrete, strain at peak stress is proximity to 0.002. However, for high strength concrete, linearity in the ascending branch of stress-strain curve is larger causing higher strain at peak stress (Attard and Setunge, 1996). The equation $\varepsilon_c = \frac{f_c'}{E_c}\frac{4.26}{\sqrt[4]{f_c'}}$ is used in determining the strain at peak stress from Setunge (1993) for crushed aggregate. Here, f'_c is the compressive strength of concrete (MPa) and E_c is the elastic modulus of concrete (MPa) calculated using the simplified formula $E_c = 4700\sqrt{f_c'}$ provided by ACI 318 (ACI, 1983) for normal-weight concrete. Splitting tensile strength is predicted using the recommended equation $f_{sp}' = 0.59\sqrt{f_c'}$ MPa from ACI (1984).

Table 5.2 Concrete properties used in analysis

Compressive strength (MPa)	Tensile splitting strength (MPa)	Elastic modulus (MPa)	Strain at peak stress
35	3.5	27806	0.00221
50	4.17	33234	0.00241
70	4.94	39323	0.00262

5.4 Design of Bridge Pier

Changed reinforced percentage possesses a significant effect on the stiffness of the structural member. During calculation of displacement demand, the effective or cracked stiffness of the structure should be incorporated. The pre-cracking response of a member is governed by the gross moment of inertia and concrete modulus, but the post-cracking behavior largely relies on the cracked moment of inertia, which depends on the longitudinal reinforcement percentage. There are two apparent methods of designing an RC member to avoid congestion of reinforcement, (1) increasing the member section dimension to make room for reinforcements, which is not an economically efficient solution and (2) decreasing longitudinal reinforcement ratio providing high strength steel. However, ACI 318 and AASHTO limits the design of longitudinal reinforcement with Grade 100 and Grade 120 reinforcement. Grade 100 steel is allowed in designing transverse reinforcements for seismically active regions. Reducing the number of reinforcement with HSR can lead to higher displacement demand due to lower flexural stiffness. A study from Rautenberg (2011) defended the concept that the initial stiffness is the driving parameter for peak drift of RC members. Laughery (2016) experimentally tested two different types of portal frames reinforce with conventional and high strength steel to check the same hypothesis. He found that the peak response of the RC structure is depended on the initial stiffness calculated from gross cross-sectional properties. He also concluded that reducing reinforcement ratio associated with HSR does not necessarily cause larger peak drift since the variation in stiffness was not large. Elastic stiffness ratios are assumed from Figure 5.3 as explained in Paulay and Priestley (1992) to calculate the cracked moment of inertia of the bridge pier sections.

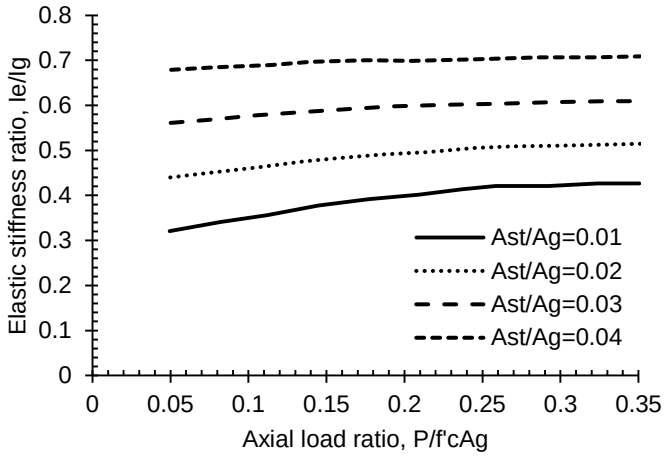

Figure 5.3 Determination of elastic stiffness ratio for circular section (from Paulay and Priestley, 1992)

5.5 Analytical Model

To get a realistic presentation of seismic response under earthquake loading, an accurate analytical model is essential that can capture both material and geometric non-linearities. A fiber element approach is employed in modeling the bridge piers using finite element analysis program SeismoStruct (SeismoStruct, 2015). The Menegotto-Pinto model (Menegotto and Pinto, 1973) for reinforcing steel and Mander et al. (1988) model is considered in modeling steel and concrete. The concrete model has the ability to consider the confinement effect on the core concrete. Recent work from Laughery (2016) employed the Manegotto-Pinto model to predict the behavior of high strength steel in concrete members. Details of the model are shown in Figure 5.4. The stress and related strain are derived using the Equations 5.1 and 5.2. The assumptions of Manegotto and Pinto (1973) steel model were: (a) time independent constitutive law of material, (b) concrete contribution in tension was ignored, (c) strain vary linearly along the section depth., (d) Bauschinger effect of steel was considered, yet material properties were assumed to be same after repeated loading, and (e) no shear stress action was considered.

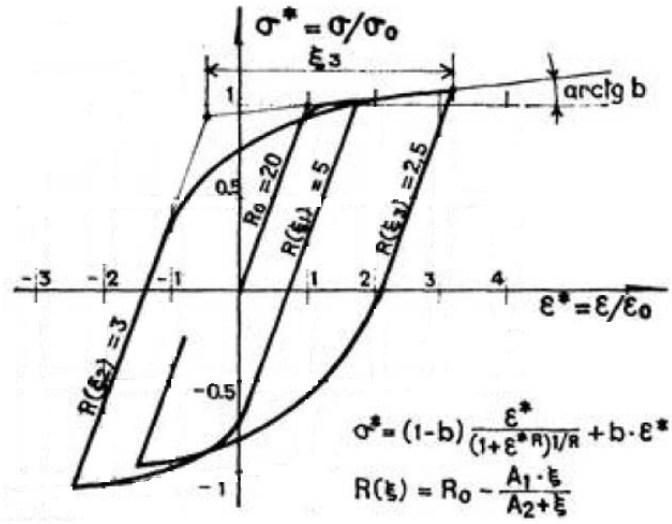

Figure 5.4 Steel model under cyclic loading (Manegotto and Pinto, 1973)

$$\varepsilon_s^* = \left|\frac{\varepsilon_s}{\varepsilon_{s0}}\right| \qquad (5.1)$$

$$\sigma_s = \left(k_s\varepsilon_s^* + \frac{(1-k_s)\varepsilon_s^*}{(1+\varepsilon_{s^*}^R)^{\frac{1}{R}}}\right)\sigma_{s0} \qquad (5.2)$$

where ε_s = steel strain, σ_s = steel stress, ε_s^* = normalized steel strain, ε_{s0} = steel strain at intersection of initial modulus line and tangent modulus at ultimate, σ_{s0} = steel stress at intersection of initial modulus line and tangent modulus at ultimate, $k_s = E_{s\infty} / E_s$, ratio of tangent modulus at ultimate to initial modulus, R_o = parameter defining the shape of the curve.

The parameters ε_{s0}, σ_{s0}, k_s, and R_o are usually adjusted to conform the stress-strain behavior of steel from tests. Program default values for the calibration parameters are considered in this study. The 3-D inelastic beam-column element is used in modeling the bridge pier. Circular section is divided into 400 discrete segments as shown in Figure 5.5c. The software can predict large deformation behavior of structural elements. The whole bridge pier is modeled in thirteen segments. Nodes are closely packed in the plastic hinge location of the bridge pier at a spacing of 250mm and about 1000mm in rest of the location. Lumped mass and 10% axial load are applied at the top of the bridge piers. Soil-structure interaction is not considered in this study, and the base is modeled fixed. The modeling details are presented in Figure 5.5. The accuracy of the program

in modeling and predicting the experimental behavior of RC bridge columns made of varying material properties are discussed in details in Chapter 3.

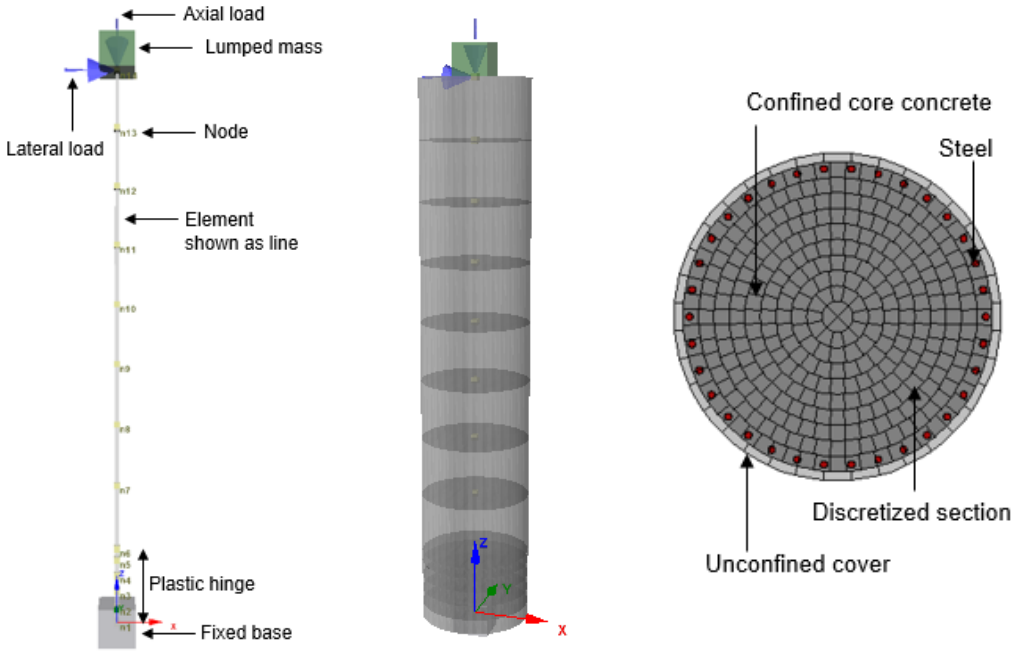

(a) (b) (c)

Figure 5.5 Finite element modeling of bridge pier (a) 2-D model, (b) 3-D elevation and (c) section model

5.6 Performance-Based Design Following CHBDC 2014

The PBD of bridge pier is based on the target performance objectives defined in CHBDC 2014. These performance criteria are presented in terms of strain in concrete and steel. Material strain more explicitly depicts the performance of structural elements than drift. However, material strain level can be correlated to associated drift in bridge pier. According to CHBDC 2014, a lifeline bridge should experience minimal damage for earthquakes with return periods of 475 years and 975 years. The damage should be repairable in a seismic event with 2475 years of return period. The minimal damage and repairable damages in the new supplement to CHBDC 2014 are defined by $\varepsilon_c \leq 0.004$ and $\varepsilon_s \leq \varepsilon_y$, and $\varepsilon_s \leq 0.015$ respectively. Here, ε_c is the compressive strain in concrete, ε_s is the tensile strain in reinforcing steel bars, and ε_y is yielding strain of steel rebar. Primary design is based on the FBD. Displacement demand on the bridge pier is calculated from

the fundamental time period of bridge pier for different hazard and performance levels. Bridge pier is subjected to static pushover loading targeting the expected displacement demand and checked for the performance criteria. This is an iterative process. The longitudinal reinforcement ratio is continually increased until the performance criteria are met for certain hazard level earthquake. Figure 5.6 portrays the pushover curves for the PBD bridge piers using different grade steel reinforcements and concrete strength. Material strain and displacement demands are also shown on the plots. As can be seen from the figures, the dominant performance criteria in designing bridge piers following CHBDC 2014 is the damage should be minimal in a seismic event with a probability of 5% in 50 years. A typical label for a bridge pier is PX/Y where P stands for the PBD, X shows the concrete compressive strength in MPa and Y is the yield strength of steel in MPa. A total of nine combinations are selected to design the lifeline bridge pier. The design outcomes and details of longitudinal reinforcement are presented in Table 5.3. It is obvious that with increment in steel grade, required reinforcement percentage will go lower. Use of Grade 60 reinforcement yields 3.58% longitudinal reinforcement. Whereas, employing ASTM A1035 120 steel results in reinforcement ratio as low as 0.98% for 35MPa concrete. Though CHBDC does not allow reinforcement ratio less than 1% to avoid temperature and shrinkage cracking, for research purpose lower reinforcement ratios are accepted in this study. HSR like ASTM A1035 can cut the design reinforcement requirement even more than 50% without compromising the target performance in design. Whereas, Grade 80 rebars can reduce the reinforcement requirement by 40%. Increasing the concrete strength does not help much in reducing the reinforcement requirement for PBD since the design performance criteria is governed by the strain in steel. For ASTM A1035 Grade 120 reinforcement, increasing the concrete strength to 70MPa from 35MPa reduces the reinforcement ratio by 12%.

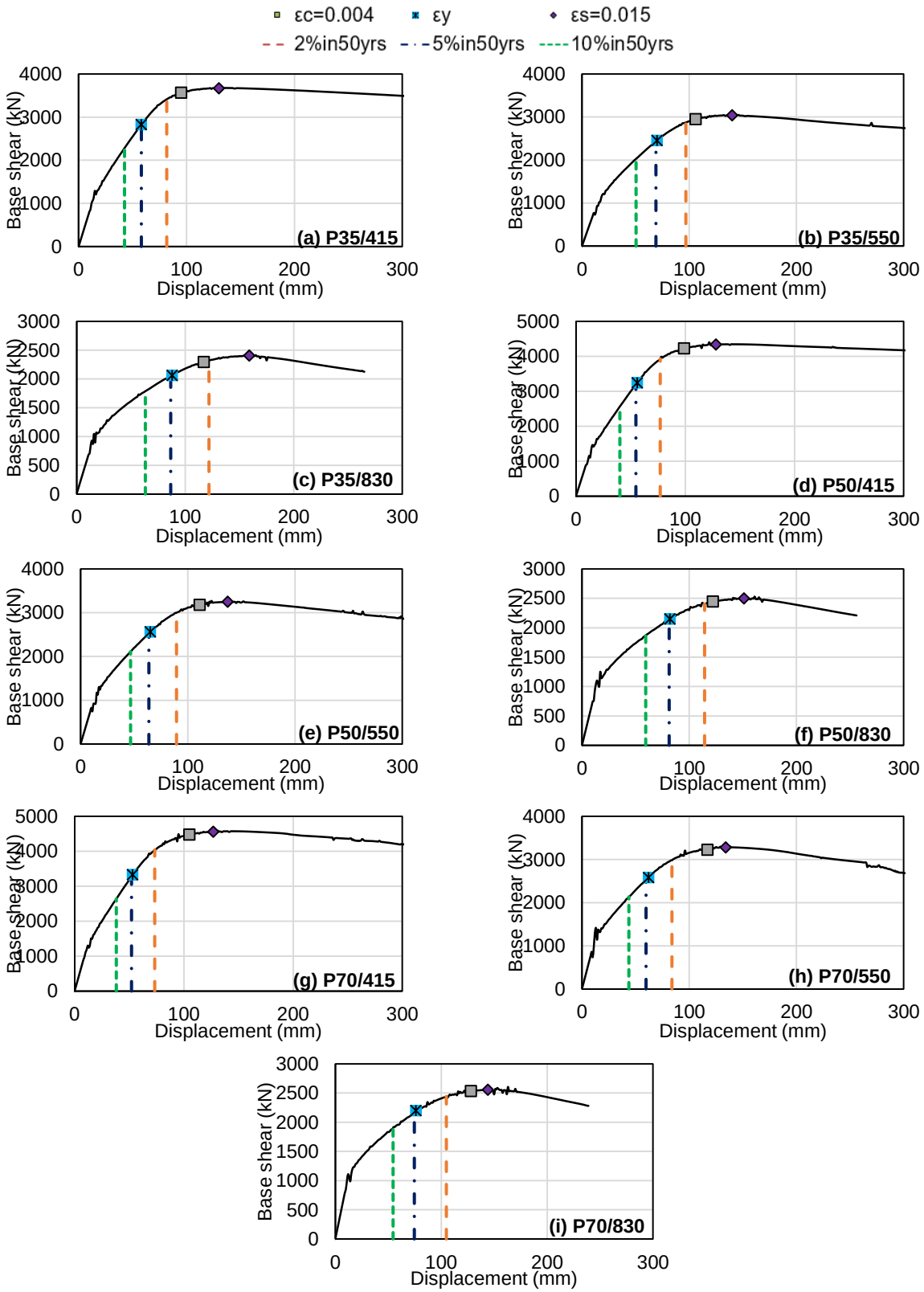

Figure 5.6 Load-displacement plot for bridge piers designed using different strength steel and concrete

Table 5.3 Design details of the bridge pier following the supplement to CHBDC 2014

ID	f'_c (MPa)	Steel grade	f_y (MPa)	Reinforcement percentage	Longitudinal rebar detail
P35/415	35	60	415	3.58%	48-50M
P35/550	35	80	550	2.1%	28-50M
P35/830	35	120	830	0.98%	32-32M
P50/415	35	60	415	4.12%	42-57M
P50/550	35	80	550	2.1%	28-50M
P50/830	35	120	830	0.92%	30-32M
P70/415	35	60	415	4.12%	42-57M
P70/550	35	80	550	1.94%	26-50M
P70/830	35	120	830	0.86%	28-32M

5.7 Moment-Curvature Relationship

Reinforcing bar number and diameter in the design of the bridge piers varied to account for the different yield strength and performance achievement. Performance criteria specified in the design code are satisfied, and they maintain a similar moment-curvature relationship for the design alternatives reinforced with similar grade steel reinforcement. Almost identical moment capacity for the Grade 120 and Grade 80 steel reinforced bridge pier sections can be noticed from Figure 5.7. Though the moment capacity increases slightly with the increase in concrete strength, the longitudinal reinforcement ratio detects the moment-curvature behavior for a section. The moment-curvature plot shows almost similar initial stiffness and post-elastic transition. The moment capacity of the section varies from 26000 kN-m to 44000 kN-m. The maximum moment capacity is observed at a curvature of 0.002 (1/m) in most of the cases.

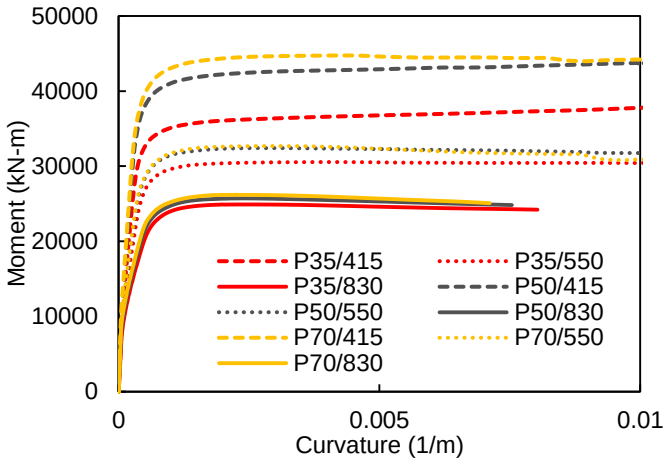

Figure 5.7 Moment-curvature relationship of designed RC bridge pier sections

5.8 Ground Motions

Twenty ground motions are selected from PEER database (PEER, 2011) as discussed in Chapter 3 to carry out the incremental dynamic analysis. The fault distances for all the ground motions are less than 10 km. Key characteristics of these motions are the *PGA/PGV* ratio that varies between 0.46 and 1.56 and the *PGA* value ranges from 0.37g to 1.07g indicating medium to strong earthquake intensity of ground motions. According to Naumoski et al. (1988), the *PGA/PGV* ratio for western Canada is close to 1. However, the 20 ground motions selected have previously been used as site-specific motions for Vancouver (Parghi and Alam, 2017). Time histories of the seismic motions are collected from PEER strong motion database (PEER, 2011). Selected ground motions are matched using the program SeismoMatch (SeismoMatch, 2014) to Vancouver design spectrum for soil class C and maximum hazard level earthquake (2% probability of exceedance in 50 years). Ground motion matching is done from time period 0.05s to 4s as suggested by Baker et al. (2011). The original ground motion spectra are presented in Figure 5.8a and the mean matched ground motions response spectrum are displayed in Figure 5.8b to match the Vancouver design spectrum.

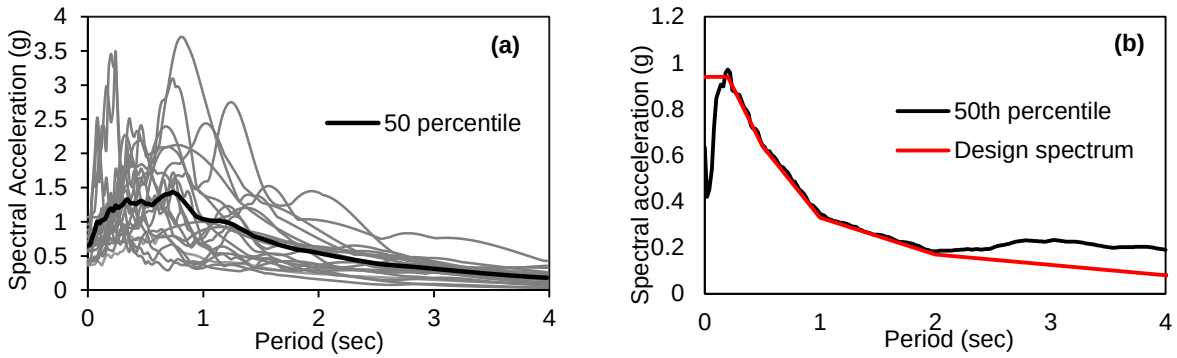

Figure 5.8 Ground motion response spectra (a) original ground motions (b) design and matched mean spectrum

5.9 Incremental Dynamic Analysis (IDA)

The PBD bridge piers reinforced with different steel strength are analyzed for the considered twenty site-specific ground motions and their *IDA* responses are plotted in Figure 5.9. *IDA* curves show the response of the bridge piers under each ground motions in term of maximum drift with varying *PGA*. Each ground motion is scaled ten times to capture the collapse behavior of the bridge piers. A single bridge pier is analyzed for 200 ground motions in that way to produce sufficient data to plot the *IDA* curves and make provision for the fragility analysis. All the plots start with somewhat similar elastic behavior before going to the non-linear range. The inelastic behaviors are quite dissimilar. Bridge piers like P35/415 and P35/550, which are reinforced with lower grade steels can take higher intensity earthquakes due to high fracture strain. The 16^{th}, 50^{th} and 84^{th} fractile plots are shown to understand their comparative performances. At certain *PGA* level 1g, 1.95%, 2.49% and 2.78% maximum drift are caused by 50% ground motions for P35/415, P35/550, and P35/830 bridge piers respectively. For bridge piers reinforce with ASTM A1035 steel experiences higher maximum drift due to decreased stiffness of the section. Increasing the concrete strength slightly reduces the reinforcement requirement, but the overall stiffness of the pier section increases due to the increased elastic modulus of high strength concrete. Thus the maximum drift reduces when concrete strength is increased for certain *PGA*. The trend of increased drift value remains the same for HSR for any concrete strength. This is because of the reduced stiffness of the piers due to lower reinforcement ratio when high strength steels are incorporated. From Figure 5.9g, the bridge pier designed using the highest strength concrete and lowest grade steel gives the best performance regarding maximum drift (1.67%) by 50% ground motions at *PGA* 1g.

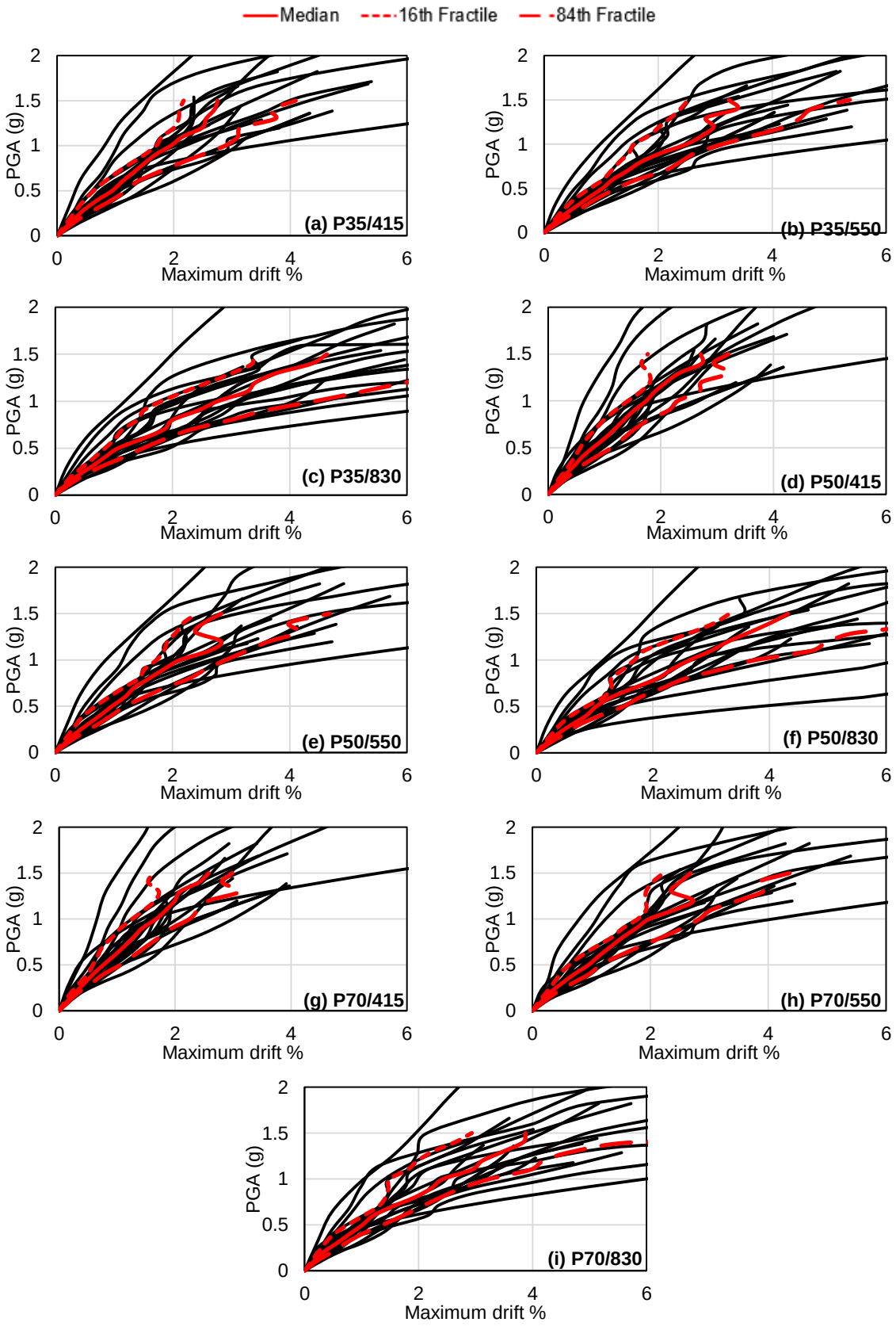

Figure 5.9 *IDA* curves of the designed bridge piers

5.10 Damage States

Inelastic static pushover analysis (*ISPA*) and incremental dynamic analysis are conducted on the PBD bridge piers reinforced with varying steel grades. Damage states of the bridge piers are defined from the non-linear static pushover analysis for both FEMA and CHBDC specified damage states. Minor deviations in yield and crushing performance from *ISAP* and *IDA* allow defining the limit states from *ISPA* with reasonable accuracy as discussed in Chapter 4. 3-D finite element models are developed using the finite element program SeismoStruct (2015). 10% axial load is considered on top of each bridge pier. Details of the modeling technique, underlying assumptions, and material models are discussed in the previous sections. Uncertainties in material properties are not considered in this study. Damage states are decided on maximum drift only.

Yielding of longitudinal steel is a critical performance benchmark for RC bridge piers. Bridge pier encounters higher residual deformation after yielding of steel rebars during dynamic loading. CHBDC 2014 (CSA, 2014) defines the minimal damage of structure in term of steel yielding. The moderate damage state outlined by FEMA (FEMA, 2003) is also characterized by yielding of longitudinal steel. Spalling and crushing of concrete eventually start after the yielding of main rebars. The yield strain of ASTM A615 Grade 60, Grade 80, ASTM A1035 Grade 120 steel reinforcements used in this study are respectively 0.002075, 0.00275, and 0.00415 mm/mm. All the reinforcing steel are assumed to have an elastic modulus of 200GPa.

The collapse of bridge pier is often defined by the crushing of confined concrete (FEMA, 2003; CHBDC 2016). This performance criterion marks the unsuitability of use of the bridge and requirement of probable replacement. The yield strength of transverse reinforcement considerably affects the crushing strain of concrete. The yield strength of transverse steel is assumed to be 400 MPa in this study. Crushing strain of confined concrete is determined using the equation, $\varepsilon_{cu} = 0.004+1.4\rho_s f_{yh}\varepsilon_{sm}/f'_c$ suggested by Paulay and Priestley (1992). Here, ε_{sm} = steel strain at maximum tensile stress (0.14); f'_c= concrete compressive strength (MPa); f_{yh} = yield strength of transverse steel (400 MPa); and ρ_s = volumetric ratio of spiral (0.6%). The crushing strain for the designed bridge piers is found to be 0.018, 0.014 and 0.011 for 35MPa, 50MPa, and 70 MPa concrete respectively. The usual range of crushing strain of concrete varies between 0.015 and 0.05 (Paulay and Priestley, 1992). However, concrete strength and transverse reinforcement configuration largely affect the crushing strain. For a fixed lateral reinforcement configuration, increased

concrete strength increases the brittleness (Setunge, 1993). Longitudinal steel strength does not necessarily affect the crushing of concrete as can be seen from the equation provided above.

5.10.1 FEMA damage states

FEMA specified onset of cracking in concrete cover and minor spalling as slight damage in bridge pier. Yielding defines the moderate damage state, which can also be described by physical phenomenon of moderate cracking and minor spalling in concrete. Extensive damage with degradation can be captured by spalling of concrete, and crushing of confined core concrete may lead to the probable collapse of the bridge pier. Priestley et al. (1996) suggested that the cracking and spalling in cover concrete occur at 0.0014 and 0.004 strain. These suggested values are used in defining slight and extensive damage states. Moderate damage is taken at a displacement when the longitudinal steel rebar yields, and collapse in bridge pier is considered at crushing strain of concrete as described earlier. Different damage criteria over the *ISPA* curves of the bridge piers are presented in Figure 5.10. Bridge reinforced with lower strength steel can undergo higher displacement due to higher total elongation capacity of steel. However, damage happens at lower drift ratio as the longitudinal steel grade is decreased. Cracking in bridge pier occurs almost at similar drift ratio. Moderate, extensive and collapse damage vary notably with the change in design reinforcement grades. The higher the reinforcing steel grade, the higher is the drift ratio for a particular damage state. P35/415 pier collapses at a drift ratio of 1.98% whereas P35/830 pier can take about 14% more drift before failure. Increasing the concrete strength helps in increasing the slight, extensive and collapse damage state, which are coupled with concrete strain limits. However, the moderate damage starts early for higher concrete strength. Moderate damage starts at 0.77% drift in pier P35/550. The same damage level is observed at 0.71%, and 0.68% drift ratio in P50/550, and P70/550 bridge piers respectively. All the damage states encounter improvement with the incorporation of high strength concrete and high yield strength reinforcing steel in PBD. Details of FEMA damage states are presented in Table 5.4 for individual bridge piers.

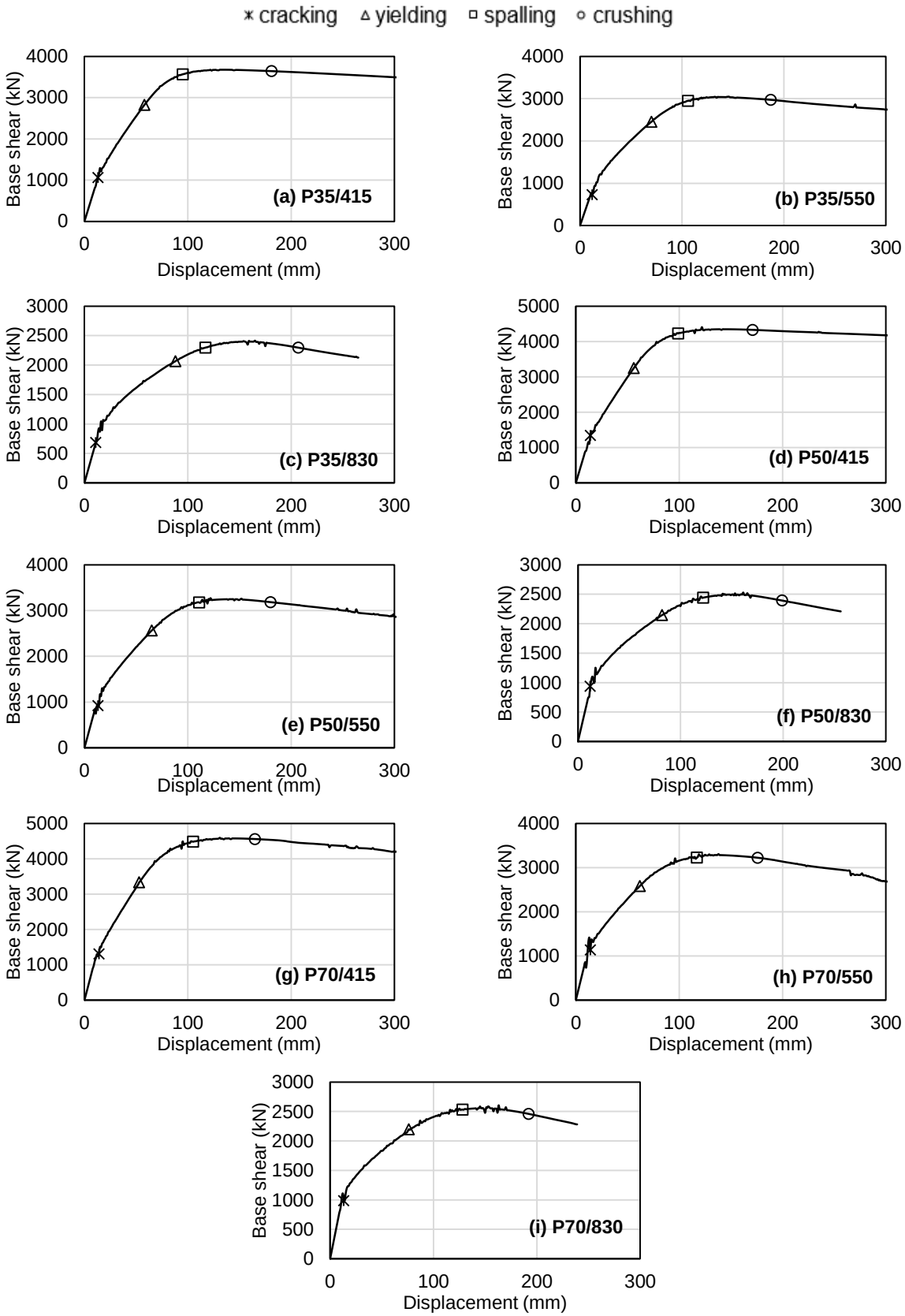

Figure 5.10 FEMA limit states from pushover analysis

Table 5.4 Damage states of bridge piers in term of drift following FEMA

Damage State →	Slight	Moderate	Extensive	Collapse
P35/415	0.14%	0.63%	1.04%	1.98%
P35/550	0.13%	0.77%	1.16%	2.05%
P35/830	0.12%	0.96%	1.28%	2.26%
P50/415	0.15%	0.61%	1.08%	1.87%
P50/550	0.14%	0.71%	1.21%	1.97%
P50/830	0.13%	0.90%	1.33%	2.18%
P70/415	0.15%	0.58%	1.15%	1.81%
P70/550	0.15%	0.68%	1.28%	1.93%
P70/830	0.14%	0.83%	1.40%	2.10%

5.10.2 CHBDC damage states

CHBDC explains the damage states of bridges in a slightly different way. The *DSs* prescribed in CHBDC 2014 (CSA, 2014) are minimal, repairable, extensive and probable replacement. Minimal damage is associated with concrete and steel strain of 0.004 and yielding respectively. It is noticeable that minimal damage in CHBDC 2014 defines the moderate damage in bridge pier by FEMA when yielding in steel governs. The concrete strain of 0.004 equals the Priestley et al. (1996) recommended value for concrete spalling, which detects the extensive damage to the pier. According to CHBDC 2014, the minimal damage starts at a drift equal to FEMA specified extensive damage limit when strain in concrete governs. In case of all the designed bridge pier, reinforcing steel yielding strain criteria governed the minimal damage state. The repairable damage is detected by steel strain of 0.015. Extensive damage is governed by the criteria that the confined core concrete strain cannot surpass the concrete crushing strain. Apparently, steel strength seems to have little effect in dictating the collapse damage state of the bridge piers. Figure 5.11 displays the CHBDC damage states over the *ISPA* curve of the designed piers and corresponding drift ratio are summarized in Table 5.5.

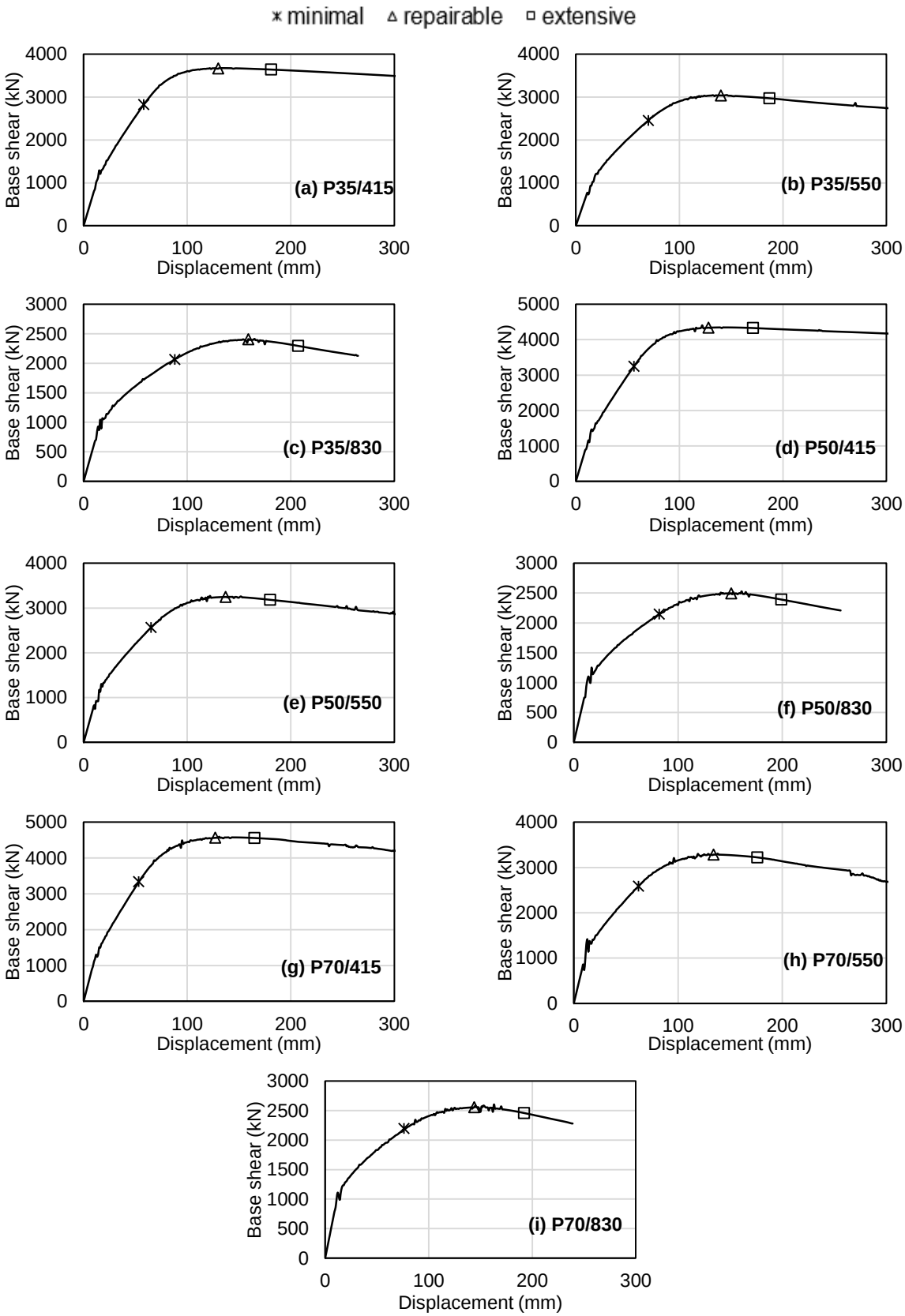

Figure 5.11 CHBDC limit states from pushover analysis

Table 5.5 Damage states of bridge piers in term of drift (%) following CHBDC 2014

Damage State →	Minimal	Repairable	Extensive
P35/415	0.63%	1.42%	1.98%
P35/550	0.77%	1.53%	2.05%
P35/830	0.96%	1.74%	2.26%
P50/415	0.61%	1.40%	1.87%
P50/550	0.71%	1.50%	1.97%
P50/830	0.90%	1.65%	2.18%
P70/415	0.58%	1.39%	1.81%
P70/550	0.68%	1.47%	1.93%
P70/830	0.83%	1.58%	2.10%

5.11 PSDMs

To determine the seismic demand on bridge pier from incremental dynamic analyses, a total of 200 bridge piers models are simulated for each bridge pier. Peak responses of the bridge piers in term of maximum drift are considered for corresponding ground motion intensity to generate the probabilistic seismic demand models (*PSDMs*). The logarithm of drift ratios is plotted in vertical axis and logarithm of *PGA* in the horizontal axis to find the parameter *a* and *b* from the regression analysis. *PSDM* plots are demonstrated in Figure 5.12. Dispersion demand, $\beta_{EDP|IM}$ is also found using the regression values. The parameters *a, b* and $\beta_{EDP|IM}$ are explained in Chapter 4. The values obtained for the designed bridge piers are exhibited in Table 5.6. Variations in the r-squared values are very small, but the values are close to 1. It indicates a reasonably good correlation between the engineering demand parameter and the intensity measure. Employing higher grade steel in the design of bridge pier slightly increases intercept (ln(a)) and slope (b) of the *PSDM* that shows higher susceptibility to ground motions. The reverse scenario is found when high strength concrete is used in design.

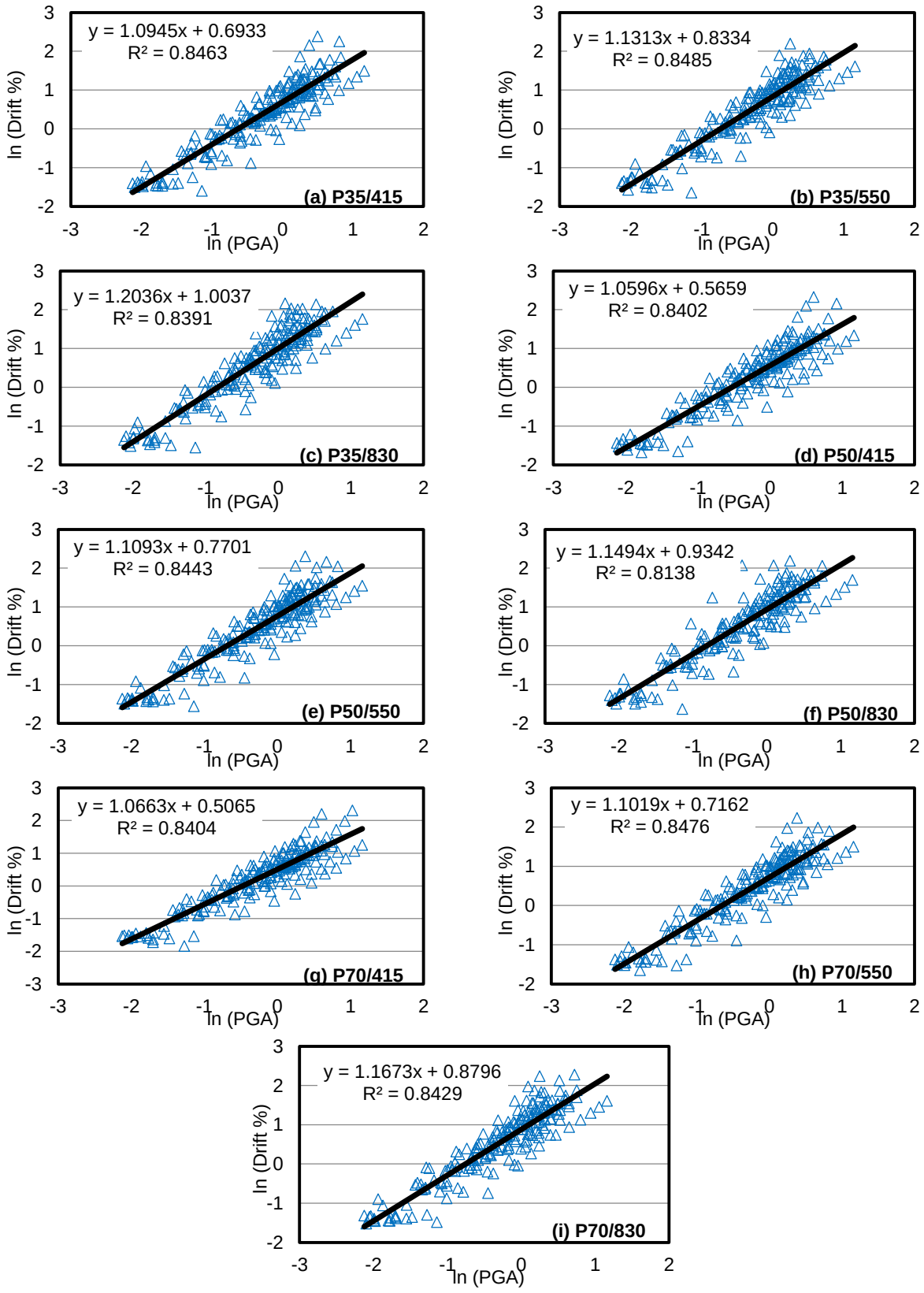

Figure 5.12 Probabilistic seismic demand models

Table 5.6 *PSDMs* parameters for the designed bridge piers

	P35/415	P35/550	P35/830	P50/415	P50/550	P50/830	P70/415	P70/550	P70/830
a	2.00	2.30	2.73	1.76	2.16	2.55	1.66	2.05	2.41
b	1.09	1.13	1.20	1.06	1.11	1.15	1.11	1.10	1.17
$\beta_{EDP\|IM}$	0.356	0.351	0.385	0.345	0.350	0.376	0.350	0.347	0.367

5.12 Fragility Analysis

Using the *IDA* results and Equations provided in Chapter 4, the fragility of various damage states for the bridge piers are developed for the selected ground motions. Maximum drift is considered as the performance measure or engineering demand parameter, and the peak ground acceleration are chosen to be the intensity measure while generating the bridge pier fragilities. Fragility curves are plotted after quantifying the normal distribution logarithm of *PGA*. Bridge pier fragilities for the FEMA and CHBDC specified damage states are discussed in the following sections.

5.12.1 Fragility curves for FEMA damage states

Slight, moderate, extensive and collapse damage probabilities of the bridge piers are demonstrated in Figure 5.13. The probability of collapse of the bridge pier reinforced with grade 60 steel and designed using 35MPa concrete is 4% at design *PGA* 0.463g. Whereas, for P35/550, and P35/830 bridge piers the collapse probabilities are 7%, and 8% respectively at the same ground motion intensity level. Collapse performance shows decrement when HSR are incorporated. No direct relation between steel strength and improved crushing of concrete draws this conclusion. Moreover, reduced longitudinal reinforcement ratio associated with HSR leads to lower stiffness of bridge pier. Though the collapse limit decreases with increased concrete strength, the collapse probability decreases by 50% when the concrete strength moves from 35MPa to 70MPa in bridge pier design. When ASTM A1035 Grade 120 rebar is used in PBD, collapse probability reduces by 12.5% at design *PGA* if 70MPa concrete replaces the 35MPa concrete. High strength concrete improves the overall stiffness of structural member due to the higher elastic modulus of concrete and reduces the drift ratio for a particular intensity earthquake. Likewise, the extensive damage probability of bridge pier also reduces with the increase in concrete strength. Incorporation of HSR

improves the moderate damage performance of the bridge piers. For 35MPa concrete, moderate damage probability reduces by 6% at design *PGA* when Grade 120 rebar is used in place of traditional Grade 60 reinforcements. For high strength concrete (70MPa), the reduction becomes 3%. Increase yielding strain of steel can be attributed to such behavior. Table 5.7 summarizes the *PGA* at which the selected ground motions cause 50% damage probability in the bridge piers. The *PGA* demand increases 15% for 50% collapse probability and about 57% for the 50% extensive damage probability from P35/415 pier to P70/415 pier. When HSR are used, the demand increases by 6.5% for 50% collapse probability from P35/830 pier to P70/830 pier. The inclusion of HSR in designing the bridge pier is greatly effective in increasing the demand for moderate damage to bridge pier (52% increment from P35/415 to P35/830 pier) since this criterion is in direct connection to the yielding of steel.

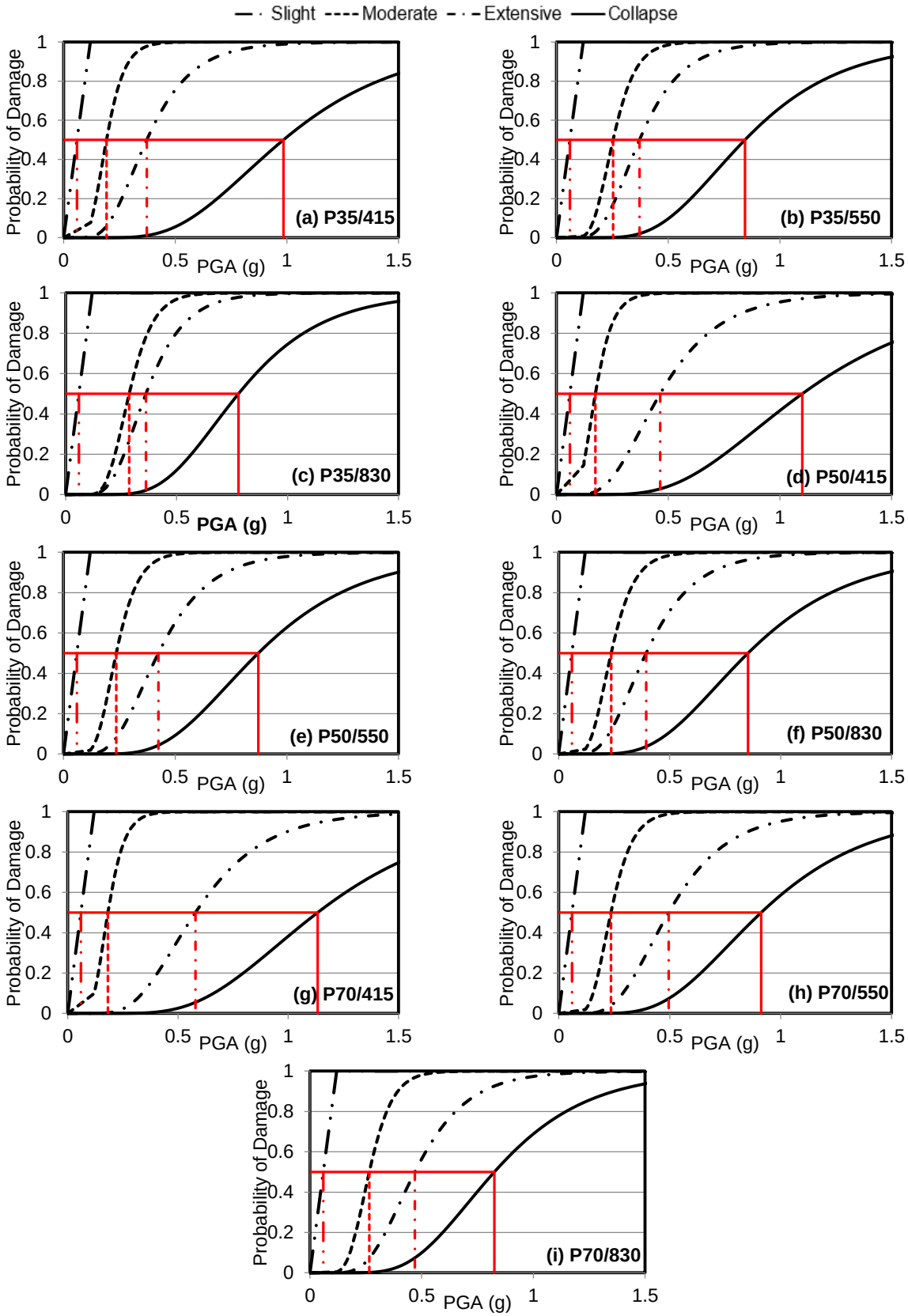

Figure 5.13 Fragility plots for FEMA limit states

Table 5.7 *PGA* at which the damage probability is 50% (FEMA *LSs*)

LS →	Slight	Moderate	Extensive	Collapse
P35/415	0.06g	0.19g	0.37g	0.98g
P35/550	0.06g	0.25g	0.37g	0.84g
P35/830	0.06g	0.29g	0.36g	0.78g
P50/415	0.06g	0.18g	0.46g	1.10g
P50/550	0.06g	0.23g	0.42g	0.87g
P50/830	0.06g	0.26g	0.39g	0.80g
P70/415	0.06g	0.18g	0.58g	1.13g
P70/550	0.06g	0.23g	0.50g	0.91g
P70/830	0.06g	0.26g	0.47g	0.83g

5.12.2 Fragility curves for CHBDC damage states

Minimal damage probability of the designed bridge piers happens when the steel strain reaches yield strain, or the concrete strain reaches 0.004 (CSA, 2014). This criterion is highly conservative compared to the slight damage criteria specified in FEMA. The damage fragilities for CHBDC *DSs* starts later compared to the fragilities of *DSs* from FEMA. Minimal damage criterion is governed by the yielding of steel in all the designed bridge piers. Demand for 50% probabilities of minimal damage is increased by 44% from P50/415 to P50/830 bridge pier. Increase in concrete strength has ignorable effect on moderate damage performance of bridge piers. Concrete strain limit governed the extensive damage in all the bridge piers, which is similar to the collapse damage fragility found following FEMA. Crushing of core concrete regulated this damage in the piers. Both the minimal and repairable damage probability reduces at design *PGA* when HSR are employed in PBD. Repairable damage probability reduces to 21% at design *PGA* 0.463g in P35/830 compared to 26% in P35/415 bridge pier. Increasing concrete strength increases the repairable damage probability insignificantly. However, repairable damage probability reduces by 11% when high strength concrete is used along with HSR. Table 5.8 demonstrates the *PGA* at which the CHBDC specified damage probabilities become 50%. ASTM A1035 Grade 120 steel reinforced bridge piers require 3.5%, 3.5%, and 3.6% higher *PGA* earthquakes for 50% repairable damage probabilities compared to the ASTM A615 Grade 60 steel reinforced bridge pier for 35MPa, 50MPa, and 70MPa concrete respectively. Bridge piers fragilities from CHBDC damage criteria are presented in Figure 5.14.

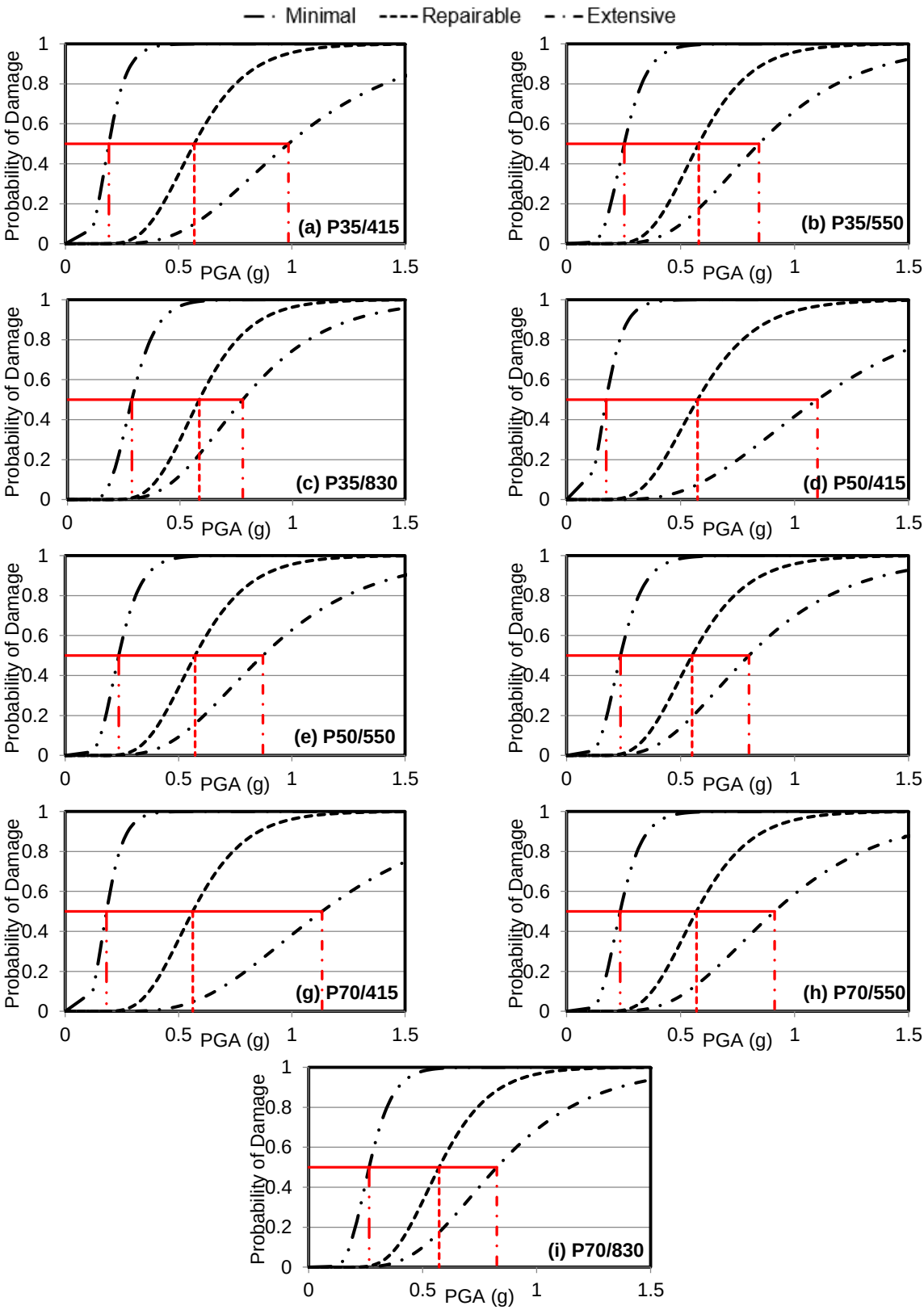

Figure 5.14 Fragility plots for CHBDC damage states

Table 5.8 *PGA* at which the damage probability is 50% (CHBDC *LSs*)

LS →	Minimal	Repairable	Extensive
P35/415	0.19g	0.57g	0.98g
P35/550	0.25g	0.58g	0.84g
P35/830	0.29g	0.59g	0.78g
P50/415	0.18g	0.57g	1.10g
P50/550	0.23g	0.57g	0.87g
P50/830	0.26g	0.59g	0.80g
P70/415	0.18g	0.56g	1.14g
P70/550	0.23g	0.57g	0.91g
P70/830	0.26g	0.58g	0.83g

5.13 Effect of Transverse Reinforcement Strength

Using high strength longitudinal rebar in designing bridge pier reduces the damage probabilities associated with steel strain such as moderate damage from FEMA and minimal and repairable damage from CHBDC guidelines. However, the collapse vulnerability of the bridge pier increases due to reduced demand in longitudinal reinforcement resulting from HSR application. Increasing the concrete strength can slightly mitigate the problem when the transverse reinforcement arrangements are kept similar. In this section, the lifeline bridge pier is designed following PBD from CHBDC 2014 for fixed concrete and longitudinal rebar strength with varying transverse reinforcement strength and analyzed for seismic actions. Three combinations of transverse reinforcements are considered and labeled as P70/830/TX as shown in Table 5.9. Here, P stands for the PBD, 70 stands for the 70MPa concrete strength, 830 represents the 830MPa longitudinal steel strength, T stands for transverse reinforcement, and X shows the yield strength of the transverse rebars. 415MPa, 550MPa and 830MPa steel are considered for transverse reinforcement to design the bridge pier. The associated material properties are shown in Table 5.1. Pitch of the spiral reinforcements is maintained 76mm in plastic hinge region and 100mm in the rest of the pier. One to one replacement is considered with higher grade steel without changing the spiral spacing for transverse reinforcement in designing the bridge pier. Inelastic static pushover analyses are carried out to check the performance criteria specified in CHBDC 2014 for a single

lifeline bridge pier. The design details are shown in Table 5.9, and the pushover curves are presented in Appendix B for brevity. Increasing the spiral strength to 550 MPa reduces the longitudinal rebar ratio by 7% compared to traditional Grade 60 spirals. However, employment of highest Grade steel (Grade 120) does not help in further reducing the longitudinal reinforcement ratio targeting the performance criteria.

Table 5.9 Design details of the bridge pier

ID	f'_c (MPa)	f_y (MPa)	f_{yh} (MPa)	Reinforcement percentage	Longitudinal rebar detail
P70/830/T415	70	830	415	0.86%	28-32M
P70/830/T550	70	830	550	0.80%	26-32M
P70/830/T830	70	830	830	0.80%	26-32M

Incremental dynamic analysis is conducted for 20 near-fault ground motions, and the *IDA* plots are shown in Appendix B (Figure B.3). Increasing the transverse reinforcement strength reduces the longitudinal rebar ratio, but increases the overall stiffness of the structure. To plot the fragility curves, limit states are defined following both FEMA and CHBDC guidelines. Limit states are plotted over *ISPA* curves and presented in Appendix B in figures (Figure B.4 and Figure B.5) and tabulated form (Table B.1 and Table B.2). Increasing spiral strength increases the limit state notably for collapse damage (9% increment when Grade 120 spiral is used instead of Grade 60). The crushing strain of concrete is calculated using the equation, $\varepsilon_{cu} = 0.004 + 1.4\rho_s f_{yh}\varepsilon_{sm}/f'_c$ suggested by Paulay and Priestley (1992). The crushing strain is found 0.012 and 0.01 for P70/830/T550 and P70/830/T830 bridge piers correspondingly. Though the crushing strain reduces with the increment in transverse reinforcement strength, it can take higher drift to reach the crushing of concrete.

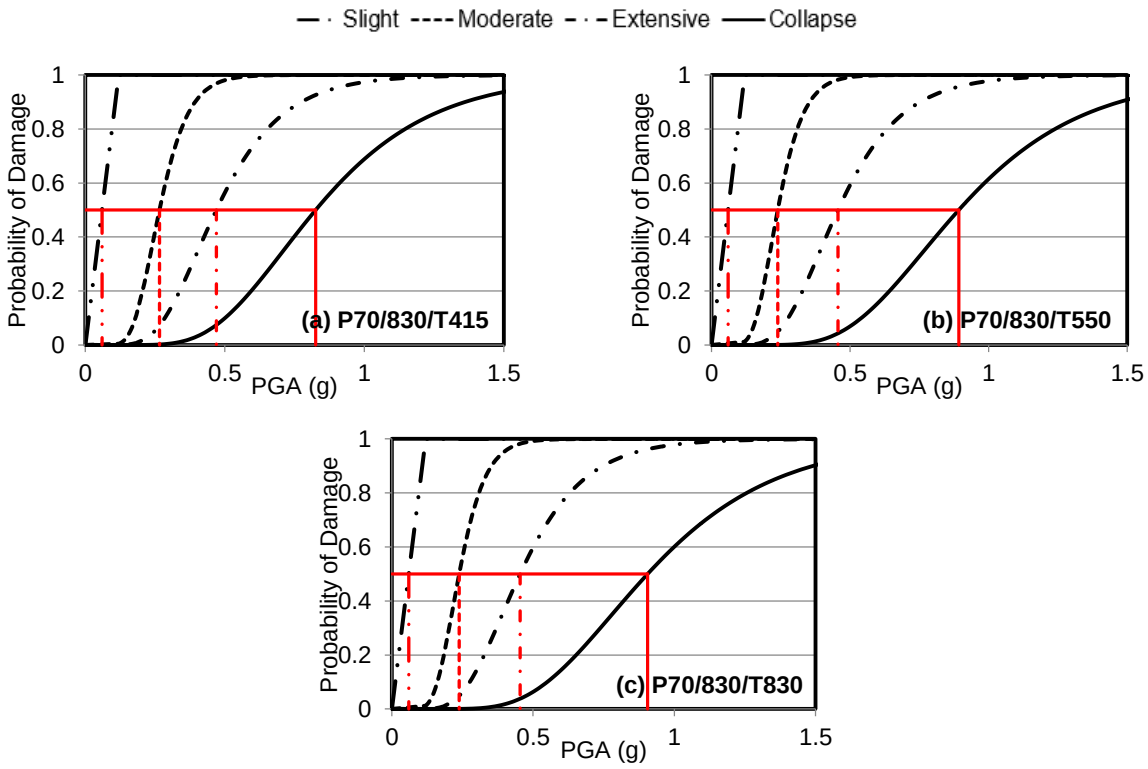

Figure 5.15 Fragility plots for FEMA damage states

Fragility curves plotted for the FEMA damage states are shown in Figure 5.15. The collapse probability curves tend to move to the right when high strength spirals are used in designing bridge pier. Other damage probability plots are essentially at similar locations. Table 5.10 demonstrates the *PGA* demand for 50% of particular limit states. Demand in *PGA* for 50% collapse probability increases 7.23% and 9.64% for Grade 80 and Grade 120 spirals compared to Grade 60 transverse reinforcements. Slight and extensive damage probability demands almost similar *PGA* with varying spiral strengths. However, extensive damage probability increases with the increase of spiral strength. Demand in *PGA* reduces by 4.26% when highest grade spirals are used in design compared to Grade 60 spirals.

Table 5.10 *PGA* at which the damage probability is 50% (FEMA *LSs*)

LS →	Slight	Moderate	Extensive	Collapse
P70/830/T415	0.06g	0.27g	0.47g	0.83g
P70/830/T550	0.06g	0.24g	0.46g	0.89g
P70/830/T830	0.06g	0.24g	0.45g	0.91g

Figure 5.16 displays the fragility curves plotted for CHBDC 2014 damage states. The extensive damage state is essentially similar to the collapse damage state from FEMA. The minimal damage state is governed by the concrete strain limit. The repairable damage limit is specified in terms of steel strain value of 0.015 in CHBDC 2014. The minimal and extensive damage vulnerability reduces with increased spiral strength in design. However, the reparable damage exhibits opposite behavior. Demand in *PGA* reduces to 0.56g when Grade 80 and Grade 120 transverse reinforcements are used from 0.57g for Grade 60 spirals (Table 5.11). For 50% minimal damage probability, demand in *PGA* increases by 14.3% when HSR are considered as transverse reinforcement.

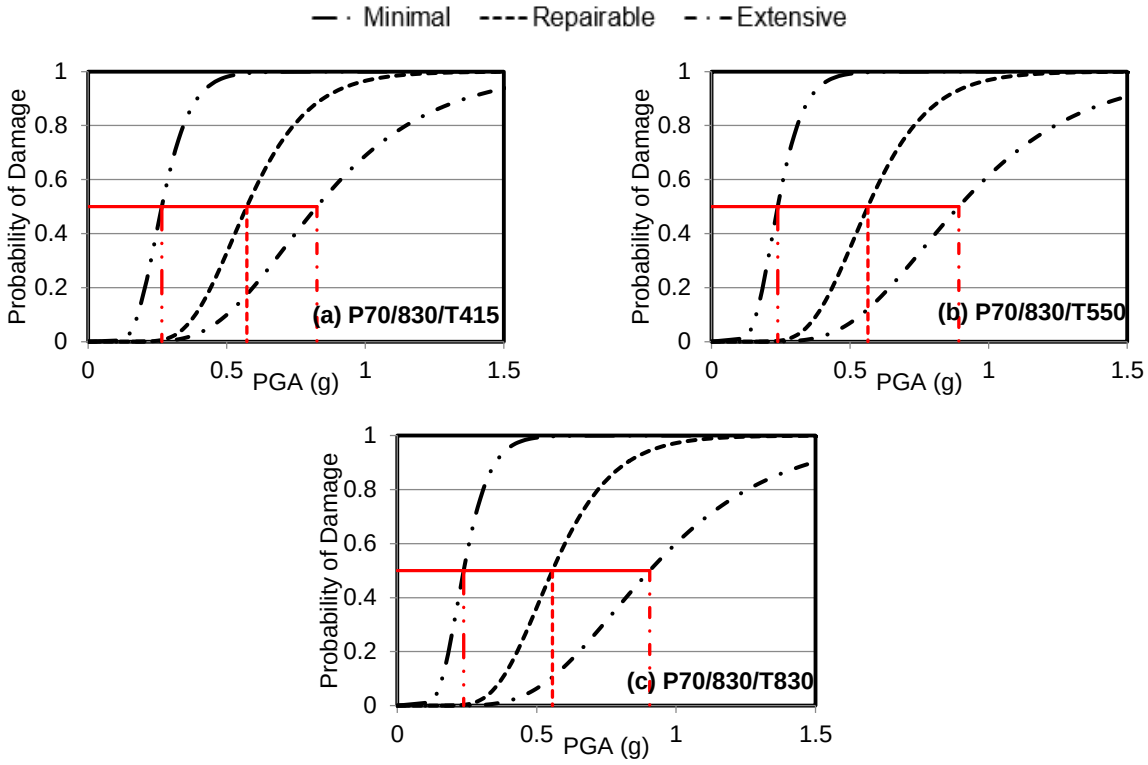

Figure 5.16 Fragility plots for CHBDC damage states

Table 5.11 *PGA* at which the damage probability is 50% (CHBDC *LSs*)

LS →	Minimal	Repairable	Extensive
P70/830/T415	0.21g	0.57g	0.83g
P70/830/T550	0.24g	0.56g	0.89g
P70/830/T830	0.24g	0.56g	0.91g

5.14 Summary

HSR are being acquainted in different RC building and bridge guidelines. CHBDC allows the use of steel reinforcement with yield strength as high as 500MPa. However, availability and production of high strength steel like ASTM A1035 Grade 100 and Grade 120 have the potential to be incorporated in CHBDC to design bridge columns. Moreover, the PBD composed of performance criteria on the tensile strain in steel and concrete where HSR and high strength concrete can perform an active role to improve the performance of bridge pier. This section of the study explicitly investigated the behavior of PBD bridge piers considering different strength steel in combination with different concrete strength under site-specific ground motions. Finally, effects of the strength of transverse reinforcement on design and seismic performance are also investigated for high strength materials. Key results from this chapter are compiled herein.

- Designing bridge piers following the PBD method and using HSR like ASTM A1035 Grade 120 can reduce the design reinforcement ratio about 50% than that of conventional Grade 60 reinforcement. ASTM A615 Grade 80 rebars also have the potential of reducing the reinforcement demand by 40% without compromising the performance criteria specified in CHBDC 2014. The cost of construction, reinforcement congestion, and cost in logistic supports can be substantially reduced when high strength steel is used in the design of bridge piers.
- Incremental dynamic analyses of the bridge piers show slightly higher susceptibility of HSR bridge piers in term of drift due to lower column stiffness. However, incorporation of high strength concrete further reduces the longitudinal rebar requirement, but *IDA* plot shows improved performance in terms of drift ratio due to increased stiffness of the bridge piers derived from the higher elastic modulus of high strength concrete.
- Damage states for the bridge piers are defined from inelastic static pushover analysis curve with reasonable accuracy. Collapse drift limit increases about 15% when HSR are used. Whereas, the moderate damage state from FEMA guideline experiences maximum uplift with 23% increment. Repairable damage limit from CHBDC specification is also increased by maximum 22% when HSR are employed.
- Moderate and repairable damage vulnerabilities decrease with the increment of steel strength in design. Collapse damage vulnerability related to concrete strain increases for

the bridge piers designed with HSR. Incorporation of high strength concrete and high strength spirals can mitigate the problem associated with HSR.

Chapter 6 : CONCLUSIONS

6.1 Summary

PBD of bridges is gaining attention in recent times from the structural engineers due to its unique ability to design targeting some definite performance criteria. CHBDC accepted the PBD in designing bridges in 2014. For major route bridge, PBD is optional and rely on the responsible authority. For critical bridges in the transportation network and disaster management like lifeline bridges, PBD is mandatory. In 2016, the performance-criteria went through noteworthy modifications. Performance limits stated in CHBDC 2014 is highly conservative and leads to excessive amount of design reinforcements as studied by researchers and the author. Relaxed performance criteria specified in the supplement to CHBDC 2014 are yet to be studied on bridge design and performance assessment of the designed bridges. Also, the effect of the strength of reinforcing steel in PBD and behavior of bridge pier under seismic loading is not available in the literature. How the strength of concrete when combined with various steel grade affect the PBD, and seismic performance of bridge pier are yet to be studied.

This thesis demonstrates the design outcomes of a lifeline RC bridge pier designed following FBD method from CHBDC 2010 and PBD methods from CHBDC 2014 and the supplement to CHBDC 2014. The governing design criteria in PBD for a lifeline bridge are identified. Inconsistencies in design results are discussed with reasoning. 20 near-fault ground motions are selected to study the seismic performance of the designed bridge piers through incremental dynamic analysis and proper analytical modeling. Reactions of the bridge piers to the dynamic loading and static pushover loading are compared on yield and crushing displacements of the piers. Performance limit states are defined from the static pushover analysis curves to generate the fragility plots of bridge piers to have an improved understanding of the seismic vulnerability of bridge piers when different design alternatives are employed.

PBD results in higher longitudinal reinforcement ratio in bridge piers to satisfy the performance criteria. However, employing high strength steel in design has the potential to reduce the required reinforcement without compromising the performance. No such study has been performed by far on the consequence of adopting HSR in PBD of bridge piers. This study is also

focused on the design of a lifeline bridge pier according to CHBDC 2014 using HSR in combination with different concrete strengths to predict the effect of HSR thoroughly. Performances of the bridge piers are investigated for static loading and site-specific earthquakes. Seismic vulnerability of the designed bridge piers under 20 near-fault ground motions are evaluated to find out optimal design solution.

6.2 Limitations of the Study

This research possesses the following limitations for simplification purposes:

- This study is based on extensive numerical analyses. However, experimental investigation of similar work can add more reliability on the outcomes.
- Regular single pier bridge bent is considered here for analysis. Selection of bridge bent with various configurations like multicolumn bridge bent, irregular bridge bent, and consideration of substructure and other bridge types in design and analysis could result in different findings.
- Uncertainties in material properties and bridge pier geometry are not considered in this study.
- Maximum drift and peak ground acceleration are chosen to be the engineering demand parameter (*EDP*) and intensity measure (*IM*) respectively. Whereas other parameters like spectral acceleration and residual drift could be selected as potential *IM* and *EDP*.

6.3 Conclusions

This research analytically studies to compare the seismic performance and fragility of three steel-reinforced concrete lifeline bridge piers designed following FBD from CHBDC 2010 and PBD from CHBDC 2014 and the supplement to CHBDC 2014 using pushover analysis. Six hundred bridge pier models are prepared to assess the responses of the bridge piers using incremental dynamic analysis method under a suit of 20 near-fault ground motions matched to Vancouver design spectrum. Later on, HSR are included in designing a bridge pier following the PBD from CHBDC 2014. HSR are also combined with varying concrete strength to analyze the complete effect of HSR on design and performance of lifeline bridge pier under seismic motions. A total of 1800 simulations are done for nine combinations of design for the *IDA*. Fragility analyses

are conducted to compare the seismic vulnerability of the bridge piers. The following conclusions can be drawn from the design and analyses results.

1. PBD following CHBDC 2014 yields very high reinforcement ratio for a lifeline bridge, even crossing the maximum reinforcement percentage limit (6%) specified. This will result in superior seismic performance, but the construction cost and difficulty will rise. Designing the bridge pier following the PBD from the supplement to CHBDC 2014 yields only 1.22% reinforcement ratio for considered loading and geometric conditions.
2. Designing the bridge pier according to the CHBDC 2010 FBD method results in 4.87% reinforcement ratio, which is 20.2% less than that of PBD pier designed according to CHBDC 2014. However, 300% more reinforcement required if FBD design is followed for a single lifeline bridge pier compared to the PBD method from the supplement to CHBDC 2014. CHBDC does not restrict the design of a lifeline bridge with single pier bent. Thus, higher importance factor with lower force reduction factor yields in very high longitudinal reinforcement ratio.
3. The governing design criteria in CHBDC 2014 is found to be the minimal damage during a seismic event of 5% probability in 50 years. This criterion ends in extremely high reinforcement requirement since the strain in steel cannot reach the yield limit. However, in the supplement to CHBDC 2014, this strain limit has been escalated to 0.01, almost five folds to the yielding strain of steel considered in this study. The governing design criterion becomes the steel strain cannot exceed 0.025 in an earthquake with a probability of 5% in 50 years, leads to lower reinforcement ratio.
4. Increasing longitudinal reinforcement percentage makes the bridge pier stiffer. As a result, PBD bridge column designed according to the supplement to CHBDC 2014 experiences 103% more maximum drift compared to the FBD pier and 125% more maximum drift compared to the pier designed following CHBDC 2014 at the same *PGA* (0.5g) by 50% ground motions.
5. PBD from CHBDC 2014 and FBD from CHBDC 2010 offer larger yield displacement capacity (36.7% and 47.8% higher respectively) during dynamic loading than that of PBD from the supplement to CHBDC 2014. Higher yield deformation capacity indicates better performance demanding a higher intensity earthquake to reach the strain limit.

6. In terms of fragility analysis, pier designed following CHBDC 2014 exhibits remarkably good performance. The supplement to CHBDC 2014 followed bridge pier increases the collapse probability at *PGA* 1g earthquake to 66% from 13% in FBD pier. Whereas, the CHBDC 2014 PBD pier reduces it to 6%. Considering construction challenge and economic feasibility, designing bridge piers following CHBDC 2014 supplement will provide reduced longitudinal reinforcement with a compromised seismic performance for a lifeline bridge pier.
7. Fragility curves using the limit states defined from CHBDC performance criteria for PBD indicate higher damage fragility of the bridge pier designed following the supplement to CHBDC 2014 compared to the CHBDC 2014 code followed bridge pier. Minimal performance criteria stated in the supplement to CHBDC 2014 are milder compared to highly conservative CHBDC 2014 entail lower longitudinal reinforcement, which increases the damage probability of bridge pier. The minimal damage criteria should be considered for further modification for a lifeline bridge pier.
8. The inclusion of HSR have the capability to reduce longitudinal reinforcement requirement in PBD to about 50% compared to Grade 60 rebars. The economy in construction projects without compromising seismic performance can be achieved by incorporating HSR in design.
9. Moderate damage state limit from FEMA guideline and repairable damage state limit from CHBDC experience improvement due to its direct link to steel strength. The demand in *PGA* of ground motion increases from 44% to 53% for 50% moderate damage possibility in a bridge pier when Grade 120 rebars is used in design in place of Grade 60 for varying concrete strength. For 50% repairable damage probability, the demand increases about 3.5%. However, the collapse vulnerability increases notably at design *PGA* earthquake when HSR are employed in the design of bridge piers due to lower reinforcement ratio. Increasing concrete strength and transverse reinforcement strength can solve this issue marginally.

6.4 Recommendation for Future Research

Design is the primary and most critical step for any large scale project. Faulty design can cause catastrophe during and after the construction of the structure. The economy in construction

and stability in performance during a seismic action without causing any major damage are expected by the stakeholders and users. This particular study tries give in insight on the PBD of lifeline bridge pier by comparing design alternatives and utilizing varying steel and concrete strength. The scope of this study could be extended to the following aspects:

- Performance criteria in the PBD may need some modification especially over minimal damage criteria for lifeline single bridge pier in future research to relate with the design outcome comparable to the FBD results.
- Recent modifications in performance criteria in CHBDC should be studied in other types of bridge structure with different configurations to extend the scope of the PBD.
- Design with high strength steel should be considered in CHBDC in near future to utilize the benefit of improved strength and performance. To improve the collapse performance of HSR bridge piers, variation in transverse reinforcement properties and details in combination with concrete and longitudinal steel strength should be studied. However, more vigorous research is expected on dynamic analysis and cost-benefit analysis of HSR bridges for better decision making.

REFERENCES

AASHTO 2007. AASHTO LRFD Bridge design specifications. American Association of State Highway and Transportation Officials, Washington, D.C.

AASHTO 2014. AASHTO LRFD Bridge design specifications. 7th ed., customary U.S. units. American Association of State and Highway Transportation Officials, Washington, DC.

AASHTO MP 18M/MP 18-15. 2015. Standard specification for uncoated, corrosion-resistant, deformed and plain alloy, billet-steel bars for concrete reinforcement and dowels. American Association of State and Highway Transportation Officials, Washington, DC.

ACI 1983. Building Code Requirements for Reinforced Concrete. ACI 318-83, ACI Committee 318, American Concrete Institute, Detroit.

ACI 1984. State-of-the-Art Report on High-Strength Concrete. ACI 363R-84, ACI Committee 363, American Concrete Institute, Detroit.

ACI 2014. Building code requirements for structural concrete and commentary. ACI 318-14, ACI Committee 318, American Concrete Institute, Farmington Hills, Michigan.

Adams, J., and Halchuk, S. 2003. Fourth generation seismic hazard maps of Canada: values for over 650 Canadian localities intended for the 2005 National Building Code of Canada. Geological Survey of Canada, Open File 4459.

Ahlborn, T., and DenHartigh, T. 2002. A comparative bond study of MMFX reinforcing steel in concrete. Michigan Tech Report CSD- 2002-03.

Alam, M.S., Bhuiyan, A.R., and Billah, A.H.M.M. 2012. Seismic fragility assessment of SMA-bar restrained multi-span continuous highway bridge isolated with laminated rubber bearing in medium to strong seismic risk zones. Bulletin of Earthquake Engineering, **10**(6): 1885-1909.

Alam, M.S., Youssef. M.A., and Nehdi, M. 2008. Analytical prediction of the seismic behaviour of superelastic shape memory alloy reinforced concrete elements. Engineering Structures, **30**(12): 3399-3411.

Allen, D.E. 1975. Limit states design-A probabilistic study. Canadian Journal of Civil Engineering, **2**(1): 36-49.

ASTM 2007. Standard specification for deformed and plain, low-carbon, chromium, steel bars for concrete reinforcement. ASTM A1035, ASTM International, West Conshohocken, Pennsylvania.

ASTM 2009. Standard Specification for Deformed and Plain Carbon-Steel Bars for Concrete Reinforcement. ASTM A615-09b, ASTM International, West Conshohocken, Pennsylvania.

Attard, M.M., and Setunge, S. 1996. Stress-Strain Relationship of Confined and Unconfined Concrete. ACI Materials Journal, **93**(5): 432-441.

ATC 1985. Earthquake damage evaluation data for California (ATC-13). Applied Technology Council, Redwood City, California.

ATC 1987. Evaluating the seismic resistance of existing buildings (ATC-14). Applied Technology Council Redwood City, California.

ATC 1996 Seismic evaluation and retrofit of existing concrete buildings (ATC-40). Applied Technology Council, Redwood City, California.

ATC 2003. Recommended LFRD guidelines for the seismic design of highway bridges. MCEER/ATC-49, Applied Technology Council, Redwood City, California.

ATC 2014. Roadmap for the use of high-strength (ATC-115). Applied Technology Council Redwood City, California.

Aoyama, H. 2001. Design of modern highrise reinforced concrete structures. Imperial College Press, London, United Kingdom.

Azizinamini, A., Chisala, M., and Ghosh, S.K. 1995. Tension development length of reinforcing bars embedded in high-strength concrete. Engineering Structures, **17**(7): 512–522.

Azizinamini, A., Stark, M., Roller, J. J., and Ghosh, S. K. 1993. Bond performance of reinforcing bars embedded in high-strength concrete. ACI Structural Journal, **90**(5): 554–561.

Baker, J.W. 2015. Efficient Analytical Fragility Function Fitting Using Dynamic Structural Analysis. Earthquake Spectra, **31(**1): 579–599.

Baker, J.W., and Cornell, C.A. 2006. Vector-valued ground motion intensity measures for probabilistic seismic demand analysis. PEER report 2006/08, PEER Center, University of California, Berkeley, CA.

Baker, J.W., Lin, T., Shahi, S.K., and Jayaram, N. 2011. New ground motion selection procedures and selected motions for the PEER transportation research program. PEER Technical report 2011/03, PEER Center, University of California, Berkeley, CA.

Banerjee, S., and Shinozuka, M. 2008. Mechanistic quantification of RC bridge damage states under earthquake through fragility analysis. Probabilistic Engineering Mechanics, **23**(1): 12–22.

Bardakis, V.G., and Fardis, M.N. 2010. A displacement-based seismic design procedure for concrete bridges having deck integral with the piers. Bulletin of Earthquake Engineering, **9**(2): 537–560.

Basöz, N., Kiremidjian, A.S., King, S.A., and Law, K.H. 1999. Statistical analysis of bridge damage data from the 1994 Northridge, CA, earthquake. Earthquake Spectra, **15**(1): 25-54.

Bentz, E.C. 2000. Sectional Analysis of Reinforced Concrete. Ph.D. Dissertation, University of Toronto, Ontario, Canada.

Bertero, V.V. 1996. The need for multi-level seismic design criteria. *In* Proceedings of the 11th World Conference on Earthquake Engineering, 23-28 June, Acapulco, Mexico.

Billah, A.H.M.M. and Alam, M.S. 2014a. Seismic performance evaluation of multi-column bridge bents retrofitted with different alternatives using incremental dynamic analysis. Engineering Structures, **62–63**: 105–117.

Billah, A.H.M.M., and Alam, M.S. 2014b. Performance-based prioritization for seismic retrofitting of reinforced concrete bridge bent. Structure and Infrastructure Engineering, **10**(8): 929-949.

Billah, A.H.M.M., and Alam, M.S. 2014c. Seismic fragility assessment of concrete bridge pier reinforced with superelastic Shape Memory Alloy. Earthquake Spectra, **31**(3): 1515-1541.

Billah, A.H.M.M. and Alam, M.S. 2015a. Seismic Fragility Assessment of Highway Bridges: A State-of-The-Art Review. Structure and Infrastructure Engineering, **11**(6): 804-832.

Billah, A.H.M.M., and Alam, M.S. 2015b. Seismic Fragility Assessment of Concrete Bridge Pier Reinforced with Superelastic Shape Memory Alloy. Earthquake Spectra, **31**(3): 1515-1541.

Billah, A.H.M.M. and Alam, M.S. 2016a. Performance-Based Seismic Design of Shape Memory Alloy–Reinforced Concrete Bridge Piers. I: Development of Performance-Based Damage States. Journal of Structural Engineering, **142**(12): 04016140.

Billah, A.H.M.M., and Alam, M.S. 2016b. Plastic hinge length of shape memory alloy (SMA) reinforced concrete bridge pier. Engineering Structures, **117**: 321–331.

Billah, A.H.M.M., Alam, M.S., and Bhuiyan, A.R. 2013. Fragility analysis of retrofitted multicolumn bridge bent subjected to near-fault and far-field ground motion. Journal of Bridge Engineering, **18**(10): 992–1004.

Bournonville, M., Dahnke, J., and Darwin, D. 2004. Statistical analysis of the mechanical properties and weight of reinforcing bars. SL Report 04-1. The University of Kansas, USA.

Bradley, B.A., Cubrinovski, M., MacRae, G.A., and Dhakal, R.P. 2009. Ground-Motion Prediction Equation for SI Based on Spectral Acceleration Equations. Bulletin of the Seismological Society of America, **99**(1): 277–285.

Brown, M., Bayrak, O., and Jirsa, J. 2006. Design for shear based on loading conditions. ACI Structural Journal, **103**(4): 541-550.

Budek, A., Priestley, M., and Lee, C. 2002. Seismic design of columns with high-strength wire and strand as spiral reinforcement. ACI Structural Journal, **99(**5):660-670.

Caltrans 1994. Initial and supplementary bridge reports for the Northridge Earthquake. California Department of Transportation, Sacramento, CA.

Caltrans. 2004. Seismic Design Criteria. California Department of Transportation. Sacramento, CA.

Chandramohan, R., Baker, J.W., and Deierlein, G.G. 2016. Quantifying the Influence of Ground Motion Duration on Structural Collapse Capacity Using Spectrally Equivalent Records. Earthquake Spectra, **32**(2): 927–950.

Chang, S. E., and Nojima, N. 2001. Measuring post-disaster transportation system performance: The 1995 Kobe earthquake in comparative perspective. Transportation Research. Part A, Policy and Practice, **35**(6): 475–494.

Chao, S. H., Naaman, A. E., and Parra-Montesinos, G. J. 2009. Bond behavior of reinforcing bars in tensile strain-hardening fiber-reinforced cement composites. ACI Structural Journal, **106**(6): 897–906.

Chen, W.F., and Duan, L. 2013. Handbook of international bridge engineering. CRC Press, NW.

China-MOC. 2008. Chinese guidelines for seismic design of highway bridges.

Choi, E. 2002. Seismic analysis and retrofit of Mid-America bridges. PhD thesis, Georgia Institute of Technology, Atlanta, GA.

Choi, E., DesRoches, R., and Nielson, B. 2004. Seismic fragility of typical bridges in moderate seismic zones. Engineering Structures, **26**(2): 187–199.

Ciancone, G.G., Michael, A.P., and Hamilton III, H.R. 2008. Behavior of standard hook anchorage with corrosion resistant reinforcement. Technical Report FDOT No. BD 545-40, Florida Department of Transportation, FL, USA.

Colley, S.D., Kleinjan, B., Bull, D.K., and Morris, G.J. 2015. Review of material and flexural overstrength factors for Grade 300E reinforcing steel used in New Zealand. *In* Proceedings of the NZSEE Conference, 10–12 April, Rotorua, New Zealand, Paper Number O-18.

Cornell, A.C., Jalayer, F., and Hamburger, R.O. 2002. Probabilistic basis for 2000 SAC federal emergency management agency steel moment frame guidelines. Journal of Structural Engineering, **128**(4): 526–532.

Correia, A.A., Almeida, J.P., and Pinho, R. 2008. Force-based versus displacement-based formulations in the cyclic nonlinear analysis of RC frames. *In* Proceedings of the 14th World Conference on Earthquake Engineering, October 12-17, Beijing, China.

CHBDC 2016. Bridge Standards and Procedures Manual. Supplement to CHBDC S6-14, Volume I, British Columbia Ministry of Transportation, BC, Canada.

CSA 2000. Canadian highway bridge design code (CAN/CSA S6-00). Canadian Standards Association (CSA), Toronto, Ontario.

CSA 2006. Canadian Highway Bridge Design Code (CAN/CSA S6-06). Canadian Standards Association.

CSA 2010. S6S1-10 Supplement No. 1 to CAN/CSA-S6-06, Canadian Highway Bridge Design Code, Canadian Standards Association, Rexdale, ON, Canada.

CSA 2014. Canadian Highway Bridge Design Code (CAN/CSA S6-14). Canadian Standards Association.

Cusson, D., and Paultre, P. 1994. High-Strength Concrete Columns Confined with Rectangular Ties. Journal of Structural Engineering, **120**(3): 783–804.

Dawood, H. M., and ElGawady, M. 2013. Performance-based seismic design of unbonded precast post-tensioned concrete filled GFRP tube piers. Composites Part B: Engineering, **44**(1): 357-367.

DeJong, S.J. 2005. Fatigue of Corrosion Resistant Reinforcing Steels. MS thesis, Queen's University.

DeJong, S.J., and MacDougall, C. 2006. Fatigue Behaviour of MMFX Corrosion-Resistant Reinforcing Steel. *In* Proceedings of the 7th International Conference on Short and Medium Span Bridges, Montreal, Canada.

Dezfuli, H.F., and Alam, M. S. 2017. Effect of different steel-reinforced elastomeric isolators on the seismic fragility of a highway bridge. Structural Control Health Monitor, **24**(2): e1866. doi: 10.1002/stc.1866.

El-Hacha, R., and Rizkalla, S. 2002. Fundamental material properties of MMFX steel rebars. Research Report: RD-02/04, North Carolina State University, page 62.

El-Hacha, R., El-Agroudy, H., and Rizkalla, S. 2006. Bond Characteristics of High-Strength Steel Reinforcement. ACI Structural Journal, **103**(6): 771–782.

Esfahani, M. R., and Kianoush, M. R. 2005. Development/splice length of reinforcing bars. ACI Structural Journal, **102**(1): 22–30.

Firas, S. A., Foret Gilles, F., and Robert, L. R. 2011. Bond between carbon fibre-reinforced polymer (CFRP) bars and ultra high performance fibre reinforced concrete (UHPFRC): Experimental study. Construction and Building Materials, **25**(2): 479–485.

Fakharifar, M., Chen, G., Dalvand, A., and Shamsabadi, A. 2015a. Collapse vulnerability and fragility analysis of substandard RC bridges rehabilitated with different repair jackets under post-mainshock cascading events. International Journal of Concrete Structures and Materials, **9**(3): 345–367.

Fakharifar, M., Chen, G., Sneed, L., and Dalvand, A. 2015b. Seismic performance of post-mainshock FRP/steel repaired RC bridge columns subjected to aftershocks. Composites: Part B, **72**: 183–198.

Faza, S., Kwok, J., Salah, O. 2008. Application of high-strength and corrosion-resistant ASTM A1035 steel reinforcing bar in concrete high-rise construction. *In* Proceedings of the CTBUH 8th World Congress, March 3-8, Dubai.

FEMA 1996. NEHRP guidelines for the seismic rehabilitation of buildings; FEMA 274, Commentary. Federal Emergency Management Agency, Washington DC.

FEMA 2000a. Commentary for the Seismic Rehabilitation of Buildings. FEMA-356, Federal Emergency Management Agency, Washington, DC.

FEMA. 2000b. Recommended seismic design criteria for new steel moment frame buildings. Rep. No. FEMA-350, SAC Joint Venture, Federal Emergency Management Agency, Washington, DC.

FEMA. 2000c. Recommended seismic evaluation and upgrade criteria for existing welded steel moment frame buildings. Report No. FEMA-351, SAC Joint Venture, Federal Emergency Management Agency, Washington, DC.

FEMA 2003. HAZUS-MH software. Federal Emergency Management Agency, Washington DC.

FHWA-NHI. 2014. LRFD Seismic analysis and design of bridges reference manual. U.S. Department of Transportation Federal Highway Administration Publication No. FHWA-NHI-15-004.

Firoze, M. 2010. Attributes of ductile reinforcing steel. *In* Proceedings of the IABSE-JSCE Joint Conference on Advances in Bridge Engineering-II, Dhaka, Bangladesh.

Floren, A., and Mohammadi, J. 2001. Performance-Based Design Approach in Seismic Analysis of Bridges. Journal of Bridge Engineering, **6**(1): 37–45.

Florida DOT. 2002. Investigation into the Structural Performance of MMFX Reinforcing Bars.

Forcellini, D., Tarantino, A., Elgamal, A., Lu, J., and Mackie, K. 2012. Performance-based seismic assessment of isolated bridge configurations on deformable soils. *In* Proceedings of the 15th World Conference on Earthquake Engineering, Lisbon, Portugal.

Gardoni, P., Mosalam, K.M., and Der Kiureghian, A. 2003. Probabilistic seismic demand models and fragility estimates for RC bridges. Journal of Earthquake Engineering, **7**(1): 79-106.

Ghobarah, A. 2001. Performance-based design in earthquake engineering: state of development. Engineering Structures, **23**(8): 878-884.

Golabi, K., and Shepard, R. 1997. A system for maintenance optimization and improvement of US bridge networks. Interfaces, **27**(1): 71-88.

Goodnight, J.C., Feng, Y., Kowalsky, M.J., and Nau, J.M. 2015. The effects of load history and design variables on performance limit states of circular bridge columns- volume 2: experimental observations. Repot No. 4000(72). Alaska Department of Transportation and Public Facilities, Channel Drive, Juneau, AK.

Gordin, E. 2010. Performance-based decision-making in post-earthquake highway bridge repair. Ph.D. Thesis, University of California, Berkeley.

Graham, S.K., and Paulson, C. 2008. Mechanical properties of ASTM A1035 high strength steel bar reinforcement. Prepared by Wiss, Janney, Elstner Associates, Inc., for the ACI Innovation Task Group 6 (ITG-6), WJE No. 2008.9901.0, Pasadena, California.

Hage, S.E., 1974. The Second-Order Analysis of Reinforced Concrete Frames. M.S. Thesis, University of Alberta, Edmonton, Canada.

Hamad, B. S., and Itani, M. S. 1998. Bond strength of reinforcement in high-performance concrete: The role of silica fume, casting position, and superplasticizer dosage. ACI Material Journal, **95**(5): 499–511.

Hamburger, R., Rojahn, C., Moehle, J., Bachman, R., Comartin, C., and Whittaker, A. 2004. The ATC-58 project: development of next-generation performance-based earthquake engineering design criteria for buildings. *In* Proceedings of the 13th World Conference on Earthquake Engineering, 1-6 August, Vancouver, British Columbia, Canada.

Harajli, M. H., Hamad, B. S., and Karam, K. 2002. Bond-slip response of reinforcing bars embedded in plain and fiber concrete. Journal of Materials in Civil Engineering, **14**(6), 503–511.

Harajli, M. H. 2004. Comparison of bond strength of steel bars in normal and high-strength concrete. Journal of Materials in Civil Engineering, **16**(4): 365–374.

Hassan, T.K., Lucier, G.W., and Rizkalla, S.H. 2012. Splice strength of large diameter, high strength steel reinforcing bars. Construction and Building Materials, **26**(1): 216-225

Hill, C., Chiaw, C.C., and Harik, I.E. 2003. Reinforcement Alternatives for Concrete Bridge Decks. Report KTC-03-19/SPR-215-00-1F.

Hognestad, E., Winter, G., Mavis, F.T., and Greaves, M. J. 1960. High-Strength Reinforcing Steels for Concrete Bridges. In Transportation Research Record: Journal of the Transportation Research Board, No. 39. Transportation Research Board of the National Academies, Washington, DC, pp. 103-119.

Holschemacher, K., Weibe, D., and Klotz, S. 2005. Bond of reinforcement in ultra high-strength concrete. Report no. SP-228-34, American Concrete Institute, Farmington Hills, MI.

Housner, G. W. 1963. The behaviour of inverted pendulum structure during earthquake, Bulletin of the Seismological Society of America, **53**: 403–417

Hsu, Y.T., and Fu, CC. 2004. Seismic Effect on Highway Bridges in Chi Chi Earthquake. Journal of Performance of Constructed Facilities, **18**(1): 47–53.

Huo, Y., and Zhang, J. 2013. Effects of Pounding and Skewness on Seismic Responses of Typical Multispan Highway Bridges Using the Fragility Function Method. Bridge Engineering, **18**(6): 499-515.

Hwang, H., Liu, J. B., and Chiu, Y. H. 2001. Seismic fragility analysis of highway bridges, Mid-America Earthquake Center report: project MAEC RR-4, University of Illinois, Urbana-Champaign.

Ji, J., Darwin, D., and Browning, J. 2005. Corrosion resistance of duplex stainless steels and MMFX microcomposite steel for reinforced bridge decks. SM Report No. 80. The University of Kansas Center for Research, Inc., Lawerence, Kansas.

Jones, M. H., Semyon Treyger, P., Pence, P. W., and Shama, A. 2013. The Gerald Desmond Cable-Stayed Bridge-A case study in performance-based seismic design. *In* Proceedings of the Structures Congress, 2-4 May, Pittsburgh, Pennsylvania.

Kabir, M.R., Billah, A.H.M.M., and Alam, M.S. 2015. Seismic vulnerability assessment of a typical 3 span highway bridge in Bangladesh. *In* Proceedings of the IABSE-JSCE Joint Conference on Advances in Bridge Engineering-III, 21-22 August 2015, Dhaka, Bangladesh, paper ID 9.

Karamlou, A., Bochini, P. 2015. Computation of bridge seismic fragility by large-scale simulation for probabilistic resilience analysis. Earthquake Engineering and Structural Dynamics, **44**(12):1959–1978.

Karim, K. R., and Yamazaki, F. 2001. Effect of earthquake ground motions on fragility curves of highway bridge piers based on numerical simulation. Earthquake Engineering and Structural Dynamics, **30**: 1839–1856.

Khan, S., and Jiang, J. 2015. Performance-based seismic design for the Vancouver Evergreen Line Rapid Transit Project-process, challenges, and innovative design solutions. Paper presented at the Structures Congress, Portland, Oregon.

Kim, S., and Shinozuka, M. 2004. Development of fragility curves of bridges retrofitted by column jacketing. Probabilistic Engineering Mechanics, **19**(1-2): 105–112.

Korinda, K., 1972. Discussion No. 3- Cracking and crack control. *In* Proceedings of the International Conference on Planning and Design of Tall Buildings, Lehigh University, Bethlehem, Pennsylvania.

Kowalsky, M.J. 2002. A Displacement-based approach for the seismic design of continuous concrete bridges. Earthquake Engineering and Structural Dynamics, **31**(3): 719–747.

Kowalsky, M.J., Priestley, M.J.N., and MacRae, G.A. 1995. Displacement-based design of RC bridge columns in seismic regions. Earthquake Engineering and Structural Dynamics, **24**(12): 1623–1643.

Laughery, L.A. 2016. Response of High-Strength Steel Reinforced Concrete Structures to Simulated Earthquakes. Ph.D. Thesis, Purdue University, West Lafayette, Indiana, USA.

Liu, M., Lu, B., and Liu, B. 2012. Study on performance index of reinforced concrete bridge column. Advances in Intelligent Soft Computing, **114**:189–98.

Lu, J., Mackie, K., and Elgamal, A. 2011. BridgePBEE: OpenSees 3D pushover and earthquake analysis of single-column 2-span bridges, User Manual, Beta 1.0.

Lubell, A., Sherwood, T., Bentz, E., and Collins, M.P. 2004. Safe shear design of large, wide beams. ACI Concrete International, **26**(1): 66-78.

Luco N., and Cornell C.A. 1998. Effects of random connection fractures on the demands and reliability for a three-story pre-Northridge (SMRP) structure. *In* Proceedings of the 6th US national conference on earthquake engineering, May 31-June 4, Earthquake Engineering Research Institute, Oakland, California.

Mackie, K.R., and Stojadinović, B. 2004. Fragility curves for reinforced concrete highway overpass bridges. 13th World Conference on Earthquake Engineering. Paper No. 1553, 1-6 August, Vancouver, B.C., Canada.

Mackie, K., and Stojadinović, B. 2007. Performance-based seismic bridge design for damage and loss limit states. Earthquake Engineering & Structural Dynamics, **36**(13): 1953-1971.

Malhas, F.A. 2002. Preliminary Experimental Investigation of the Flexural Behavior of Reinforced Concrete Beams using MMFX Steel. Final Report for MMFX Technologies Corporation, University of North Florida, Jacksonville, Florida.

Mander, J. B., Priestley, M. J. N., and Park, R. 1988. Theoretical stress strain model for confined concrete. Journal of Structural Engineering, **114**(8): 1804-1826.

Marsh, M. L., and Stringer, S. J. 2013. Performance-based seismic bridge design. TRB's National Cooperative Highway Research Program (NCHRP) Synthesis 440 Transportation Research Board, Washington, D.C.

Mast, R.F., Dawood, M., Rizkalla, S.M., and Zia, P. 2008. Flexural Strength Design of Concrete Beams Reinforced with High-Strength Steel Bars. ACI Structural Journal, **105**(4): 570–577.

McNally, M.M. 2003. MMFX Rebar Evaluation for I-95 Service Road Bridge 1-712-B. MS thesis, University of Delaware, Delaware, USA.

Menegotto, M., and Pinto, P. E. 1973. Method of analysis for cyclically loaded R.C. plane frames including changes in geometry and nonelastic behaviour of elements under combined normal force and bending. Symposium on the Resistance and Ultimate Deformability of Structures Acted on By Well-Defined Repeated Loads, International Association for Bridge and Structural Engineering, Zurich, Switzerland, 15–22.

Mirza, S. 2007. Danger ahead: The coming collapse of Canada's municipal infrastructure. Report for the Federation of Canadian Municipalities, Ottawa, Ont., 1-25.

Mirza, S. A., and MacGregor, J. G. 1979. Variability of Mechanical Properties of Reinforcing Bars. Structural Division, ASCE, **105**: 921-937.

Mitchell, D., Paultre, P., Tinawi, R., Saatcioglu, M., Tremblay, R., Elwood, K.J., Adams, J., and DeVall, R. 2010. Evolution of seismic design provisions in the national building code of Canada. Canadian Journal of Civil Engineering, **37**(9): 1157–1170.

Moehle, J.P. 1996. Displacement-based seismic design criteria. *In* Proceedings of the 11th World Conference on Earthquake Engineering, 23-28 June, Acapulco, Mexico. Paper no. 2125.

Moran, J.D.G., and Lubell, A.S. 2008. Behavior of Concrete Deep Beams with High Strength Reinforcement. Report No. 277. University of Alberta. Alberta, Canada.

Muguruma, H., Nishiyama, M., Watanabe, F., and Tanaka, H. 1991. Ductile Behavior of High Strength Concrete Columns Confined by High Strength Transverse Reinforcement. ACI SP-128 - Evaluation and Rehabilitation of Concrete Structures and Innovations in Design, **128**: 877–891.

Munikrishna, A. 2008. Shear Behavior of Concrete Beams Reinforced with High Performance Steel Shear Reinforcement, M.S. Thesis, North Carolina State University, Raleigh, North Carolina.

Nagashima, T., Sugano, S., Kimura, H., and Ichikawa, A. 1992. Monotonic Axial Compression Test on Ultrahigh Strength Concrete Tied Columns. *In* Proceedings of the 10th World Conference on Earthquake Engineering, 19-24 July, Madrid, pp 2983–2988.

Naumoski, N., Tso, W.K., and Heidebrecht, A.C. 1988. A selection of representative strong motion earthquake records having different A/V ratios. EERG Rep. 88-01, Dept. of Civil Engineering, McMaster Univ., Hamilton, ON, Canada.

Nawy, E.G. 1968. Crack Control in Reinforced Concrete Structures, Journal of the American Concrete Institute, Farmington Hills, MI, **65**: 825–838.

Nielson, B.G. 2005. Analytical Fragility Curves for Highway Bridges in Moderate Seismic Zones. Ph.D. Thesis, Georgia Institute of Technology, Atlanta, GA.

Nielson, B.G., and DesRoches, R. 2007a. Seismic fragility methodology for highway bridges using a component level approach. Earthquake Engineering and Structural Dynamics, **36**: 823-839.

Nielson, B.G., and DesRoches, R. 2007b. Seismic fragility curves for typical highway bridge classes in the central and southeastern United States. Earthquake Spectra, **23**: 615-633. doi: 10.1193/1.2756815.

Nishiyama, M., Fukushima, I., Watanabe, F., and Muguruma, H. 1993. Axial Loading Tests on High Strength Concrete Prisms Confined by Ordinary and High Strength Steel. *In*

Proceedings of the Symposium on High Strength Concrete, 20-23 June, Norway, pp 322–329.

NIST 2014. Use of High-Strength Reinforcement in Earthquake-Resistant Concrete Structures. National Institute of Standards and Technology GCR 14-917-30, prepared by the NEHRP Consultants Joint Venture, a partnership of the Applied Technology Council and the Consortium for Universities for Research in Earthquake Engineering, for the National Institute of Standards and Technology, Gaithersburg, Maryland.

NRC 2017. 2010 National Building Code of Canada seismic hazard values. <http://earthquakescanada.nrcan.gc.ca/> (March. 05, 2017)

NRCC 2005. National building code of Canada. National Research Council of Canada, Ottawa, Ontario.

NRCC. 2010. National building code of Canada. National Research Council of Canada, Ottawa, Ontario.

NZ-Transport. 2014. New Zealand bridge manual. New Zealand Government.

Ortiz, J. 2006. Displacement-based design of continuous concrete bridges under transverse seismic excitation. European School for Advanced Studies in Reduction of Seismic Risk (ROSE School).

Ou, Y., Kurniawan, D., and Handika, N. 2012. Shear behavior of reinforced concrete columns with high strength steel and concrete under low axial load. *In* Proceedings of the ACI Fall Convention, 21-25 October, Toronto, Ontario, Canada.

Overby, D., Kowalsky, M., and Seracino, R. 2015. A706 Grade 80 Reinforcement for Seismic Applications. Report No. CA16-2563, California Department of Transportation, Sacramento, CA.

Özer, E., and Soyöz, S. 2015. Vibration-based damage detection and seismic performance assessment of bridges. Earthquake Spectra, **31**(1): 137-157.

Padgett, J.E. 2007. Seismic vulnerability assessment of retrofitted bridges using probabilistic methods. Ph.D. Thesis, Georgia Institute of Technology, Atlanta, GA.

Padgett J., and DesRoches, R. 2007. Bridge functionality relationships for improved seismic risk assessment of transportation networks. Earthquake Spectra, **23**: 115–130.

Padgett, J. E., and DesRoches, R. 2008. Methodology for the development of analytical fragility curves for retrofitted bridges. Earthquake Engineering and Structural Dynamics, **37**: 157–174.

Pang, Y., Wu, X., Shen, G., and Yuan, W. 2014. Seismic fragility analysis of cable-stayed bridges considering different sources of uncertainties. Journal of Bridge Engineering, **19**(4): 1—1.

Parghi, A., and Alam, M.S. 2017. Collapse Fragility Analysis of Non-Seismically Designed Bridge Columns Retrofitted with FRP Composites. *In* Proceedings of the Structures Congress 2017: Bridges and Transportation Structures, 6–8 April, Denver, Colorado.

Paulay, T., and Priestley, M. N. J. 1992. Seismic design of reinforced concrete and masonry buildings, Willey, New York.

Paulson, C., Graham, S.K., and Rautenberg, J.M. 2013. Determination of Yield Strength for Nonprestressed Steel Reinforcement, prepared by Wiss, Janney, Elstner Associates, Inc., for the Charles Pankow Foundation, RGA 04-13, WJE No. 2013.4171, Pasadena, California.

Paultre, P., Légeron, F., and Mongeau, D. 2001. Influence of Concrete Strength and Transverse Reinforcement Yield Strength on Behavior of HighStrength Concrete Columns. ACI Structural Journal, **98**(4): 490-501.

PEER 2011. New ground motion selection procedures and selected motions for the PEER transportation research program. PEER Rep. 2011/03, PEER center, University of California, Berkeley, CA.

Peterfreund, P. 2003. Development length of MMFX steel reinforcing bars used in bridge deck applications. MSc thesis, University of Massachusetts-Amherst.

Pinho, R., Casarotti, C., and Antoniou, S. 2007. A Comparison of singlerun pushover analysis techniques for seismic assessment of bridges. Earthquake Engineering Structural Dynamics, **36**(10): 1347–1362.

Price, K.R., Fields, D., and Lowes, L.N. 2014. The impact of high-strength reinforcing steel on current design practice. Research Grant Agreement #01-13, Charles Pankow Foundation, Vancouver, Washington.

Priestley, M. 2000. Performance based seismic design. Bulletin of the New Zealand Society for Earthquake Engineering, **33**(3): 325-346.

Priestley, M.J.N., Calvi, G.M., and Kowalsky, M.J. 2007. Displacement-based seismic design of structures. IUSS Press, Pavia, Italy.

Priestley, M.J.N., Seible, F., and Calvi, G.M. 1996. Seismic design and retrofit of bridges. Willey, New York.

Rautenberg, J.M. 2011. Drift capacity of concrete columns reinforced with high-strength steel. PhD thesis, Purdue University, West Lafayette, USA.

Razvi, S.R., and Saatcioglu, M. 1994. Strength and deformability of high strength concrete columns. ACI Structural Journal, **91**(6): 678–687.

Restrepo, J.I., Seible, F., Stephan, B., and Schoettler, M.J. 2006. Seismic testing of bridge columns incorporating high-performance materials. ACI Structural Journal, **103**(4): 496–504.

Reza, S.M. 2012. Seismic Performance of Multi-Span RC Bridge with Irregular Column Heights. M.A.Sc. Thesis, the University of British Columbia, Canada.

Reza, S.M., Alam, M.S., and Tesfamariam, S. 2014. Seismic performance comparison between direct displacement-based and force-based design of a multi-span continuous reinforced concrete bridge with irregular column heights. Canadian Journal of Civil Engineering, **41**: 440–449.

Rizkalla, S., Zia, P., Seliem, H., and Lucier, G. 2005. Evaluation of MMFX steel for NCDOT concrete bridges. Report FHWA/NC/2006-31, NCDOT Project 2004-27.

Roy, N., Paultre, P., and Proulx, J. 2010. Performance-based seismic retrofit of a bridge bent: Design and experimental validation. Canadian Journal Civil Engineering **37**: 367–379.

Russell, H.G., Miller, R.A., Harries, K.A., and Shahrooz, B.M. 2011. Design of concrete structures using high-strength steel reinforcement. NCHRP report 679. Transportation research board, Washington, D.C.

Saiidi, M. 2011. Managing seismic performance of highway bridges evolution in experimental research. Structure and Infrastructure Engineering, **7**(7–8): 569–586.

Saleem, M.A., Mirmiran, A., Xia, J., and Mackie, K. 2013. Development length of high-strength steel rebar in ultrahigh performance concrete. Journal of Materials in Civil Engineering, **25**(8): 991-998.

Salomon, A.L., and Moen, C.D. 2014. Structural design guidelines for concrete bridge decks reinforced with corrosion-resistant reinforcing bars. Report No. FHWA/VCTIR 15-R10. U.S. Department of Transportation Federal Highway Administration. Charlottesville, Virginia.

SEAOC Vision 2000. 1995. Performance based seismic engineering of buildings, vols. I and II: Conceptual framework. Sacramento Structural Engineers Association of California, CA.

SeismoMatch. 2014. SeismoMatch help file. Available from www.seismsoft.com

SeismoStructure. 2015. SeismoStruct help file. Available from www.seismsoft.com

Seliem, H., Hosny, A., Dwairi, H., and Rizkalla, S. 2006. Shear behavior of concrete beams reinforced with MMFX steel without web reinforcement. NC State Report IS-06-08.

Seliem, H.M., Hosny, A., Rizkalla, S., Zia, P., Briggs, M., Miller, S., Darwin, D., Browning, J., Glass, G.M., Hoyt, K., Donnelly, K., and Jirsa, J.O. 2009. Bond characteristics of ASTM A1035 steel reinforcing bars. ACI Structural Journal, **106**(4): 530–539.

Seliem, H.M., Lucier, G., Rizkalla, S.H., and Zia, P. 2008. Behavior of concrete bridge decks reinforced with high-performance steel. ACI Structural Journal, **105**(1): 78-86.

Setunge, S. 1993. Structural Properties of Very High-Strength Concrete. Ph.D. Thesis, Monash University, Australia.

Setzler, E.J., and Sezen, H. 2008. Model for the lateral behavior of reinforced concrete columns including shear deformations. Earthquake Spectra, **24**(2): 493-511.

Shahrooz, B.M., Miller, R.A., Harris, K.A., and Russell, H.G. 2011. Design of concrete structures using high-strength steel reinforcement. National Cooperative Highway Research Program (NCHRP) Report 679, Transportation Research Board of the National Academies, Washington, D.C.

Shahrooz, B.M., Reis, J., Wells, E., Miller, R.A., Harries, K., and Russell, H.G. 2010. Flexural behavior and design with high-strength bars and those without well-defined yield point. In Transportation Research Record: Journal of the Transportation Research Board. Transportation Research Board of the National Academies, Washington, DC, **10**: 103-111.

Sheikh, M. N., and Légeron, F. 2014. Performance based seismic assessment of bridges designed according to Canadian Highway Bridge Design Code. Canadian Journal of Civil Engineering, **41**: 777–787.

Shinozuka, M., Feng, M.Q., Kim, H.K., and Kim, S.H. 2000. Nonlinear static procedure for fragility curve development. ASCE Journal of Engineering Mechanics, **126**: 1287– 1296.

Shinozuka M, Feng M.Q, Kim H, Uzawa, T., and Ueda, T. 2003. Statistical analysis of fragility curves. MCEER Report-03-0002.

Shiro, M., and Hitoshi, S. 1996. Development of high strength mild steel deformed bars for high performance reinforced concrete structural members. *In* Proceedings of the 11th World Conference on Earthquake Engineering, 23-18 June, Acapulco, Mexico, Paper no. 1742.

Siqueiraa, G., Sandab, A., Paultreb, P., and Padgettc, J. 2014. Fragility curves for isolated bridges in eastern Canada using experimental results. Engineering Structure, **74**: 311–324.

Somerville, P.G. 2002. Characterizing near fault ground motion for the design and evaluation of bridges. *In* Proceedings of the 3rd National Conference and Workshop on Bridges and Highways, April 28-May 1, Portland, Oregon.

Sperry, J., Al-Yasso, S, Searle, N., DeRubies, M.,Darwin, D., O'Reilly, M., Matamoros, A., Feldman, L., Lepage, A., Lequesne, R., and Ajam, A. 2015. Anchorage of high-strength reinforcing bars with standard hooks. SM Report No. 111. The University of Kansas Center For Research, Inc., Lawrence, Kansas

Stephan, B., Restrepo, J., and Seible, F. 2003. Seismic Behavior of Bridge Columns Built Incorporating MMFX Steel. UCSD Report SSRP- 2003/09.

Suarez, V., and Kowalsky, M. 2006. Implementation of displacement based design for highway bridges. *In* Proceedings of the 5th National Seismic Conference on Bridges & Highways, San Francisco, Canada.

Sumpter, M.S. 2007. Behavior of high performance steel as shear reinforcement for concrete beams. ACI Structural Journal, **106**(2): 171–177.

Tadros, M.K. 2017. High-strength steel in bridge applications. Concrete Bridge Technology. ASPIRE.

Tavares, D. H., Padgett, J. E., and Paultre, P. 2012. Fragility curves of typical as-built highway bridges in eastern Canada. Engineering Structures, **40**: 107-118.

Tureyen, A.K., and Frosch, R.J., 2003, Concrete shear strength: Another perspective. ACI Structural Journal, **100**(5): 609-615.

Vamvatsikos D, and Cornell CA. 2002. Incremental dynamic analysis. Earthquake Engineering Structural Dynamic, **31**(3): 491–514.

Vijay, P.V., GangaRao, H.V.S., and Prachasaree, W. 2002. Bending Behavior of Concrete Beams Reinforced with MMFX Steel Bars, West Virginia University.

Wagstaffe, J. 2016 Oct 11. The 'Big One' near Vancouver you may not know about. Retrieved from http://www.cbc.ca

Wang, Z. 2006. Understanding seismic hazard and risk assessments: An example in the New Madrid Seismic Zone of the central United States. *In* Proceedings of the 8th National Conference on Earthquake Engineering. San Francisco, California.

Xu, S.Y., and Zhang, J. 2011. Hysteretic shear–flexure interaction model of reinforced concrete columns for seismic response assessment of bridges. Earthquake Engineering and Structural Dynamics, **40**(3): 315–337.

Yotakhong, P. 2003. Flexural performance of MMFX reinforcing rebars in concrete structures. M.S. Thesis, North Carolina State University, Raleigh, North Carolina.

Yun, S., Hamburger, RO., Cornell, C.A., and Foutch, DA. 2002. Seismic performance evaluation for steel moment frames. Journal of Structural Engineering, **128**(4): 534–45.

Zelaschi, C., Monteiro, R., and Pinho, R. 2015. Improved fragility functions for RC bridge populations. *In* Proceedings of the 5th ECCOMAS Thematic Conference on Computational Methods in Structural Dynamics and Earthquake Engineering, 25–27 May, Crete Island, Greece.

Zeno, G.A. 2009. Use of High Strength Steel Reinforcement in Shear Friction Applications. MSCE thesis, University of Pittsburgh, Pennsylvania.

Zhang, Q. 2015. Performance based design and evaluation of reinforced concrete bridges. M.A.Sc. Thesis, the University of British Columbia, Kelowna, Canada.

Zhang, Q., Alam, M.S., Khan, S. and Jiang, J. 2016. Seismic performance comparison between force-based and performance-based design as per Canadian Highway Bridge Design Code (CHBDC) 2014. Canadian Journal of Civil Engineering, **43**: 741–748.

Zhang, J., and Huo, Y. 2009. Evaluating effectiveness and optimum design of isolation devices for highway bridges using the fragility function method. Engineering Structures, **31**(8): 1648-1660.

Ziehl, P.H., Cloyd, J.E., and Kreger, M.E. 1998. Evaluation of Minimum Longitudinal Reinforcement Requirements for Reinforced Concrete Columns, Research Report 1473-S, Center for Transportation Research, University of Texas, Austin, Texas.

Ziehl, P.H., Cloyd, J.E., and Kreger, M.E. 2004. Investigation of minimum longitudinal reinforcement requirements for concrete columns using present-day construction materials. ACI Structural Journal, **101**(2): 165-175.

APPENDICES

Appendix A: Longitudinal Reinforcement Design for FBD

The following column-interaction diagram (Figure A.1) is used to determine the longitudinal reinforcement percentage for the FBD method of the bridge pier.

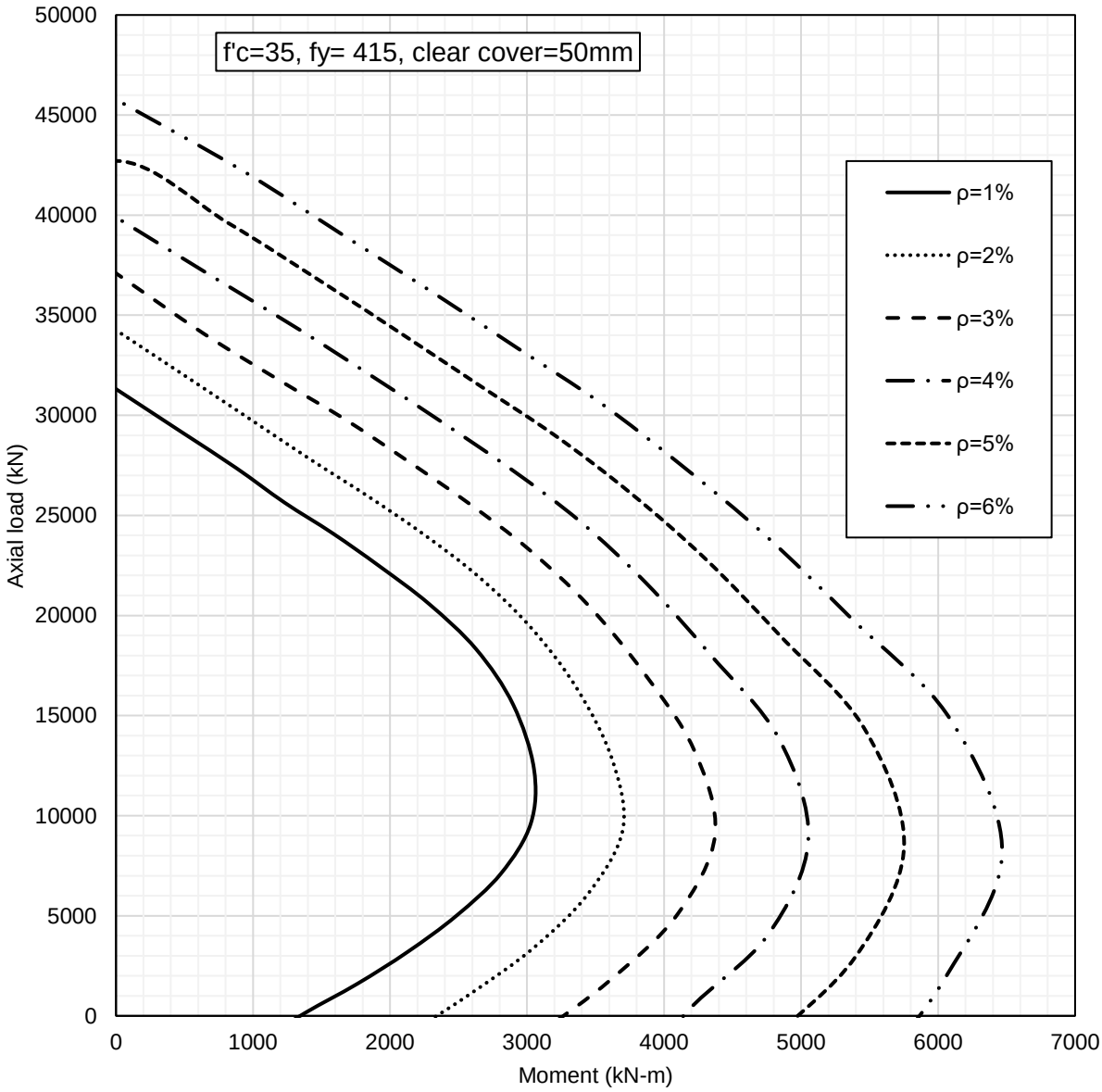

Figure A.1 Column interaction diagram for FBD

FBD calculation details for a lifeline single bridge pier following CHBDC 2010:

$Diameter\ of\ the\ pier, d = 915mm$

$Clear\ cover = 50mm$

$Height\ of\ the\ pier, L = 5.25m$

$Concrete\ strength = 35MPa$

$Longitudinal\ steel\ reinfrocement\ strength = 415MPa$

$Lumped\ mass, m = 2300kN = 234455kg$

$Axial\ load\ ratio = 10\%\ of\ gross\ capacity; W = 10\%x657556x35 = 2300kN$

$Modulus\ of\ elasticity\ of\ concrete = 26273.08MPa$

$Cross - sectional\ are\ of\ the\ pier = 657556.5mm^2$

$Gross\ moment\ of\ inertia\ of\ pier\ section, I_g = \frac{\pi d^4}{64} = 3.44x10^{10}mm^4$

$Zonal\ acceleration\ ratio\ for\ Vancouver, A = 0.2$

$Importance\ factor\ for\ a\ lifeline\ bridge, I = 3$

$Site\ co - efficient\ for\ soil\ profile\ III, S = 1.5$

$Response\ modification\ factor\ for\ single\ pier, R = 3$

$Assuming\ 4\%\ longitudinal\ reinforcement, elastic\ stiffness\ ratio\ from\ Fig.\ 5.3,$

$\frac{I_{eff}}{I_g} = 0.76\ ; I_{eff} = 0.76xI_g = 2.61x10^{10}mm^4$

$Stiffness\ of\ the\ pier, k = \frac{3EI_{eff}}{L^3} = 14243.71\frac{N}{mm}$

$Time\ period, T = 2\pi\sqrt{\frac{m}{k}} = 0.806sec$

$$Elastic\ seismic\ response\ coefficient, C_{sm} = \frac{1.2AIS}{T^{\frac{2}{3}}} = 1.247 \leq 2.5AI$$

$$Elastic\ base\ shear\ demand, V_{elastic} = C_{sm}xW = 2850kN$$

$$Inelastic\ base\ shear\ demand, V_{inelastic} = \frac{V_{elastic}}{R} = 950kN$$

$$Design\ moement, M = V_{elastic}xL = 5020kN - m$$

From the column interaction diagram (Figure A.1), required longitudinal reinforcement ratio is found to be 4.6%, which is close to the assumed ratio. 16-55M longitudinal rebar is selected, and the spirals are designed for elastic base shear demand. Provided longitudinal reinforcement ratio becomes 4.87%.

Appendix B: Effect of Transverse Reinforcement Strength on Design and Seismic Performance

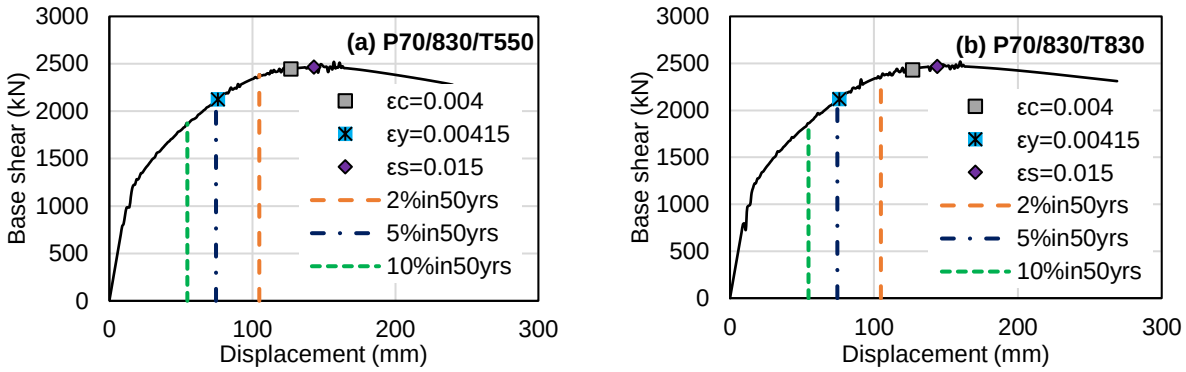

Figure B.2 Static pushover analysis curves

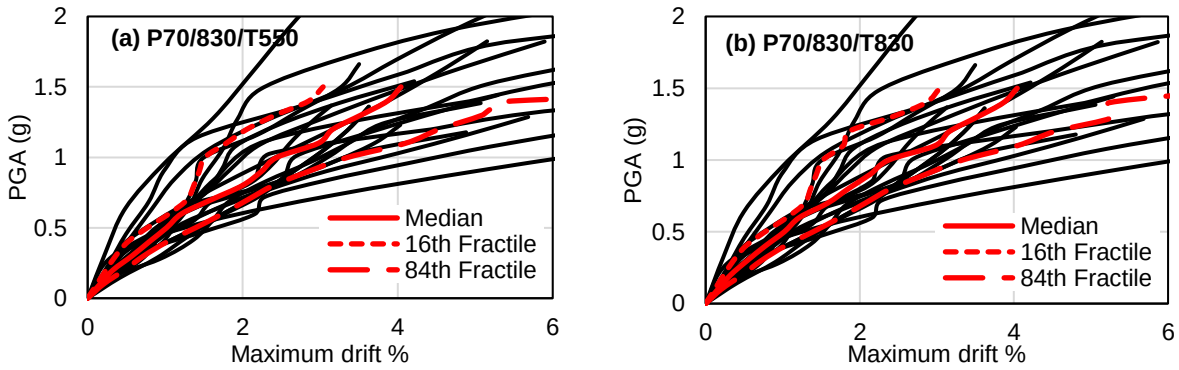

Figure B.3 *IDA* curve for maximum drift

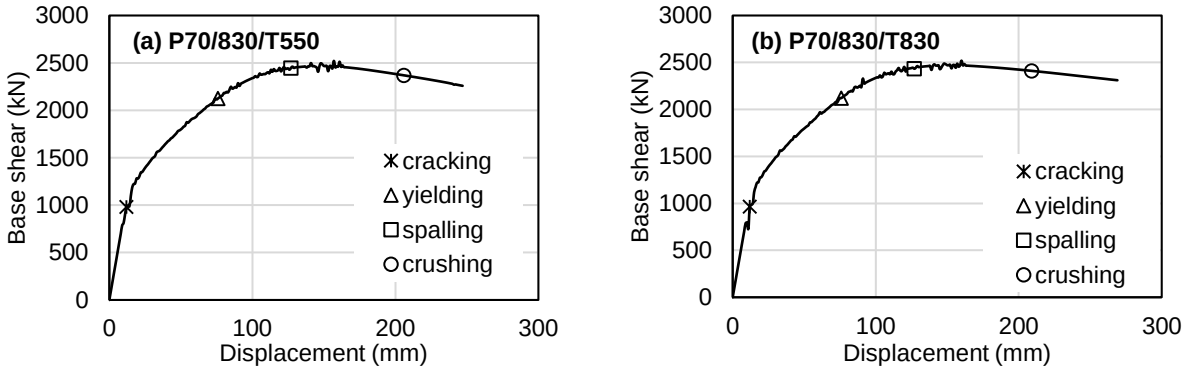

Figure B.4 FEMA limit states

Table B.1 LSs of bridge pier following FEMA for Drift%

Damage State →	Slight	Moderate	Extensive	Collapse
P70/830/T415	0.14%	0.83%	1.40%	2.10%
P70/830/T550	0.13%	0.83%	1.38%	2.25%
P70/830/T830	0.13%	0.83%	1.39%	2.29%

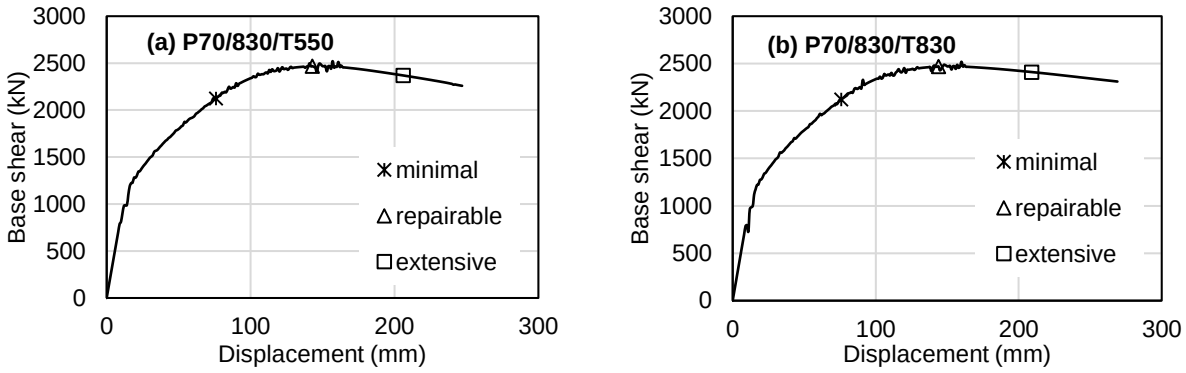

Figure B.5 CHBDC limit states

Table B.2 *LS*s of bridge pier following CHBDC for Drift%

Damage State →	Minimal	Repairable	Extensive
P70/830/T415	0.83%	1.58%	2.10%
P70/830/T550	0.83%	1.56%	2.25%
P70/830/T830	0.83%	1.58%	2.29%

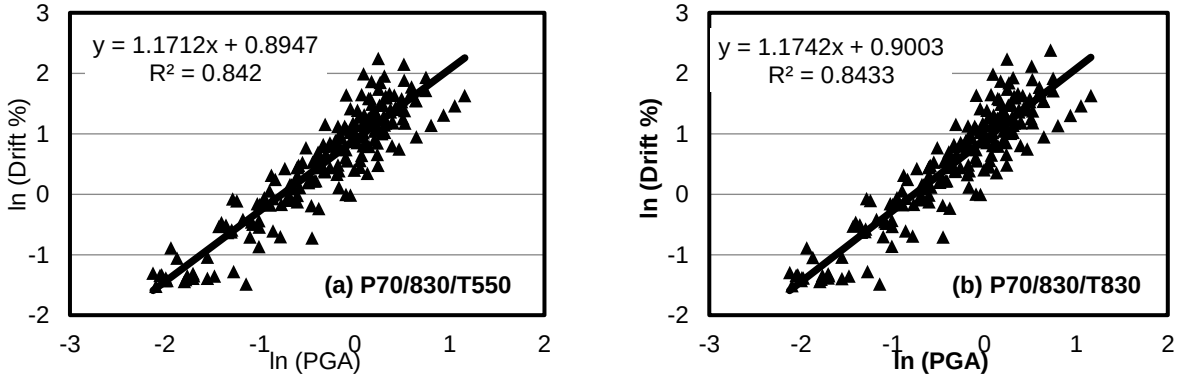

Figure B.6 Probabilistic seismic demand models